GUSTAVO FERREIRA CORREIA

Bauxite mining and shipping: transportable moisture limit (TML) tests and further cargo assessments for safe shipping

Dissertation presented to *Escola Politécnica da Universidade de São Paulo* for the degree of Master of Science

Advisor: Prof. Dr. Arthur Pinto Chaves

São Paulo

2020

GUSTAVO FERREIRA CORREIA

Bauxite mining and shipping: transportable moisture limit (TML) tests and further cargo assessments for safe shipping

Corrected version

Dissertation presented to *Escola Politécnica da Universidade de São Paulo* for the degree of Master of Science

Concentration area: Mineral Engineering

Advisor: Prof. Dr. Arthur Pinto Chaves

São Paulo
2020

Este exemplar foi revisado e corrigido em relação à versão original, sob responsabilidade única do autor e com a anuência de seu orientador.

São Paulo,_____de_____de _____

Assinatura do autor: _____

Assinatura do orientador: _____

Catalogação-na-publicação

Correia, Gustavo
Bauxite mining and shipping: transportable moisture limit (TML) tests and further cargo assessments for safe shipping / G. Correia – versão corr. -- São Paulo, 2020.
133 p.

Dissertação (Mestrado) - Escola Politécnica da Universidade de São Paulo. Departamento de Engenharia de Minas e Petróleo.

1.Bauxite 2.Transportable moisture limit 3.Particle size distribution 4.Solid bulk cargo 5.Cargo classification I.Universidade de São Paulo. Escola Politécnica. Departamento de Engenharia de Minas e Petróleo II.t.

Correia, Gustavo Ferreira. **Bauxite mining and shipping: transportable moisture limit (TML) tests and further cargo assessments for safe shipping**. São Paulo. 2020, 133 p. (Mestrado) Escola Politécnica, Universidade de São Paulo, São Paulo, 2020.

ACKNOWLEDGEMENTS

To Heloisa Ruggeri, for supporting the projects related to this research in every opportunity. To Professor Arthur P. Chaves for the great contribution to my training as a mining engineer, for advising me and for providing valuable inputs beyond the work covered on these pages. To Rodrigo Ferreira, for all the amazing work done on the subject of this dissertation and for sharing so much!

To Tim Evans, for the impacting contributions to all those involved in shipping Group A cargoes, for the high standard of commitment and for the decisive leadership to deliver the joint bauxite industry research. To Dany Policarpo, for the unparalleled technical skills and never-ending willingness to socialize knowledge. To Robin Castello, for the great spirit and for always providing the best routes for the team to navigate.

To Rodrigo Ferreira and to Professors Homero Delboni Jr., Fernando Marinho and Arthur P. Chaves for all the suggestions for improvement of this text.

To Railson Maciel, Maelson Moutinho, Diomedes Santarém, Diana Martins, Edelina Viana, Robson Machado, Lucivaldo Fernandes, Luiz Sérgio Oliveira, Agissé Matos and all those in laboratory, port operations and quality control teams for the great support, friendship and commitment to good work.

To Newton Oliveira, Bárbara Fiorito, Hydeckel Lima and José Danza for the feedbacks and companionship along the way.

To Mônica Paiva, Giovanni Moraes, Bernardo Bandeira, and Débora Motomatsu, for the friendship and all the help in classes. To Paula Figueiredo, for the great support on this journey.

To the professionals and companies involved in the research carried by the Global Bauxite Working Group for the effort and accomplishments.

To Associação Brasileira do Alumínio and its associates for the sponsorship of initiatives to produce and share knowledge within the Brazilian aluminum industry and its stakeholders.

“The cure for anything is saltwater:
sweat, tears or the sea.”

ABSTRACT

Solid bulk cargoes relatively fine and wet may become unstable during ocean voyages and put a risk to the stability of the ship and life of the crew. To prevent instabilities related to the moisture content of the cargo, the international regulation on maritime transportation establishes that certain cargoes can only be shipped if its moisture content is below the so-called transportable moisture limit (TML), a regulatory parameter determined in a laboratory test to provide the maximum moisture content of the cargo to assure safe shipping. In 2015, the loss of lives and ship related to instability of wet and fine bauxite cargo under adverse sea conditions led to amendments on relevant bauxite shipping regulations. The Proctor/Fagerberg test method is widely used to determine the TML of solid bulk cargoes. Recent studies have led to improvements in test apparatus and procedures to Proctor/Fagerberg test to make it more suitable and reliable on the TML determination of specific cargoes. This study applied changes on the original Proctor/Fagerberg test and analyzed the effect of variables (compaction energy, type of bauxite and top size) on the TML determination of bauxites. All variables analyzed showed influence on TML results and the level of compaction energy provided by different compaction hammers was the single variable with the highest effect. By the light of joint research carried by bauxite industry players, it was developed a particle size criterion to distinguish between finer bauxites that may exhibit instabilities due to moisture and coarser bauxites that may not present such risk. The borderline defined is 30% in weight passing 1 mm and 40% in weight passing 2.5 mm. The fundamentals behind the particle size criterion developed are presented, while their implementation, adequacy, and relevance for the safety of bauxite shipping are discussed. Finally, a study case of bauxite cargo classification for shipping in accordance with the aforementioned particle size criterion is presented. A particle size distribution database of nearly 500 bauxite shipments since 2015 was analyzed to verify the variation in particle size distributions, the likelihood of variation in cargo classification and relevant practices to assure safe and compliant shipping.

Keywords: Bauxite, transportable moisture limit, design of experiments, particle size distribution, solid bulk cargo, cargo classification, safe shipping.

RESUMO

Cargas sólidas a granel relativamente finas e úmidas podem se tornar instáveis durante o transporte oceânico, colocando a estabilidade do navio e a vida da tripulação em risco. Para evitar instabilidades provocadas por umidade da carga, a regulamentação internacional em transporte marítimo estabelece que certas cargas só podem ser embarcadas se sua umidade estiver abaixo do t*ransportable moisture limit* (TML), um parâmetro regulatório determinado em testes laboratoriais para se obter o máximo de umidade que poderá estar contida na carga para garantir a segurança do transporte marítimo. Em 2015, a perda de vidas e navio devido à instabilidade de carga de bauxita fina e úmida em condições adversas de navegação levou a alterações na regulamentação pertinente ao transporte marítimo de bauxita. O método de teste Proctor/Fagerberg é largamente utilizado para determinar o TML de cargas sólidas a granel. Estudos recentes levaram a ajustes em aparatos de teste e procedimentos do teste Proctor/Fagerberg para torna-lo mais adequado e confiável para a determinação do TML de cargas específicas. Este estudo aplicou mudanças no teste Proctor/Fagerberg original e analisou o efeito de variáveis (energia de compactação, tipo de bauxita e *top size*) na determinação do TML de bauxitas. Todas as variáveis analisadas apresentaram influência nos resultados de TML e a energia de compactação obtida a partir de diferentes soquetes de compactação foi a variável com maior efeito. À luz da pesquisa conjunta desenvolvida por atores da indústria da bauxita, foi estabelecido um critério granulométrico para distinguir bauxitas finas que podem apresentar instabilidades devido à umidade e bauxitas mais grossas que não apresentam tal risco. O limite definido foi 30% em peso passante em 1 mm e 40% em peso passante em 2.5 mm. Os fundamentos que sustentam o critério granulométrico definido são apresentados, enquanto se discute sua implementação, adequação e relevância para a segurança dos embarques de bauxita. Por fim, um estudo de caso de classificação de carga de bauxita para embarque de acordo com o critério granulométrico em questão é apresentado. Uma base de dados de distribuição granulométrica de cerca de 500 embarques de bauxita desde 2015 foi analisada para se verificar a probabilidade de variação de classificação da carga, bem como as práticas relevantes para a garantia da segurança e conformidade dos embarques.

Palavras-chave: Bauxita, limite de umidade transportável, planejamento experimental, distribuição granulométrica, carga sólida à granel, classificação de carga, segurança do transporte marítimo .

LIST OF FIGURES

LIST OF FIGURES

LIST OF FIGURES

LIST OF FIGURES

LIST OF TABLES

LIST OF EQUATIONS

ACRONYMS / GLOSSARY

Bulk carrier: A ship designed to carry bulk solids.

Cargo Schedule: Individual cargoes are listed as 'schedules' in Appendix 1 of the IMSBC Code. These schedules describe cargo's properties and classifications (for example, 'Group A') and detail the requirements for handling, stowing and carrying it safely. Schedules may also contain tests specific to that cargo.

CCC: IMO's S/ub-Committee on Carriage of Cargoes and Containers.

Competent Authority: The authority in charge of domestic enforcement of the IMSBC Code.

CTT: Cyclic triaxial test. A laboratory testing method used to determine the cyclic strength of soils by the load-controlled cyclic triaxial technique to evaluate the ability of a soil to resist the shear stresses induced due to earthquake or other cyclic loading, such as vessel motions.

Degree of Saturation (*S*): Volume of water within the inter-particle voids of granular material (such as a bulk commodity). It is expressed as a percentage, where water completely fills the voids at S=100% and the material is completely dry at S=0%.

DWT: Deadweight tonnage, which is a measure in metric tons of how much weight a ship can carry, considering cargo, fuel, crew, freshwater, and provisions.

Flow Moisture Point (FMP): The minimum moisture content at which cargo liquefaction may occur, as determined from test methods (Proctor/Fagerberg test and Flow table test) within the IMSBC Code.

Flow Table test (FTT): One of the three general methods within the IMSBC Code used to determine the TML of a Group A cargo.

FSE: Free Surface Effect, which is the reduction of stability of the ship caused by changes of the ship's center of gravity position with the movement of liquid cargoes or solid cargoes with liquid behavior.

ACRONYMS / GLOSSARY

GBWG: Global Bauxite Working Group.

GM: Metacentric height, which is the height of M in relation to G, where M represents the point of intersection of vertical forces acting on the ship and G represents the center of gravity of the ship.

Group A cargo: Cargo liable to liquefy (current IMSBC Code definition).

Group B cargo: Cargo that may possess chemical hazard (current IMSBC Code definition).

Group C cargo: Cargo that is neither liable to liquefy nor to possess chemical hazards (current IMSBC Code definition).

Hold / Cargo hold / Vessel hold / Ship hold: space where cargo is loaded and carried in a ship.

IMO: International Maritime Organization.

IMSBC Code: International Maritime Solid Bulk Cargoes Code.

List: When the ship assumes an angle of rotation over the transverse axis, often due to a change in center of gravity of the cargo that follows cargo shift.

Master / Captain of the ship: a licensed mariner in ultimate command of the ship.

OMC: Optimum Moisture Content. The moisture content at which a material presents its higher level of compaction, which can be observed as the highest point of density or lowest point of voids on the compaction curve of a Proctor or Proctor/Fagerberg test.

Proctor/Fagerberg test (PFT): One of the three general methods within the IMSBC Code used to determine the TML of a Group A cargo.

PSD: Particle Size Distribution.

PTT (Penetration Test): One of the three general methods within the IMSBC Code used to determine the TML of a Group A cargo.

ACRONYMS / GLOSSARY

ROM: Run of Mine. Raw material after it is mined and prior to any form of processing.

Shipper: The merchant who delivers the goods to the carrier. Example: commodity producers, such as mining companies.

Solid bulk cargo/bulk cargo: Any material, other than liquid or gas, which consists of a combination of particles, granules or any other larger pieces of material that is loaded directly into the cargo spaces of a ship without any intermediate form of containment.

TML: Transportable moisture limit, read as gross water content in weight. It is a concept within the IMSBC Code that represents the maximum moisture at which a Group A cargo can be safely loaded to prevent moisture-related instability of the cargo.

WA: Western Australia.

LIST OF SYMBOLS

B	mass of mold + sample
C	wet mass of sample
d	density of solid material determined in the picnometer
D	mass of dry sample
e	void ratio
e_v	net water content
E	mass of water
V	volume of the mold
γ	dry bulk density
S	degree of saturation
u_w	pore water pressure
W	net water content
W_1	gross water content
σ	normal stress
σ'	effective stress

CONTENTS

OBJECTIVES

- To analyze the effect of variables (compaction energy, type of bauxite and top particles size) on the TML determination of bauxites through the original Proctor/Fagerberg test procedure;

- To review the fundamentals behind the particle size criterion developed for bauxite classification, while discussing its implementation, adequacy, and relevance for the safety of bauxite shipping;

- To provide a case study of bauxite cargo classification in Juruti mine in accordance with the particle size criterion prescribed by most updated relevant regulation, verifying the likelihood of variation in cargo classification and relevant practices to assure safe and compliant shipping.

1. INTRODUCTION

The aluminum industry relies on mining and transportation of bauxite, as it has been the primary source of aluminum for over a century. The world total bauxite production in 2018 was nearly 300 million tons, from which about 100 million tons were transported by ships (CLARKSON, 2017; GBWG, 2017; USGS, 2019).

Sufficiently fine and wet solid bulk cargoes may shift in cargo holds under vessel motions in ocean voyages, causing displacement of ship's center of gravity and diminishing its stability. The ship may develop a list or even capsize, putting in risk the life of the crew and integrity of the ship and its cargo (MUNRO; MOHAJERANI, 2016a; JU et al., 2017; EVANS et al., 2018; FERREIRA; PEREIRA; LIMA, 2019).

From 2009 to 2018, 9 ships and 101 lives were lost in the maritime transportation of solid bulk cargoes due to cargo shift triggered by moisture-related mechanisms such as liquefaction and dynamic separation of cargoes. Out of the 9 ships lost, 6 were carrying nickel ore, 2 were carrying iron ore fines and one was carrying bauxite (INTERCARGO, 2019). The event related to bauxite cargo occurred in 2015 when the bulk carrier Bulk Jupiter was carrying 19 men and 46.000 tons of bauxite from Malaysia to China. The ship sunk off the coast of Vietnam, accounting for 18 casualties (BMTA, 2015).

The maritime transportation of people and goods shall comply with the international regulatory frame provided by the International Maritime Organization (IMO), which is a United Nations agency responsible for the safety and prevention of pollution in maritime transportation. The IMO's provisions related to solid bulk cargoes are found on the International Maritime Solid Bulk Cargoes (IMSBC) Code. It contains instructions and requirements for safe and compliant handling of solid bulk cargoes. Such cargoes are categorized in 3 Groups: i) Group A – those liable to liquefy; ii) Group B – those that may possess chemical hazard; iii) Group C – those that are neither liable to liquefy nor to possess chemical hazards (IMO, 2018).

To prevent potential cargo instability due to moisture, the IMSBC Code establishes that Group A cargoes can only be shipped if the moisture content of the cargo is less than its transportable moisture limit (TML) – a regulatory parameter determined through

laboratory test methods acknowledged by the IMO. The TML is the maximum moisture content of a Group A cargo for safe carriage and its accurate determination is key for the safety of the crew, vessel, and cargo.

The TML became a key parameter for the mining industry and failing to provide accurate moisture content and TML figures may put the safety of the crew, ships, and cargoes in risk while jeopardizing the continuity of operations. This makes knowledge and proficiency in TML testing of high concern for those involved in the production and transportation of bauxite and all other cargoes classified as Group A.

Until 2015, bauxite cargoes were shipped as Group C cargoes. After the Bulk Jupiter incident, companies in the bauxite industry formed an interdisciplinary Global Bauxite Working Group (GBWG) to research the behavior of bauxite during shipping. The group aimed to develop a globally applicable science-based criterion for distinguishing Group C and Group A bauxite cargoes; and to develop a TML test method for Group A bauxites. The GBWG gathered a variety of stakeholders and expertise, including shippers (mine owners/operators), transporters (shipowner/operators), users (alumina refinery operators) and consultants with diversified backgrounds, such as geotechnical and hydraulic engineering, maritime science, chemical and process engineering, and port and ship operations.

From 2015 to 2017, the GBWG research analyzed bauxite samples from Australia, Brazil, Indonesia, India, Malaysia, Guinea, Guyana, and Jamaica, representing over 90% of all seaborne traded bauxite at the time. Following simulations of vessel motions of a wide variety of bauxites, the GBWG was able to verify the bauxites modes of instability due to moisture content (GBWG, 2017).

As an employee of Alcoa, the author was a member of the GBWG, providing information of bauxite shipped by the company and participating in the research developed with key inputs for the development of the TML test specific for finer bauxites. Founded 130 years ago, Alcoa is a global company operating in all stages of the aluminum production chain, including bauxite mining and metallurgical processing in refineries (Bayer process) and smelters (Hall-Héroult process). In 2018, Alcoa has produced 45.8 million dry metric tons on its 7 bauxite operations around the globe, including Juruti mine, located in the state of Pará, in Brazil (ALCOA, 2019).

In summary, the GBWG research led to the recommendation of a particle size criterion to distinguish coarse stable bauxites (Group C cargoes) and fine potentially unstable bauxites (Group A cargoes). For those Group A cargoes, the GBWG proposed a suitable TML test procedure (the Modified Proctor/Fagerberg Test for Bauxite) and noted that the cargo instability due to moisture took place due to a progressive dynamic separation of water and finer particles from the whole cargo under ship motions, resulting in the formation of a free slurry surface that could move freely above a layer of compacted cargo, reducing the stability of the vessel. The recommendations made by GBWG were peer-reviewed by Imperial College London and fed regulation updates on bauxite carriage by the IMO in September of 2017. By the light of the GBWG findings, the IMO has established a particle size criterion to distinguish between finer bauxites that may exhibit instabilities due to moisture and coarser bauxites that may not. This work presents an overview of the GBWG research while discussing practical aspects of its application and measures for safer bauxite shipping.

In 2015, Alcoa started to ship bauxite cargoes as Group A in Juruti, in accordance with updated IMO regulations at the time. In order to assure safety and compliance of shipping, the TML determination and keen moisture management of the bauxite to be shipped became part of Juruti mine and port routine operations.

The Proctor/Fagerberg test is widely used to determine TML and improvements in the original Proctor/Fagerberg test have been proposed to make it more suitable and reliable on the TML determination of specific cargoes. This study applied changes on standard Proctor/Fagerberg test procedures and assessed the effect of variables on the TML results of bauxites from Juruti mine. Factorial design with 3 variables and 2 levels was applied: different compaction hammers (C and D); different bauxites (washed and unwashed); and samples top size (5 mm and 25.4 mm). This approach allowed assessment of how the TML responds to variations of bauxite characteristics and changes in procedures of the standard Proctor/Fagerberg test. It provided relevant insights on bauxite TML testing and the effects of potential amendments to the standard Proctor/Fagerberg test when developing a modified test version to make it more adequate to determine the TML of a specific cargo.

Following 2017’s regulatory update – providing the particle size criterion to classify

bauxite cargoes as Group C or A –, this work presents a case study on bauxite cargo classification for shipping. The particle size distribution (PSD) database of cargoes shipped since 2015 was assessed to verify the variability, the likelihood of variation in cargo Group and relevant practices to assure safe and compliant shipping of bauxite cargoes.

2. LITERATURE REVIEW

2.1 BAUXITE

Bauxite is the primary source of aluminum, the third most abundant element in the crust of earth, after oxygen and silicon. Bauxites are formed from the weathering processes of silicate rocks (granite and basalt) and carbonate rocks (limestone and dolomite) in wet tropical or subtropical climates. The weathering processes are related to leaching of silica and formation of higher concentrations of aluminous minerals lying above an aluminosilicate base. As a weathered product of the underlying parent rock, the bauxites deriving from silicate rocks are commonly regarded as “lateritic bauxites”, while those deriving from carbonate rocks are known as “karst bauxites”. Lateritic bauxites account for approximately 90% of the world's exploitable reserves of bauxite (FREYSSINET, P.H., BUTT, C.R.M., MORRIS, R.C., PLANTONE, 2005).

In lateritic bauxites, the aluminous minerals are predominately gibbsite, while boehmite may also occur in lower amounts. In karst bauxites, boehmite and diaspore are the main aluminous minerals (Table 1). In both types of bauxite, kaolinite is the main silicate mineral. Karst bauxites can be found in Eastern Europe and Northern Asia, while all other bauxite occurrences worldwide are regarded as lateritic bauxites (BARDOSSY G., 1990; SMITH, 2009)

Table 1 – Typical mineralogical composition of lateritic and karst bauxites

Oxides	Lateritic	Karst
Al_2O_3	Gibbsite, boehmite	Boehmite, diaspore
SiO_2	Kaolinite, quartz	Kaolinite, quartz, chamosite, ilite
Fe_2O_3	Hematite, goethite	Hematite, goethite, magnetite
TiO_2	Anatase, rutile	Anatase, rutile, ilmenite
CaO	Calcite, apatite, crandallite	Calcite, apatite, crandallite

Source: Adapted from SMITH, 2009

Approximately 85% of world bauxite production is processed into alumina and aluminum in refineries and smelters. It is necessary to consume 5 to 7 tons of Bauxite to produce 2 tons of alumina (aluminum oxide), which is then processed to make 1 ton of aluminum (IAI, 2018). The bauxites used for aluminum production are regarded as

metallurgical bauxites, while those used for the production of refractory materials, chemicals or cement are known as non-metallurgical bauxites. The typical composition of profitable bauxites is 40-60% of Al_2O_3; 10-30% of H_2O combined; 1-15% of SiO_2; 1-30% of Fe_2O_3; 3-4% of TiO_2; 0,05-2% of other elements and oxides (GREENWOOD; EARNSHAW, 1997).

Bauxite has its name after the Les Baux village in southern France, where it was first recognized as containing aluminum by the French geologist Pierre Berthier in 1821. Bauxite has an earthy luster and its color may vary from white to red, brown or yellow. The color is highly influenced by proportions of iron oxides contained in the rock: white bauxites contain 2-4% of iron oxides, while red bauxites contain up to 25%. (GBWG, 2017).

2.2 BAUXITE RESERVES, PRODUCTION AND SEABORNE TRADE

The ore is typically found in tropical and subtropical areas with the largest bauxite reserves found in Guinea, Australia, and Brazil. Figure 1 shows locations where commercially viable deposits of bauxite are found (GBWG, 2017). World total bauxite production was about 300 million tons in 2017 and 2018 (Table 2), with the largest producers being Australia, China, Guinea, Brazil, and India (USGS, 2019).

Figure 1 – Commercially viable bauxite deposits in the world

Source: GBWG, 2017

Table 2 - Bauxite world production and reserves. Figures in dry tons.

	Production (*in million tons*) 2017	2018	Reserves *(in million tons)*
Australia	87.9	75.0	6,000.0
Brazil	38.5	27.0	2,600.0
China	70	70.0	1,000.0
Guinea	46.2	50.0	7,400.0
India	22.9	24.0	660.0
Indonesia	2.9	7.1	1,200.0
Jamaica	8.2	10.0	2,000.0
Malaysia	2.0	2.0	110.0
Russia	5.5	5.5	500.0
Vietnam	2.4	2.5	3,700.0
Other countries	22.5	22.0	5,200.0
World total (rounded)	309.0	300.0	30,000.0

Source: USGS, 2019

Annually, nearly 100 million tons of bauxite are transported by sea. The major shipping countries are Australia, Brazil, and Guinea, accounting for over 80% of the seaborne traded bauxite. It is worth noting that Indonesia supplied up to 50 million tons of seaborne bauxite to China before an export ban was imposed on the ore by the Indonesian government in 2014. This led other suppliers, notably Malaysia, Guinea, and

China to an increase in bauxite production to fulfill the demand of Chinese refineries.

In terms of ship sizes (Figure 2) carrying bauxite in the freight market, Panamax vessels (~80.000 deadweight tonnage) account for nearly 80% of the seaborne bauxite, while Capesize (~170.000 deadweight tonnage) and Handymax (~50.000 deadweight tonnage) account for approximately 10% each (GBWG, 2017).

Figure 2 - Sizes of bulk carriers

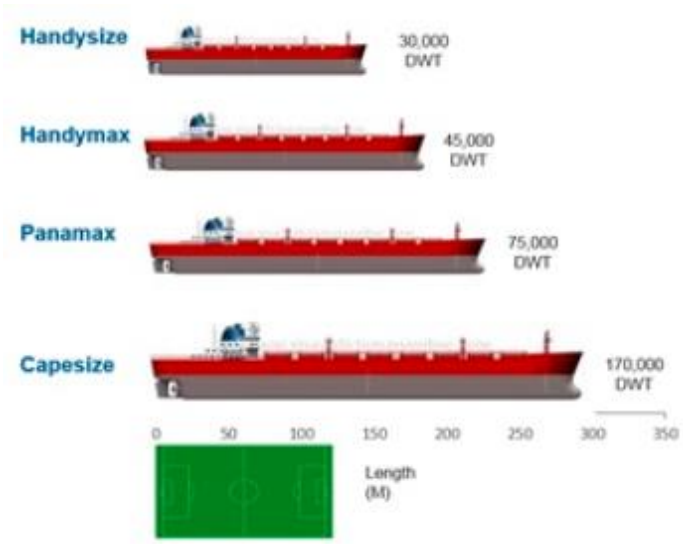

Source: Adapted from GOLD PALM GLOBAL BHD, 2019

2.3 INCIDENTS DUE TO INSTABILITY OF SOLID BULK CARGOES IN MARITIME TRANSPORTATION

If excessively wet, fine solid bulk cargoes may shift in cargo holds under vessel motions, adversely affecting the stability of the vessel, which may ultimately develop a list or even capsize, causing loss of vessel and crew (EVANS et al., 2018).

The cargo shift may take place due to liquefaction, in which ship motions lead to reductions in cargo volume and spaces between particles, resulting in an increase of pore water pressure. This pressure undermines the shear strength of the cargo (IMO, 2018). As a result, the cargo may flow in a viscous fluid manner (MUNRO; MOHAJERANI, 2016b, 2016a; JU et al., 2017; FERREIRA; PEREIRA; LIMA, 2019).

In 1920, Hazen firstly used the term ‘liquefies’ referring to the failure of a dam (HAZEN, 1920). The term ‘liquefaction’ has been used to describe the liquid behavior of

soil after its shear strength is reduced to near zero under cyclic, static or shock loading (SLADEN; D'HOLLANDER; KRAHN, 1985; ESELLER-BAYAT et al., 2013; MUNRO; MOHAJERANI, 2017a). During his research on soil consolidation, Terzaghi applied the principle of effective stress to develop the theory behind the liquefaction of soils. As shown in Equation 1, the effective stress (σ') is considered a function of normal stress (σ) and pore water pressure (u_w) (TERZAGHI, 1925, 1943). If pore water pressure increases, the resulting effective stress may approach zero, resulting in the flow of the wet granular material. The liquefaction theory is often applied to assess the stability of dams and potential collapse of structures built on soils where the liquefaction phenomena may be triggered by an earthquake in locations more susceptible to seismic events.

Equation 1

$$\sigma' = \sigma - u_w$$

If the whole cargo or part of it flows (Figure 3), the center of gravity of the vessel may be displaced (Figure 4), affecting the stability of the ship and increasing the probability of ship developing a list or capsizing (Figure 5) (ZHANG; WU; HU, 2017; CORREIA et al., 2018; DAOUD et al., 2018).

Figure 3 - Unstable fine and wet cargoes of iron ore fines and nickel ore in vessel holds

Source: Adapted from GRANT; UK P&I CLUB, 2008; KAI; NICK; BROOKSBELL, 2009; BUREAU VERITAS; THE LONDON P&I CLUB; TMC MARINE, 2017

Figure 4 - Displacement of the ship's center of gravity due to cargo shift

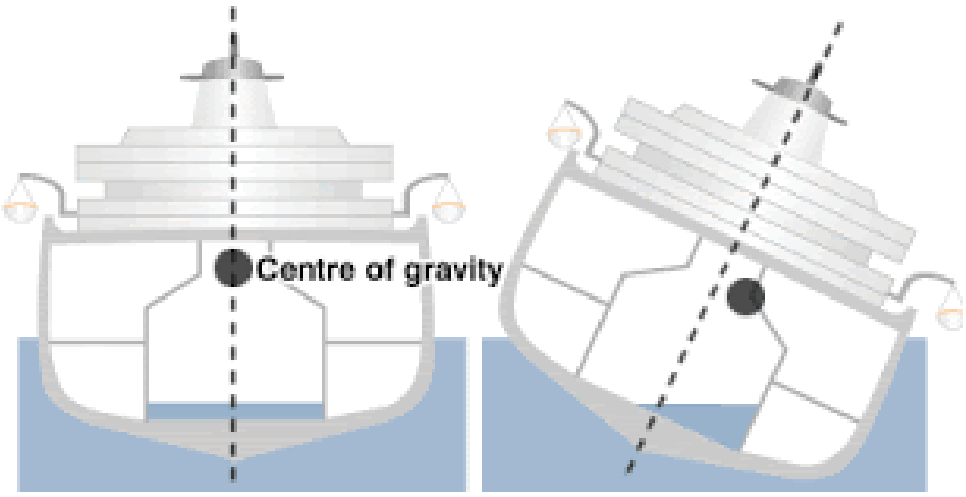

Source: Adapted from NEXT GENERATION, 2013

Figure 5 - Reported vessels listing and capsizing due to instability of bulk cargo

Source: THE HONG KONG MARINE DEPARTMENT, 2005; KAI; NICK; BROOKSBELL, 2009; ZOGRAFAKIS, 2014; LEE, 2017

On the other hand, the pore water pressure increase will be inhibited during compaction if the cargo is sufficiently dry or if the water is allowed to pass through particle spaces. Therefore, liquefaction will not take place if the cargo consists of low moisture content or predominantly of large particles. (JU; VASSALOS; BOULOUGOURIS, 2016; JU et al., 2017, 2018; IMO, 2018).

Previous research on bauxite behavior in maritime transportation has noted that the cargo instability due to moisture may also occur due to a dynamic separation of the cargo in which a progressive separation of water and fine particles from the whole cargo take place under ship motions, resulting in the formation of a free slurry surface that may move freely in the vessel hold, reducing the stability of the vessel (AMSA, 2017; GBWG, 2017; IMO, 2017).

Figure 6 - Moisture related cargoes' instability mechanisms: liquefaction and dynamic separation

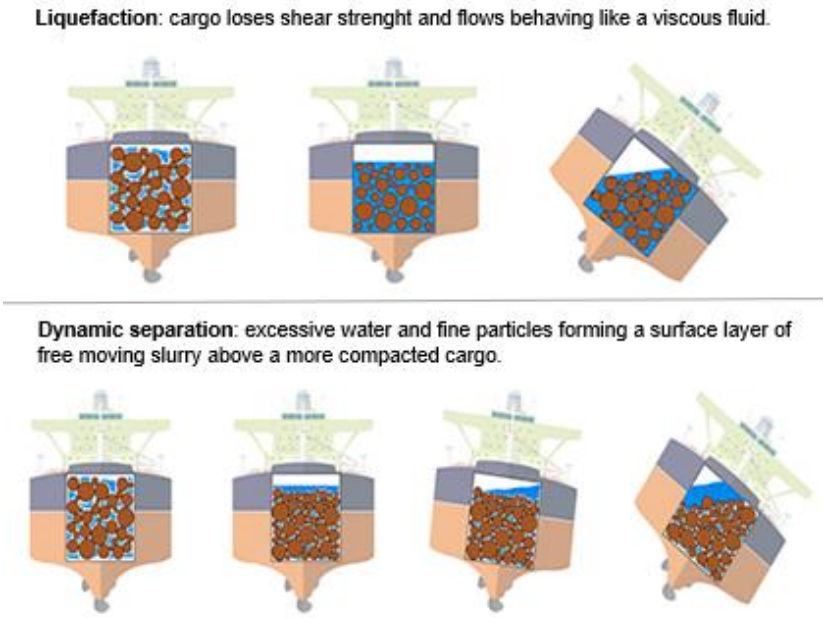

Source: Adapted from AMSA, 2017

During shipping, moisture migration of the cargo may also lead to the formation of a wet base in vessel holds. This wet base may be a source of instability and, whenever possible, the drained water shall be pumped out of the ship through bilge systems (CHEN et al., 2017, 2018; IMO, 2018).

Incidents related to liquefaction have been reported since the loss of the M/S Bengal in 1910 (SANDVIK; REIN, 1992) and the rise in the number of events in the past years led to increased interest in the subject (FERREIRA et al., 2017; JU et al., 2017)**.** Previous studies (MUNRO; MOHAJERANI, 2017a) have shown that some of the episodes reported as cargo liquefaction may be more accurately described as cyclic instability as a form of unstable behavior related to strain softening and caused by a series of dynamic load cycles.

From 2009 to 2018, 101 seafarers and 9 ships were lost due to cargo instability incidents, as outlined in Table 3 (INTERCARGO, 2019). Most of these losses are related to reported cases of liquefaction of unprocessed nickel ore cargo (Figure 7) whose safe carriage must be further researched by the industry (LEE, 2017).

Table 3 - Causes of losses of lives and ships from 2009 to 2018

Reported cause	Losses of human life	Losses of ships	Likely root cause	Losses of ships
Cargo shift / liquefaction	101	9	Cargo failure	9
Collision	0	4	Machinery failure	1
			Unknown	2
			Human element	1
Fire / explosion	16	3	Unknown	2
			Cargo safety	1
Flooding	0	6	Unknown	5
			Machinery failure	1
Grounding	10	19	Machinery failure	4
			Navigation	3
			Unknown	3
			Weather	1
			Human element	8
Structutal	0	1	Collision	1
Unknown	61	6	Unknown	5
			Machinery failure	1
Total	188	48		48

Source: Casualties report, INTERCARGO, 2019

Figure 7 - Vessels lost per cargo from 2009 to 2018

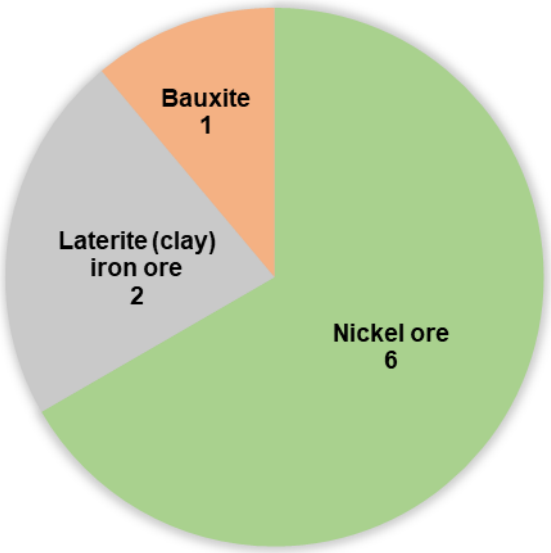

Source: Adapted from Intercargo, 2019

Although shipped for many decades, concern about potential moisture-related

hazards of bauxite cargoes arose in January 2015, when the bulk carrier MV Bulk Jupiter sank off the coast of Vietnam while carrying a crew of 19 men and 46,400 tons of bauxite from Malaysia to China. Only one man survived the vessel capsize and an investigation carried by the vessel flag state pointed to liquefaction and free surface effects as root cause of the incident (BMTA, 2015).

The fine bauxite cargo carried by Bulk Jupiter was loaded over the course of 13 days under heavy rainfall. The bauxite loaded in the port of Kuantan, in Malaysia, was exposed to the rain, increasing its moisture content. Tests conducted as cargo was loaded indicated an average moisture content of 21.3%. The investigation of the incident concluded that cargo instability was likely the root cause of vessel listing and capsizing due to the absence of structural failure of the ship summed to the very wet condition of the cargo, reports from sole survivor and conditions of other bauxite cargoes (Figure 8) shipped on that port right after the Bulk Jupiter (BMTA, 2015).

Figure 8 - Cargo holds of the ship Orchid Island, loaded with bauxite and shipped right after Bulk Jupiter in the same Malaysian port.

Source: Bahamas Maritime Authority, 2015

Following the Bulk Jupiter incident, the Malaysian port of Kuantan – where the bauxite cargo was loaded – announced improvements to prevent the occurrence of a similar episode. By the end of 2016, 100% of Malaysian bauxite was shipped at the Kuantan port, which also loads iron ore and coal. At the time, the bauxite stockpiles area was said to have a capacity of 200,000 tons and duplication of this capacity was in course. Other construction works included roof and drainage system for bulk cargoes storage area. The port facility allows loading and unloading of solid bulk cargoes. Between the Bulk Jupiter

episode and November of 2016, two vessels loaded with bauxite had to be unloaded due to moisture content above the TML (personal communication, November 2016).

Figure 9 - Area where bauxite used to be kept in Kuantan port prior to Bulk Jupiter (top) and area where bauxite has been kept after the event (middle and bottom)

Source: personal file

2.4 REGULATORY FRAME ON CARRIAGE OF SOLID BULK CARGOES

The maritime transportation of goods and people shall comply with international

regulations set by the International Maritime Organization (IMO), which is a United Nations agency responsible for the safety of shipping and prevention of pollution by ships.

For the solid bulk cargoes transportation, the IMO provides a rulebook known as International Maritime Solid Bulk Cargoes Code (IMSBC Code), which contains a general description of solid bulk cargoes, tests to assess cargoes parameters, information on risks related to the cargoes and procedures to be adopted for safe handling of cargoes. The IMSBC Code categorizes the cargos in three groups: Group A – cargoes which may liquefy; Group B – cargoes which possess chemical hazards; Group C – those which are neither liable to liquefy nor to possess chemical hazards (IMO, 2018). The IMSBC Code is annually reviewed and updated by IMO's Sub-Committee on Carriage of Cargoes and Containers (CCC) and by IMO's Maritime Safety Committee (MSC).

Group A cargoes can only be shipped if the cargo's moisture content is below the maximum moisture content for safe shipping of the cargo. This maximum moisture content is known as the transportable moisture limit (TML), which can be determined by test methods listed in the IMSBC Code.

2.5 TRANSPORTABLE MOISTURE LIMIT

To prevent the risk of cargo instability due to moisture, the IMO establishes that Group A cargoes can only be shipped if the moisture content of the cargo is less than its transportable moisture limit (TML). This is a regulatory parameter determined through laboratory test methods prescribed by the IMO, namely the Penetration test, the Flow Table test, the Proctor/Fagerberg test, the Modified Proctor/Fagerberg test for Iron Ore Fines, the Modified Proctor/Fagerberg test for Coal and the Modified Proctor/Fagerberg test for Bauxite, accredited by the IMO since 2017 (IMO, 2017, 2018). The TML represents the maximum moisture content of a Group A cargo for safe carriage and its accurate determination is paramount to assure safety and compliance of shipping operations, as inaccuracies in moisture and TML determinations may pose a risk to seafarers and ships.

Table 4 outlines key aspects of the TML test methods acknowledged by the IMSBC

Code and applied to Group A cargoes in general: Flow table test, Proctor/Fagerberg test, and Penetration test.

Table 4 - Overview of TML tests applied to Group A cargoes in general

IMSBC Code test method	Flow Table (FTT)	Proctor/ Fagerberg (PFT)	Penetration (PTT)
Recommended top size	7 mm	5 mm (or > 5 mm if "extensive investigation for adoption and improvement is undergone")	10 mm for small cylinder, 25 mm for large cylinder
Volume of sample molds	Conical mold volume = 296.6 cm3	Proctor mold volume = 1000 cm3	1,700 cm3 or 4,700 cm3
Energy input (compaction) parameters	Tamper head = 30mm; Tamper pressure = density × max cargo depth × g Table drop height = 12.5 mm Number of cycles = 50 Frequency = 25 Drops / minute (0.62 Hz)	Tamper head = 50mm Drop height = 20cm Hammer mass = 350 g 25 drops per layer / 5 layers	Vertical vibration Frequency: 50 or 60 Hz Acceleration: 2g rms ± 10% Vibration Time: 6 min.
TML	Flow moisture point (FMP) measured from observed deformation of sample. TML = 90% x FMP	TML determined from intersection of the compaction curve with the 70% saturation line.	Flow moisture point (FMP) determined as penetration depth >5 cm TML = 90% x FMP
Procedure	Tests at different moisture contents are conducted until a visual deformation of sample is detected. The mold is filled with 3layers of sample. The first one is tamped 25x, the second one is tamped 25x, and the third one is tamped 20x. The tamping pressure is calculated.	After tamping essays, the relation between moisture and void ratio is identified. 5 to 10 tests at different moisture contents are conducted with the Proctor mold filled with 5 layers of sample, each of them receiving 25 drops of the tamping hammer.	Tests at different moisture contents are conducted until at least one of the bits penetrates 5 cm or more in the sample. The mold is filled with 3 layers of sample and compaction is conducted until a leveled surface of the sample is obtained.
Origin	Originally developed for the cement industry. Adapted in Canada for TML determination and firstly adopted by the IMO in 1965.	Developed in Sweden. Adopted by the IMO in 1992.	Developed in Japan to determine the TML of coal. Adopted by the IMO in 1992.
Test Apparatus		 Source: FERREIRA et al., 2017	

Source: ASTM, 1952, 1971; FAGERBERG, 1965; FAGERBERG; STAVANG, 1971; ROSE, 2014; FERREIRA et al., 2017; IMO, 2018

Concerned about practical implications of TML determination, previous works have discussed the rationale behind the Proctor/Fagerberg test (FERREIRA; PEREIRA; LIMA, 2019) and verified the TMLs of cargoes tested by different accredited test methods,

(MUNRO; MOHAJERANI, 2014; ROSE, 2014; MUNRO; MOHAJERANI, 2016d; FERREIRA et al., 2017; MUNRO; MOHAJERANI, 2017b).

Ferreira et al. determined the TML of 35 samples of iron ore fines through the 3 general test methods accredited by the IMSBC Code. The minimum average difference of TML among different test methods was 0.45% (FTT x PTT) and the maximum average difference was 1.32% (PFT x PTT) – Table 5 (FERREIRA et al., 2017). When analysing a pair of TML results determined through different test methods, the absolute difference was over 2% in some cases.

Table 5 - Absolute difference of TMLs determined through different test methods

	Proctor/Fagerberg (PFT) x Flow Table (FTT)	Proctor/Fagerberg (PFT) x Penetration (PTT)	Flow Table (FTT) x Penetration (PTT)
Absolute average difference	0.93	1.32	0.45
Absolute minimum difference	0.33	0.82	0.13
Absolute maximum difference	1.65	2.14	0.96
Standard deviation	0.36	0.32	0.24

Source: FERREIRA et al., 2017

Munro and Mohajerani discussed the results of TML determined through the 3 general test methods accredited by the IMSBC Code for 13 samples of iron ore fines - Figure 10. This study showed minimum average difference of TML among different test methods of 0.6% (PFT x FTT) and a maximum average difference of 1.9% (PFT x PTT) (MUNRO; MOHAJERANI, 2014). As in the work of Ferreira et al., when analysing a pair of TML results determined through different test methods, Munro and Mohajerani also noted absolute differences above 2%.

Figure 10 - TMLs results of different test methods

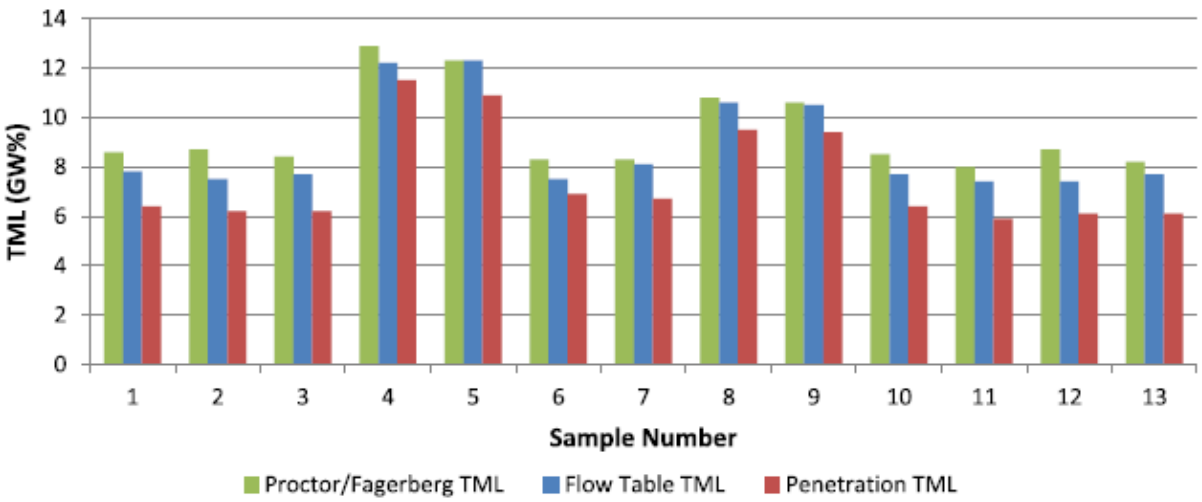

Source: MUNRO; MOHAJERANI, 2014

Until 2015, all bauxite cargoes were shipped as Group C cargoes, although particle size characteristics of bauxites cargoes shipped worldwide often did not match those of Group C bauxite cargo listed on the IMSBC Code up to that time (GBWG, 2017; HASAN; AZIZ; WAN JUSOH, 2017; HASAN et al., 2018). Following the Bulk Jupiter incident in 2015, some bauxite cargoes became classified as Group A cargoes and the TML determination became mandatory when shipping such cargoes (IMO, 2015, 2017). As per IMO regulations, the TML shall be determined through an accredited test method by an accredited laboratory and the moisture content of the cargo to be shipped must be lower than the determined TML. If such conditions are not met, shipping is not allowed.

From 2015 to 2017, the TML of bauxites had to be determined through one of the three general test methods listed on the IMSBC Code. The research carried by the bauxite industry (GBWG) into the behavior of bauxite during maritime transportation developed amendments to the original Proctor/Fagerberg test to make it more suitable to test bauxite. Based on the GBWG work, the IMO has firstly published the Modified Proctor/Fagerberg test procedure for bauxite in September of 2017, encouraging those involved in bauxite shipping to adopt this test method to determine the TML of Group A bauxites (GBWG, 2017; IMO, 2017).

2.5.1 THE PROCTOR/FAGERBERG TEST METHOD

Among the accredited test methods for TML determination, the Proctor/Fagerberg test procedure has been widely used in the mining industry for ores classified as Group A cargoes due to its good repeatability, reproducibility and solid basis in Soil Mechanics (IOFTWG, 2013; ROSE, 2014; GBWG, 2017). Previous improvements on standard Proctor/Fagerberg test procedures and apparatus to make the test more suitable and reliable on the TML determination of specific cargoes have led to the development of the Modified Proctor/Fagerberg test for Iron Ore Fines (IOFTWG, 2013; IMO, 2018), for Coal (ACARP, 2014; IMO, 2018) and for Bauxite (GBWG, 2017; IMO, 2017).

The Proctor/Fagerberg test is based on adaptions of the Proctor test, a laboratory test widely used in soil mechanics to verify the optimum moisture content (OMC) at which soils exhibit the maximum dry density for a given compaction effort. This information is obtained by plotting moisture contents and dry densities obtained through a series of tests with samples at various moisture contents and applying standard compaction energy on the samples filling a 1,000 cm^3 mold (PROCTOR, 1933a, 1933b). Figure 11 shows an example of compaction curve of a standard Proctor test, highlighting the point of maximum dry density and respective moisture content, where the OMC is read.

Figure 11 - Compaction curve of a standard Proctor test

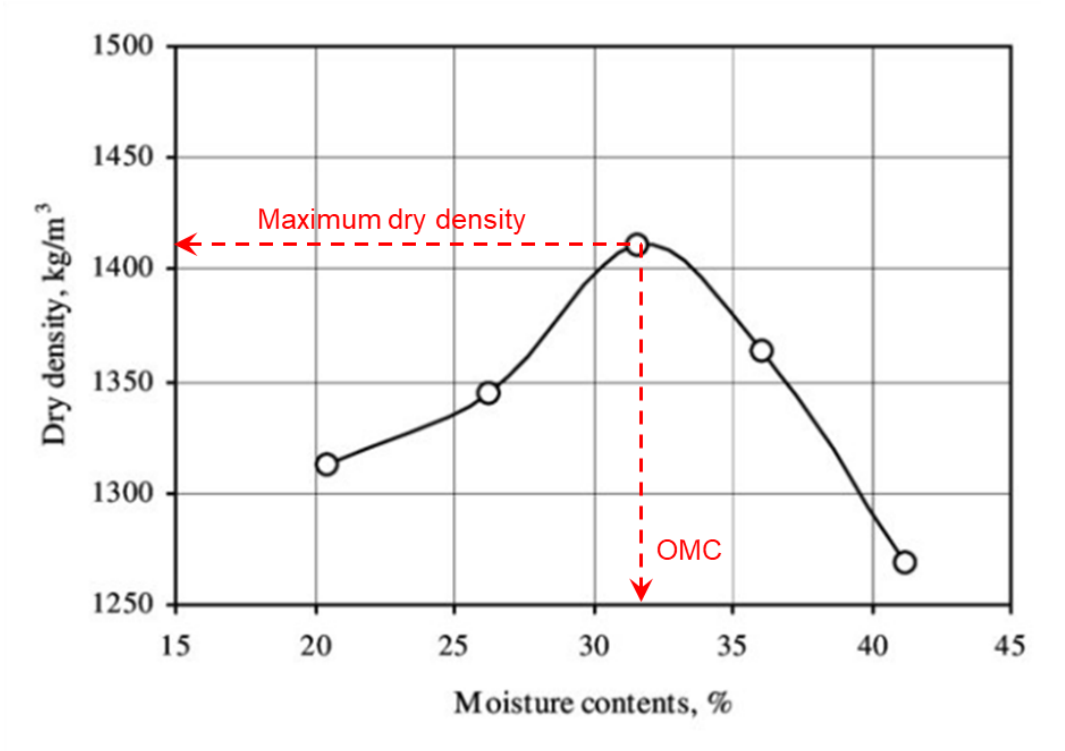

Source: Adapted from AHMAD; KASSIM; TAHA, 2006.

Aiming to develop a simple test method to determine the TML of ore concentrates, Fagerberg analyzed the degrees of saturation at which the OMCs took place for different levels of compaction energy (Figure 12). For a given compaction effort that matched the density of ore concentrate cargoes in vessel holds, Fagerberg considered the TML to be the gross water content (GWC) at 70% of saturation, once this saturation was noted as consistently below the saturation degree of the OMC for the tested Scandinavian ore concentrates (FAGERBERG; STAVANG, 1971). The OMC marks a change of behavior of the tested material: as it goes beyond this point on the way to full saturation, it is more susceptible to develop excessive pore water pressures and expel water. Therefore, making sure that moisture of the cargo to be shipped is always below the OMC provides a prevention of cargo instability due to excessive moisture content, while defining the TML as a point below the OMC makes for the addition of safety margin.

Figure 12 - Saturation lines and compaction curves of ore concentrate at different levels of compaction effort tested on Fagerberg's research on the development of the Proctor/Fagerberg test

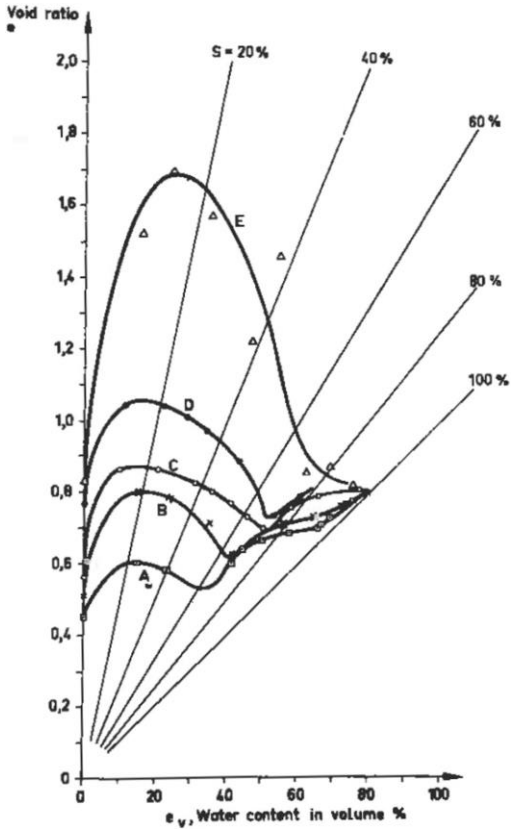

Source: FAGERBERG; STAVANG, 1971

In summary, the Proctor/Fagerberg test procedure consists of compacting samples at varying moisture contents inside a cylinder mold with drops of a hammer through a guided pipe (Figure 13). By determining the density of the solid material[1] in a pycnometer, it is possible to calculate the volumes of voids, solids and water at different moisture contents and determine the parameters required for plotting the compaction curve and calculating the TML, which is the GWC at 70% of degree of saturation, as depicted in Figure 14 (IMO, 2018).

[1] The "density of the solid material" or simply "density of the solid" or "solid density" are the terminologies more typically used in Proctor/Fagerberg tests. These are synonyms of "particle density" or "true density" of the solid material and do not depend on the degree of compaction or moisture content of the material, as is the case in bulk densities. In Proctor/Fagerberg tests, the density of the solid material is typically expressed in g/cm^3. The specific gravity (or relative density) of the material is obtained by dividing the density of the solid material by the density of water at a specified temperature.

Figure 13 - Mold and hammer applied in compaction of samples as per Proctor/Fagerberg test method

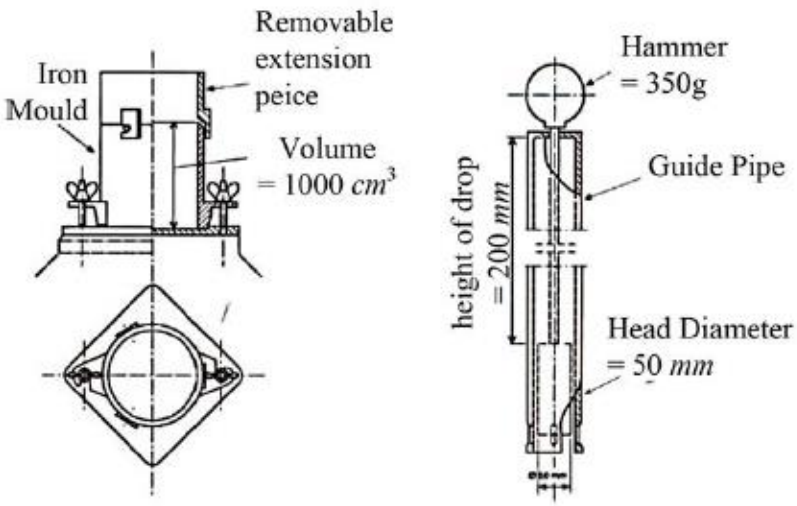

Source: Adapted from IMO, 2018

Figure 14 - Illustration of compaction curve and saturation lines obtained through the Proctor/Fagerberg test

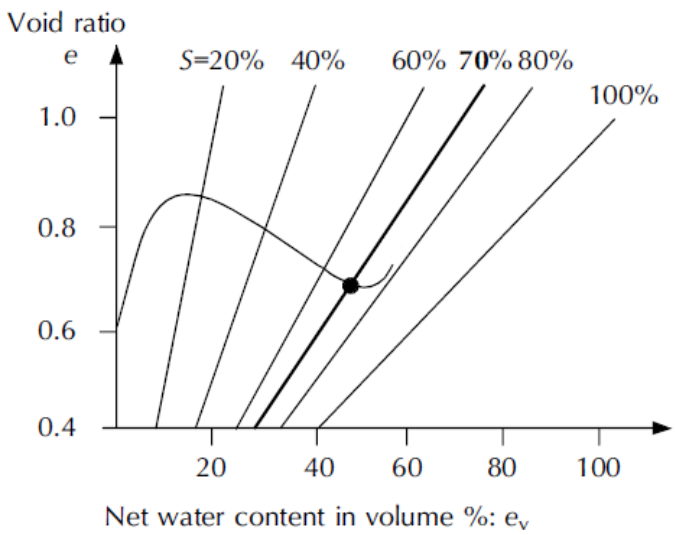

Source: Adapted from IMO, 2018

The Proctor/Fagerberg test compaction curve is plotted after 5 to 10 compaction tests with samples at different moisture contents and the same compaction effort. At moisture contents below the OMC, increasing moisture content of samples leads to higher densities and lower volume of voids of samples compacted with the standard compaction energy. Above the OMC, the samples containing more moisture will exhibit lower density and higher volume of voids. The appearance of samples and the increase in moisture

content followed by decrease in the void ratio is outlined in Figure 15, which shows samples of bauxite out of the mold after compaction tests at different moisture contents and the compaction curve plotted with results of the compaction tests (GBWG, 2017).

Figure 15 - Compacted bauxite samples and compaction curve of a Proctor/Fagerberg test

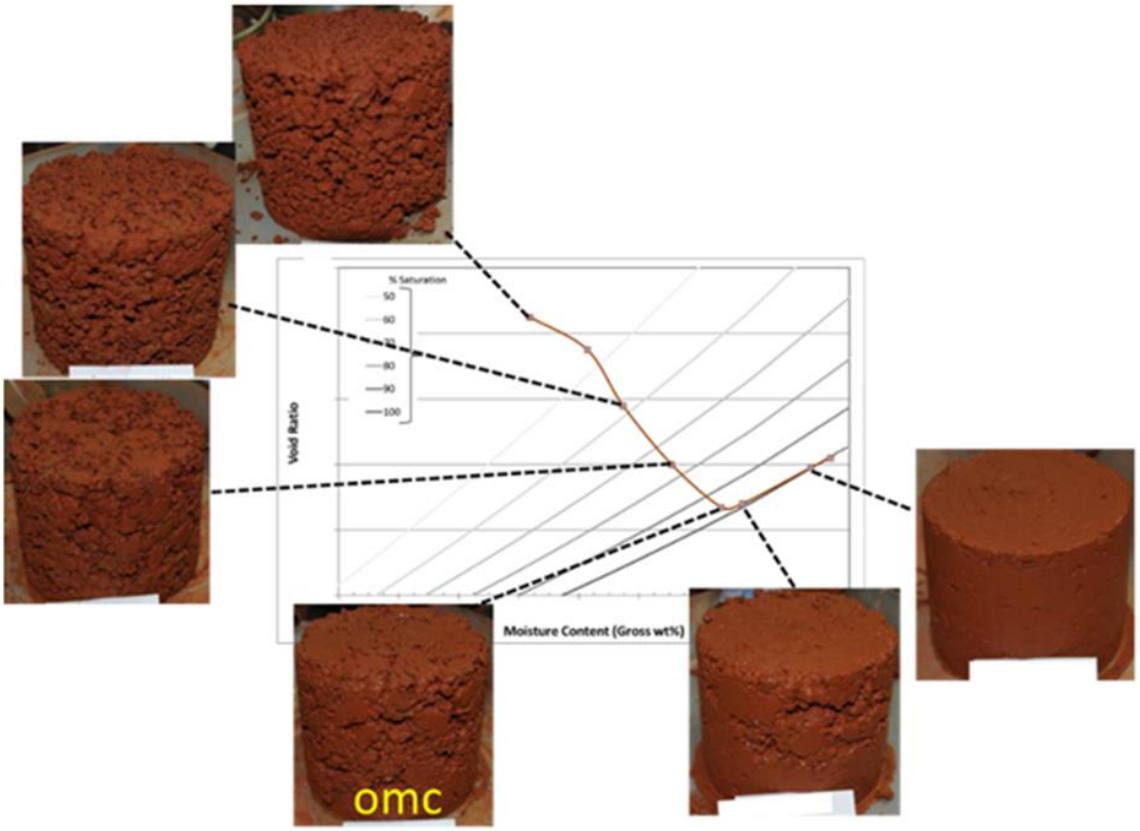

Source: Adapted from GBWG, 2017

The PFT modified versions to test specific cargoes take into account the bulk density of the shipped cargoes. Extensive research carried by iron ore, coal, and bauxite industries has shown that the compaction energy of the original Proctor/Fagerberg test returns densities significantly above the bulk densities of shipped cargoes (IOFTWG, 2013; ACARP, 2014; GBWG, 2017; IMO, 2017, 2018). The original PFT method's "C hammer" – containing 20 cm of height and 350 g of weight – was replaced by the "D hammer" – containing 15 cm of height and 150 g of weight – in the modified versions for iron ore fines and bauxite fines. A common design of C and D hammers is shown in Figure 16. In the Proctor/Fagerberg test modified for coal, an adapted version of D

hammer was developed.

Figure 16 - C and D hammers

Source: MUNRO; MOHAJERANI, 2016d

The D hammer used in the iron ore fines, bauxite fines and coal versions of the modified PFT matches the bulk densities of those shipped cargoes, providing calibration of the original PFT for such cargoes. An overview of the molds, hammers and compaction protocols applied in the original Proctor/Fagerberg test and its modified versions is presented in Table 6 and Figure 17.

Table 6 - PFT equipment and compaction protocol

Test	No. of layers	No. of drops per layer	Drop height (mm)	Hammer foot diameter (mm)	Hammer weight (g)	Mold inner diameter (mm)	Mold height (mm)	Mold volume (cm^3)	Compaction effort (kJ/m^3)
Original PFT	5	25	200.0	50.0	350.0	100.0	127.3	1000.0	85.8
IOF PFT	5	25	150.0	50.0	150.0	100.0	127.3	1000.0	27.6
Coal PFT	5	25	150.0	75.0	337.5	150.0	120.0	2120.6	29.3
Bauxite PFT	5	58	150.0	50.0	150.0	152.0	127.0	2304.5	27.8

Source: Adapted from GBWG, 2017

Figure 17 - Hammers utilized in the different PFT versions

Source: Personal file

The modified PFT for iron ore fines has the TML read at 80% saturation. Since iron ore fines typically exhibit OMC above 90% saturation, reading TML at 80% saturation provides a minimum of 10% of safety margin between the saturation degree of the TML and the saturation degree of the OMC. The Modified PFT for iron ore fines can only be applied when the verified OMC is 90% or higher. If this condition is not met, one of the three general TML test methods shall be applied (IOFTWG, 2013; WILLIAMS et al., 2017; IMO, 2018).

The Modified PFT for coal adopts a larger mold, which is more adequate to test particles with 25 mm top size. As some coals may contain particles larger than 25 mm,

a particle size reconstitution is adopted. After scalping the initial sample at 25 mm, the amount of removed mass of particles larger than 25 mm is replaced by a size fraction of particles larger than 16 mm and smaller than 25 mm from a different sample. This allows testing a sample with a particle size distribution more similar to the original sample, while still testing only the size fraction below 25 mm. This reconstitution scheme is illustrated in Figure 18. The adapted version of D hammer used in the modified PFT for coal has larger diameter and larger weight, while the mold filled with the sample is also larger than that of the original PFT. Adjusting these parameters, the compaction effort produced is similar to that of the original D hammer in the original Proctor mold.

Figure 18 - Overview of the sample reconstitution scheme in the Modified PFT for coal

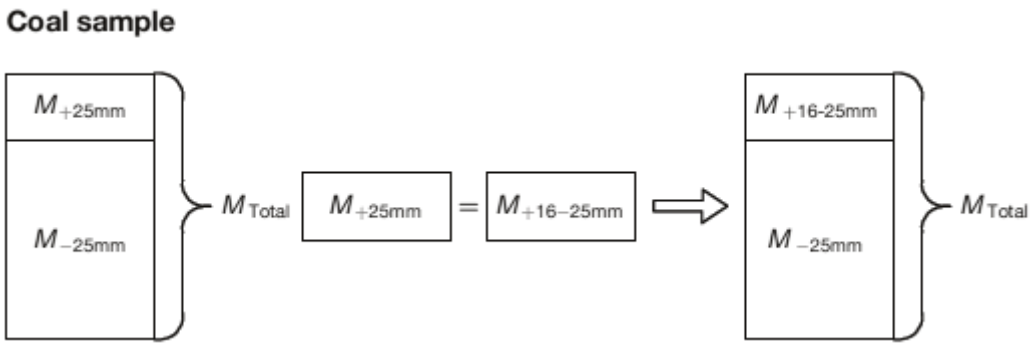

Source: IMO, 2018

The Modified PFT for bauxite fines applies the standard D hammer and a larger mold, which is the standard mold applied on the California Bearing Ratio (CBR) test (ASTM, 1999). The larger diameter and volume of the CBR mold makes it more adequate than the standard Proctor mold to test particles with top size larger than the 5 mm top size reference of the original PFT.

Sample reconstitution is also adopted in the Modified PFT for bauxite. Samples are scalped at 25 mm and to compensate the removal of particles larger than 25 mm, the mass of particles larger than 25 mm removed is replaced by equivalent mass of particles in size fraction -25 mm +6.3mm (Figure 19), to improve the similarity between shipped material and tested samples, while still testing samples with a 25 mm top size. The sample reconstitution procedure is only applied for bauxite fines containing more than 10% of mass with particles larger than 25 mm. If the sample contains less than 10% of the mass of particles larger than 25 mm, no reconstitution is necessary.

Figure 19 - Schematic diagram of sample reconstitution procedure in the Modified PFT for bauxite tines

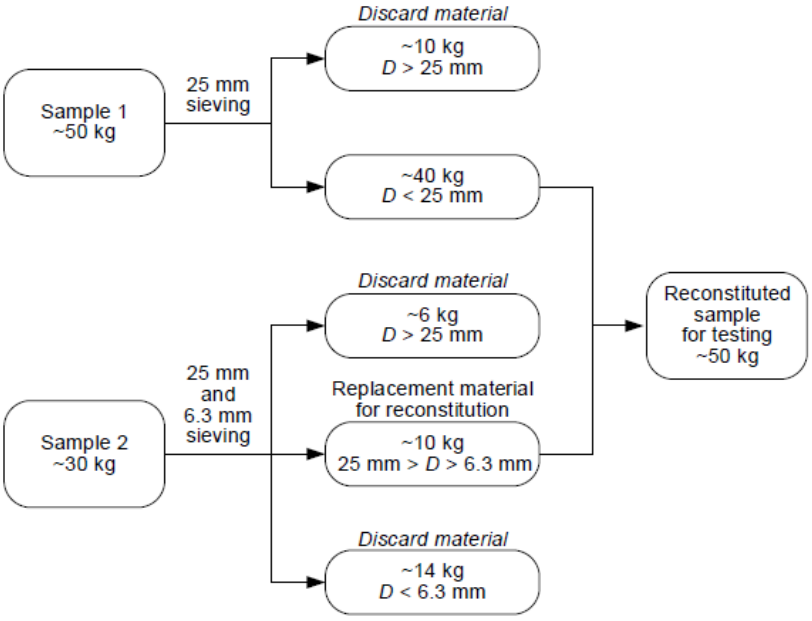

Source: IMO, 2017

Figure 19 exhibits comparison of a theoretical particle size distribution of bauxite as it is shipped (with top size of approximately 76 mm) with particle size distributions of sample scalped at 25 mm (light blue line), of sample scalped at 5 mm (purple line) and of sample scalped at 25 mm with reconstitution of -25 mm +6.3 mm fraction (green line). The reconstituted sample has the most similar particle size distribution to the as shipped material, while the sample scalped at 5 mm is the most different and represents less than 50% of the whole material.

Figure 20 - Theoretical PSD of as shipped bauxite, scalped at different meshes and scalped followed by reconstitution

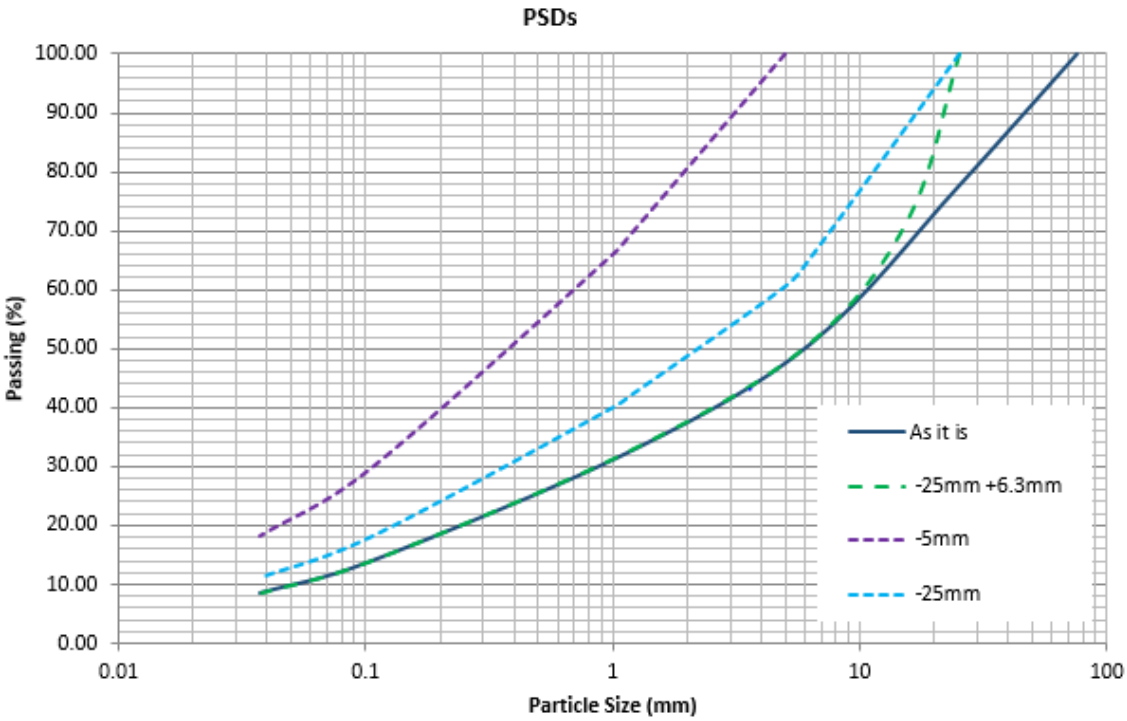

Source: GBWG, 2017

The Modified PFT for bauxite fines allows reading the TML at 70% or 80% saturation, depending on the saturation in which the OMC occurs. If OMC is above 90% saturation, the TML can be read at 80% saturation degree, as in the Modified PFT for Iron Ore Fines. When the OMC is below 90% or when it cannot be clearly defined, a more conservative approach is adopted and TML is read at 70% saturation degree (Figure 20).

Figure 21 - Schematic illustration of the saturation degree at which the TML is determined in the Modified PFT for bauxite fines

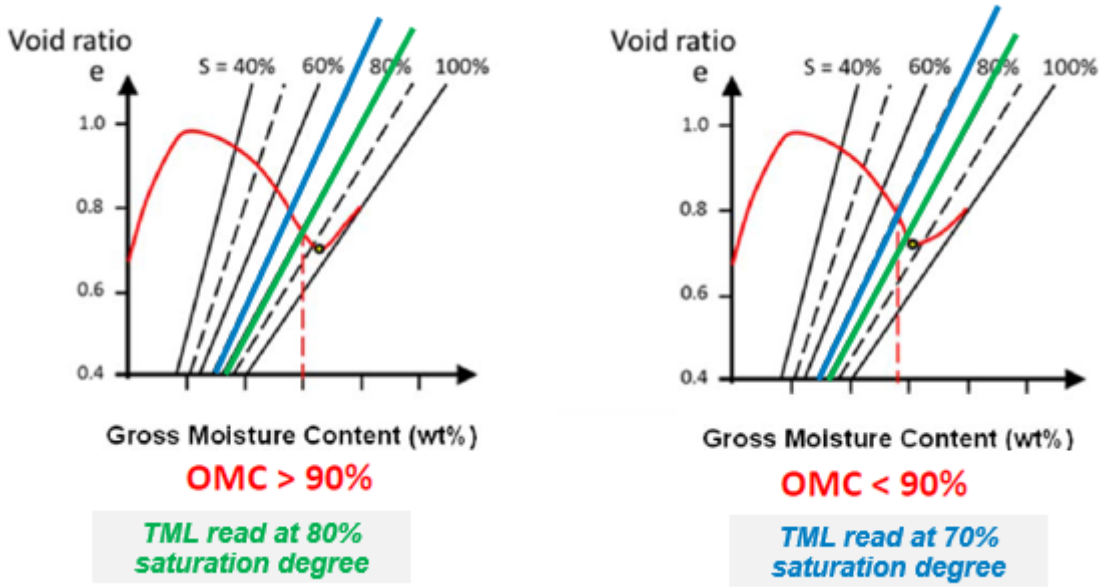

Source: Personal file

2.5.2 PFT CALCULATIONS

A granular material, such as soils or ores in general, is composed of 3 phases: air, water and solid. The illustration and notation presented in Figure 22 support the calculations necessary to plot the compaction curve and determine the TML in all versions of the Proctor/Fagerberg test.

Figure 22 - Schematic illustration of a granular material and its phases to support comprehension and calculations in the PFT

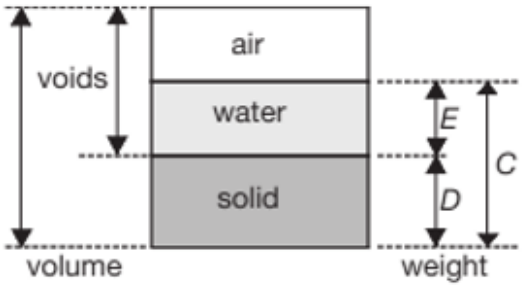

Source: IMO, 2018

After compaction, the sample is weighted and the wet mass of sample (*C*) is verified. The sample is dried and the mass of dry sample (*D*) is verified. Then, the water mass (*E*)

– which is equivalent to the volume of water – is determined:

Equation 2

$$E = C - D$$

The net water content (e_v) in percentage by volume is calculated as:

Equation 3

$$e_v = \frac{E}{D} \times 100 \times d$$

Where *d* is the density of solid material determined in the picnometer.

The void ratio (*e*), which is the volume of voids divided by the volume of solids is calculated as:

Equation 4

$$e = \frac{d}{\gamma} - 1$$

Where *γ* is the dry bulk density, which is calculated as:

Equation 5

$$\gamma = \frac{D}{V}$$

Where *V* is the volume of the mold.

The degree of saturation (S), which is the percentage of the volume of voids filled with water, is calculated as:

Equation 6

$$S = \frac{e_v}{e}$$

Each compaction test carried for samples at a different moisture content corresponds to a point of the compaction curve plotted in a chart with void ratio (*e*) in the y-axis and net water content (e_v) in the x-axis. The chart also contains the curves of saturation degrees and the e_v corresponding to 70% or 80% of saturation (depending on the PFT

version and on the OMC) allows calculation of the TML as:

Equation 7

$$TML = \frac{100e_v}{100d + e_v}$$

2.6 RESPONSE TO INCIDENT INVOLVING BAUXITE CARGO

The IMSBC Code 2018 version (and also the previous versions) contains a bauxite schedule informing characteristics of bauxite cargoes. The document regards bauxite as a Group C cargo – not liable to liquefy nor to possess chemical hazard. Furthermore, the schedule states that bauxite cargoes contain up to 10% moisture content and up to 30% of particles finer than 2.5mm (Figure 23). This description shall be considered outdated as it does not meet the characteristics of most of the bauxite cargoes shipped worldwide (GBWG, 2017; HASAN; AZIZ; WAN JUSOH, 2017; CORREIA et al., 2018; HASAN et al., 2018).

Figure 23 - Characteristics of bauxite cargoes in the IMSBC Code

Individual schedules of solid bulk cargoes

BAUXITE

Description

A brownish-yellow clay-like and earthy mineral. Moisture content: 0% to 10%. Insoluble in water.

Characteristics

Angle of repose	Bulk density (kg/m^3)	Stowage factor (m^3/t)
Not applicable	1190 to 1389	0.72 to 0.84
Size	**Class**	**Group**
70% to 90% lumps: 2.5 mm to 500 mm 10% to 30% powder	Not applicable	C

Source: IMO, 2018

After the MV Bulk Jupiter episode, in September 2015, IMO's CCC has issued a circular entitled "Carriage of bauxites which may liquefy". This regulatory provision established that bauxite cargoes containing characteristics different than those listed in

the Code's schedule (i.e., more than 10% moisture and/or more than 30% in weight passing 2.5mm) should be shipped as Group A cargo, unless assessed by the competent authority as a cargo that does not present Group A properties (IMO, 2015).

Meanwhile, an interdisciplinary Global Bauxite Working Group was initiated by representatives of bauxite producers and shippers to research the behavior of bauxite during shipping. The group aimed to develop globally applicable science-based criterion for distinguishing Group C and Group A bauxite cargoes; and to develop a TML test method for Group A bauxites.

2.7 THE BAUXITE INDUSTRY RESEARCH INTO CARGO BEHAVIOR IN MARITIME TRANSPORTATION

The GBWG gathered a variety of stakeholders and expertise, including shippers (mine owners/operators), transporters (shipowner/operators), users (alumina refinery operators) and consultants with diversified backgrounds, such as geotechnical and hydraulic engineering, maritime science, chemical and process engineering, and port and ship operations. From 2015 to 2017, the GBWG research analyzed bauxite samples (Figure 24) from Australia, Brazil, Indonesia, India, Malaysia, Guinea, Guyana, and Jamaica, representing over 90% of all seaborne traded bauxite at the time. (Global Bauxite Working Group, 2017)

Figure 24 - Some of the tested bauxite samples

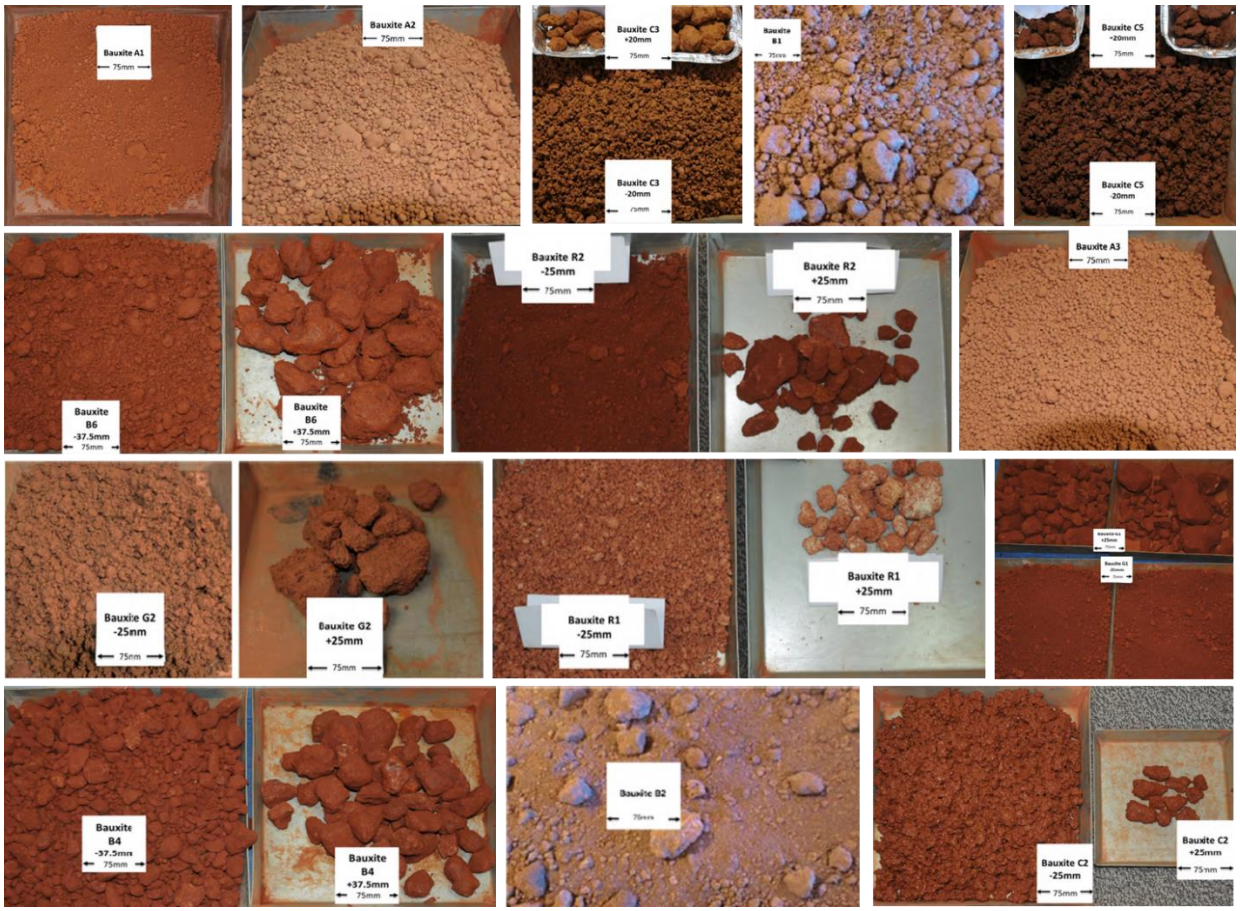

Source: GBWG, 2017

2.7.1 OVERVIEW OF TEST METHODS

Before the bauxite industry research, two other cargoes had research conducted on their behavior during shipping that led to amendments on the IMSBC Code: iron ore fines (IOFTWG, 2013) and coal (ACARP, 2014). The research conducted on these cargoes provided a significant contribution to the understanding of cargo behavior during ocean transportation and the GBWG assessed the test methods applied in these previous studies when developing its test program to verify how bauxite cargoes behave in maritime transportation.

Techniques utilized by the GBWG to investigate possible modes of instabilities of bauxite due to moisture included; vessel monitoring and cargo observations, cyclic

triaxial tests, small scale physical modeling – including hexapod and dynamic centrifuge testing, and numerical modeling. For those cargoes exhibiting instabilities at high moisture contents, TML tests were also conducted. The GBWG test methods took into account experimental and modeling tools applied in recent studies aiming to assess moisture effect in cargoes stability, such as tensiometers measurements (WIJDEVELD; EVANS; PENNEKAMP, 2016), numerical modelling (CHEN et al., 2018; DAOUD et al., 2018) and physical modelling (MUNRO; MOHAJERANI, 2016e; EVANS et al., 2018; MUNRO; MOHAJERANI, 2018).

The particle size distributions of the typical bauxites shipped from different sources including; Australia, Brazil, Guinea, Guyana, Indonesia, India, Jamaica, and Malaysia, were determined through wet screening at Tyler mesh sizes down to 0.037 mm, while finer size ranges were measured using a hydrometer.

Cargo observations were conducted to provide relevant cargo behavior information. The observations included measurements of cargoes in-hold bulk densities using laser scanning and photogrammetry techniques, as well as photo records of cargoes right after vessels were loaded and right before they were discharged. In addition to that, records of bilge water removal added to the understanding of cargo drainage during the sea voyages.

Simulation software for ship motion modeling, SAFETRANS™ was applied to provide statistics on motions and forces a cargo may experience which were used to estimate the stresses induced in the cargo due to the ship motions. Simulations were conducted for different ship sizes (Handymax, Panamax, and Capesize) and different routes (Figure 25), such as Malaysia, Australia, Brazil and Guinea to China. From 300 to over 900 trips were simulated for each route and the results were later taken as reference against geotechnical tests, comparing the induced stresses observed in numerical modeling to the samples' resistance to stress verified in the geotechnical tests.

Figure 25 - Routes investigated: from Malaysia (top left), Australia (top right), Brazil (bottom left) and Guinea (bottom right) to China

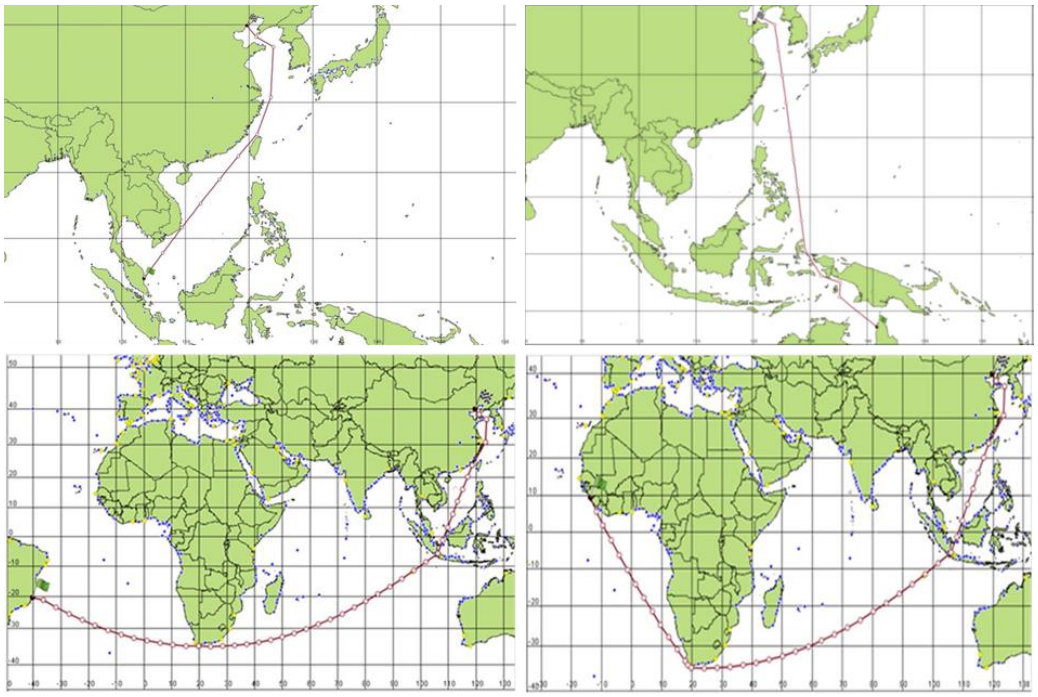

Source: GBWG, 2017

The cargoes' resistance to liquefaction was assessed through Cyclic Triaxial Tests (CTTs) (Figure 26), which allow controlled application of stresses to samples while measuring water pressures within the tested samples. The amount of pore water pressure increase and straining in the sample was measured. CTTs were carried taking into account stresses of extreme vessel motions for saturated samples under undrained conditions, hence a worst-case scenario of drainage and an overall conservative test condition. The cyclic stress ratios and numbers of cycles observed in vessel motions simulations were then applied in the CTTs protocols to determine excess pore water pressure and strain of the sample under these worst-case conditions.

Figure 26 - Cyclic triaxial test apparatus

Source: GBWG, 2017

The different modes of the instability of bauxite samples were assessed through small scale physical modeling in hexapod (Figure 27) and dynamic centrifuge (Figure 28) tests, which allow mimicking vessel motions – by setting amplitude, roll, and frequency of movements – applied in bauxite sample piles containing a wide variation of moisture contents. In the hexapod tests, a container with a small cargo pile is actuated in six degrees of freedom to mimic different sea state conditions. In the dynamic centrifuge test, a sample of a pile is oscillated as in the hexapod and the confining pressures can be correctly scaled. Previous works have applied centrifuge in the simulation of rolling motions (TAYLOR; SKINNER, 1998). In both hexapod and dynamic centrifuge tests, pore water pressure sensors were installed in different points of the container to assess the pore water pressure variations throughout the tests. The hexapod tests were conducted with a rolling frequency from 0.1 Hz to 0.4 Hz and motions up to 25 degrees for samples of 100kg in piles of approximately 0.5m. The dynamic centrifuge tests considered similar amounts of samples and moving parameters but applied a g-force of 50G. This way, vessel rolling frequencies of 0.1 Hz, need to be adjusted to 5.0 Hz due to scaling in the dynamic centrifuge environment.

Figure 27 - Hexapod test apparatus and container for cargo sample

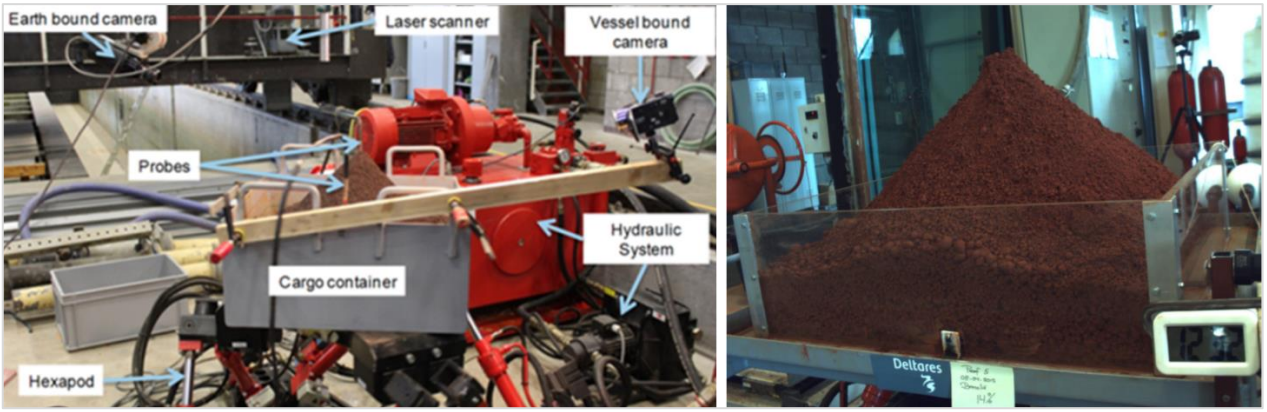

Source: Adapted from GBWG, 2017

Figure 28 – Dynamic centrifuge test apparatus and container for cargo sample

Source: Adapted from GBWG, 2017

For those bauxites that showed some mode of instability in CTTs or physical modeling tests performed, it was necessary to evaluate improvements in TML test procedure to test bauxite more properly and make the test method more reliable. Among the TML test methods prescribed in the IMSBC Code, the Proctor/Fagerberg test may be seen as the preferred one, as it is the least subjective and most precise, while it is also the only test method built upon solid geotechnical fundamentals. Previous improvements in Proctor-Fagerberg test method to make it more suitable to specific cargoes have led to the development of the Modified Proctor/Fagerberg test for iron ore fines and the Modified Proctor/Fagerberg test for coal. Following this line, the GBWG considered improvements in test procedure and test apparatus to develop a Proctor/Fagerberg test more suitable to bauxite. To do so, inputs such as densities of cargoes after voyages, particle size

distributions of shipped bauxites and saturation degrees of Optimum Moisture Content verified after Proctor/Fagerberg compaction assays were taken into account.

To assess the potential reduction in stability of a ship carrying a bauxite that may have undergone a moisture-related instability mechanism in which a free moving slurry is formed, the loss of GM[2] (distance from ship's center of gravity to its metacenter, as illustrated in Figure 29 and 30) due to FSE[3] (free surface effect) was calculated for a typical Handymax (~50.000 deadweight tonnage). This exercise considered a total reduction in GM as FSE occurs in 1 to 5 holds for a ship homogeneously loaded with bauxite in all 5 holds. The FSE considered is due to a 1.5 t/m^3 density surface slurry of 1 m above a flattened bauxite cargo.

Figure 29 - The metacentric height (GM) of a ship

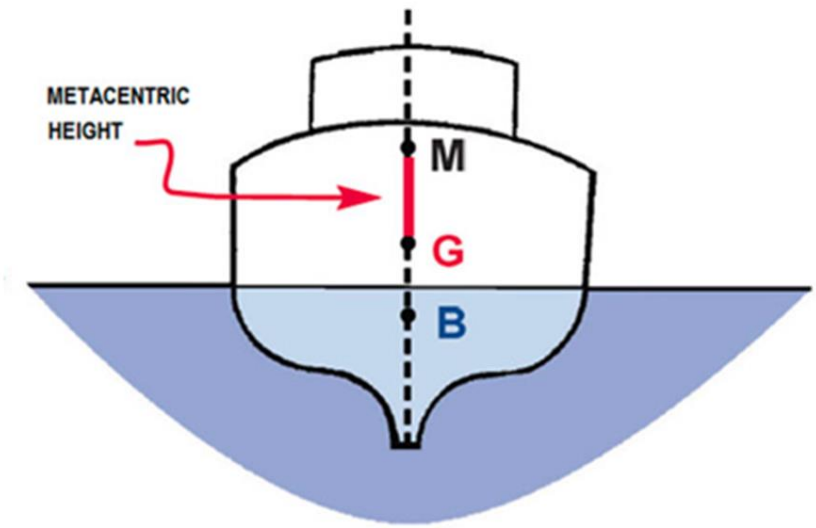

Source: VEFNÁMSKEID, 2019

[2] Metacentric height, which is the height of M in relation to G, where M represents the point of intersection of vertical forces acting on the ship and G represents the center of gravity of the ship (WARTSILA, 2019a).
[3] Free Surface Effect, which is the reduction of stability of the ship caused by changes of ship's center of gravity position with the movement of liquid cargoes or solid cargoes with liquid behavior (RNLI, 2014; WARTSILA, 2019b).

Figure 30 - Overview of key parameters related to ship stability theory [4]

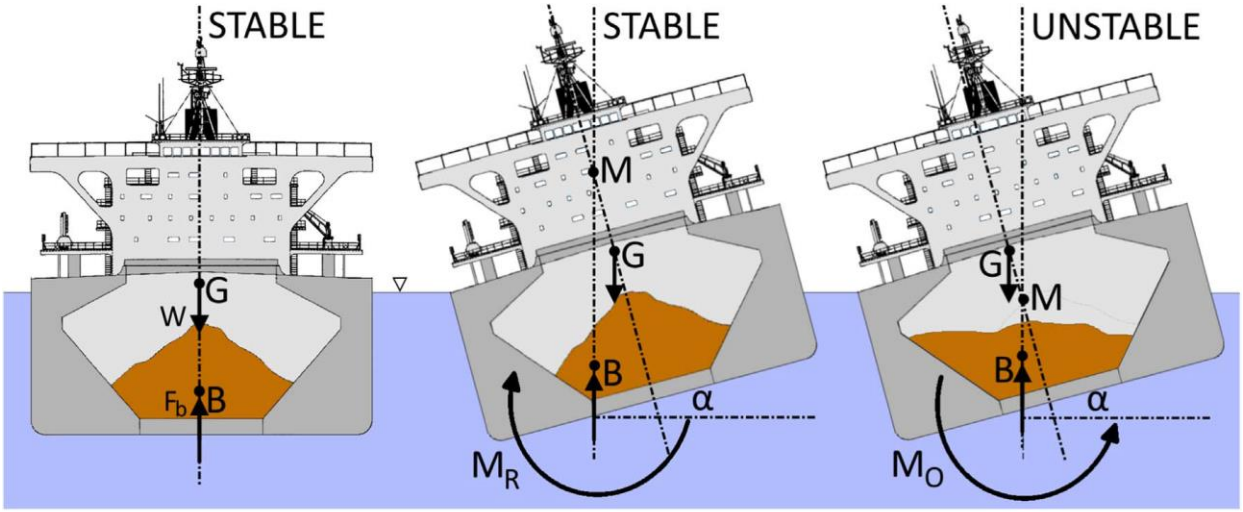

Where: B = Centre of buoyancy of hull; F_b = Buoyancy force; G = Centre of gravity of vessel; M = Metacentre; M_O = Overturning moment; M_R = Restoring moment; W = Vessel weight; α = Angle of heel.

Source: MUNRO; MOHAJERANI, 2017b

To further verify how the free surface slurry of bauxite affects vessel behavior, a Handymax model in the 1:180 scale was constructed. The model was loaded with fixed weights to mimic loaded conditions. Out of the 5 vessel holds, 4 contained a “ramp” with a ball bearing free to move across the ramp, simulating the calculated FSE. Each set of ramp and ball represents a cargo hold that developed a free slurry surface layer with 1 m of height and 1.5 t/m^3 of density (Figure 31).

[4] A stable ship has a positive metacentric height (GM) when the metacenter (M) is found to be above the center of gravity (G). On the other hand, an unstable ship exhibits a negative metacentric height (GM) when the metacenter (M) is found to be below the center of gravity (G) (VEFNÁMSKEID, 2019).

Figure 31 - 1:180 scale model of a Handymax

Source: GBWG, 2017

2.7.2 OVERVIEW OF RESULTS OF THE GBWG

Although generally composed of similar minerals, the tested bauxites exhibited large differences in particle size distributions and top sizes (Figure 32) as these may depend on the geology of the deposit and subsequent processing. The letters on labels below correspond to the bauxite supplier, while the numbers represent different nominal products. The “A” stands for Australia (bauxite exporter), “B” stands for Brazil (bauxite exporter), “C” stands for China (bauxite importer providing samples from Indonesia, India, and Malaysia), “G” stands for Guinea (bauxite exporter) and “R” stands for Refinery (bauxite importer providing samples from Guinea, Guyana, and Jamaica).

Figure 32 - Particle size distributions of the nominal bauxite products tested

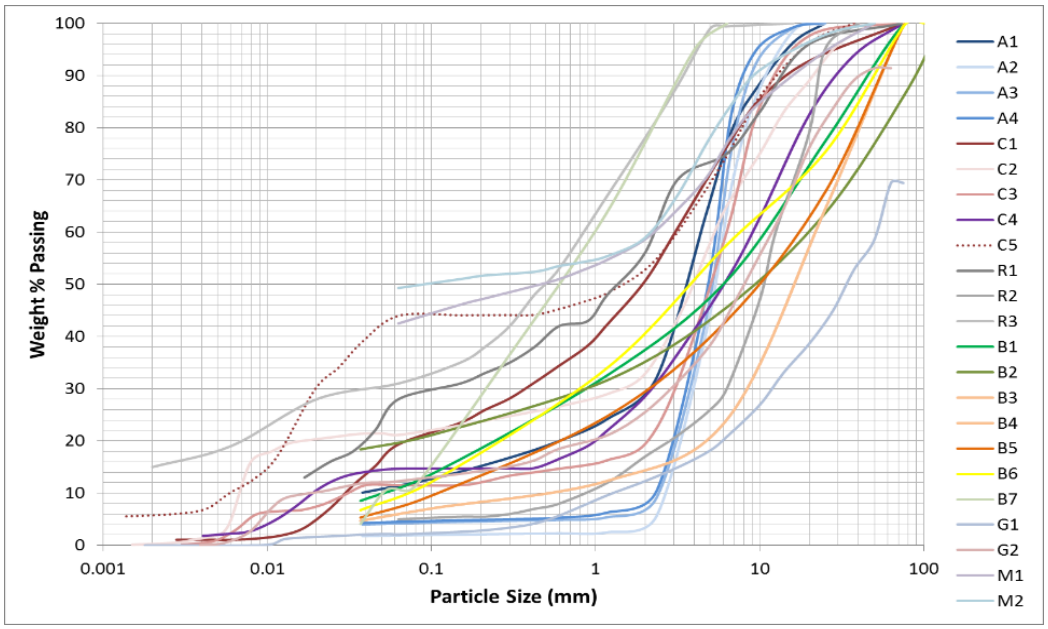

Source: GBWG, 2017

Regarding geotechnical classification of the bauxites tested in terms of particle sizes, the globally shipped bauxites range from silt with much gravel to silty gravel with sand and cobbles, while particle shapes range from spherical to angular (GBWG, 2017). Figure 33 shows the boundaries of particle sizes separating potentially liquefiable sandy soils from fine-grained soils that are not vulnerable to liquefaction, as proposed by Tsuchida (TSUCHIDA, 1970). These boundaries were defined after analyses on a number of soils known to have liquefied or not to have liquefied in past earthquakes.

Figure 33 - Particle size boundaries separating liquefiable and unliquefiable soils

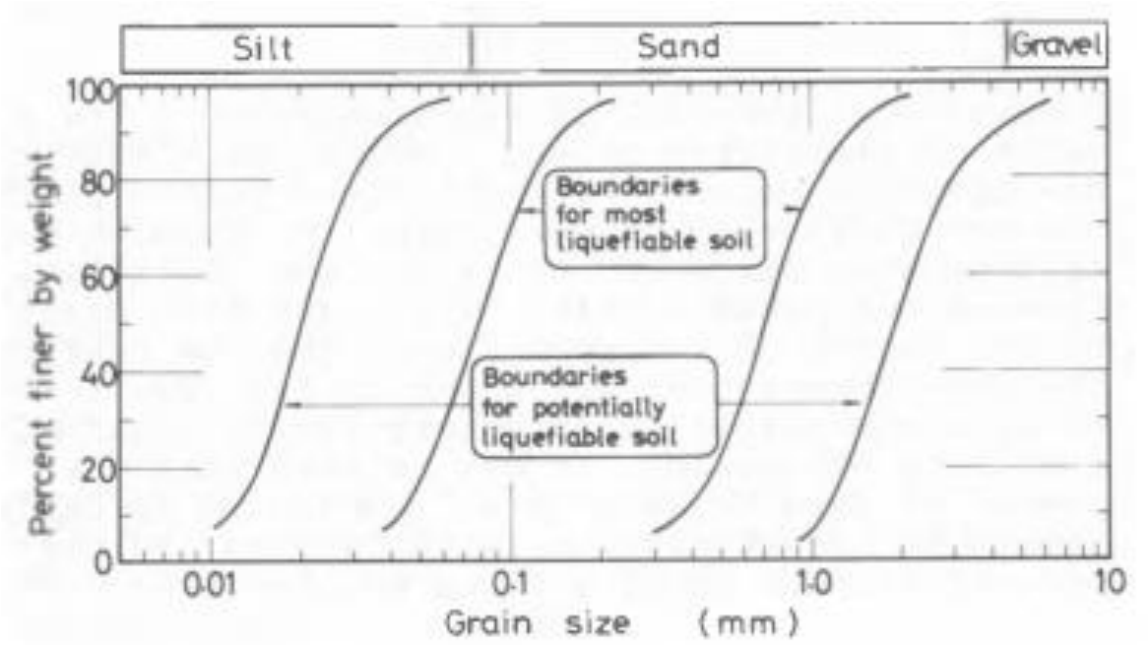

Source: TSUCHIDA, 1970

Limitations to the boundaries of liquefiable soils established by Tsuchida have been discussed by Ishihara, who pointed that characteristics other than particle sizes – such as cohesiveness and plasticity – play an important role in fine soils susceptibility to liquefaction (ISHIHARA, 1985). A comparison of the particle size distributions of shipped bauxites and Tsuchida's boundaries for potentially liquefiable soils is provided in Figure 34. The GBWG noted that bauxites are not susceptible to earthquake-induced liquefaction, as the particle size distribution curves of shipped bauxites cut across the boundaries of liquefiable soils. This comparison supports the theory that bauxites do not liquefy, although the levels of energy provided in shipping are significantly smaller than those of earthquake events (GBWG, 2017).

Figure 34 - PSDs of shipped bauxites and boundaries for potentially liquefiable soil

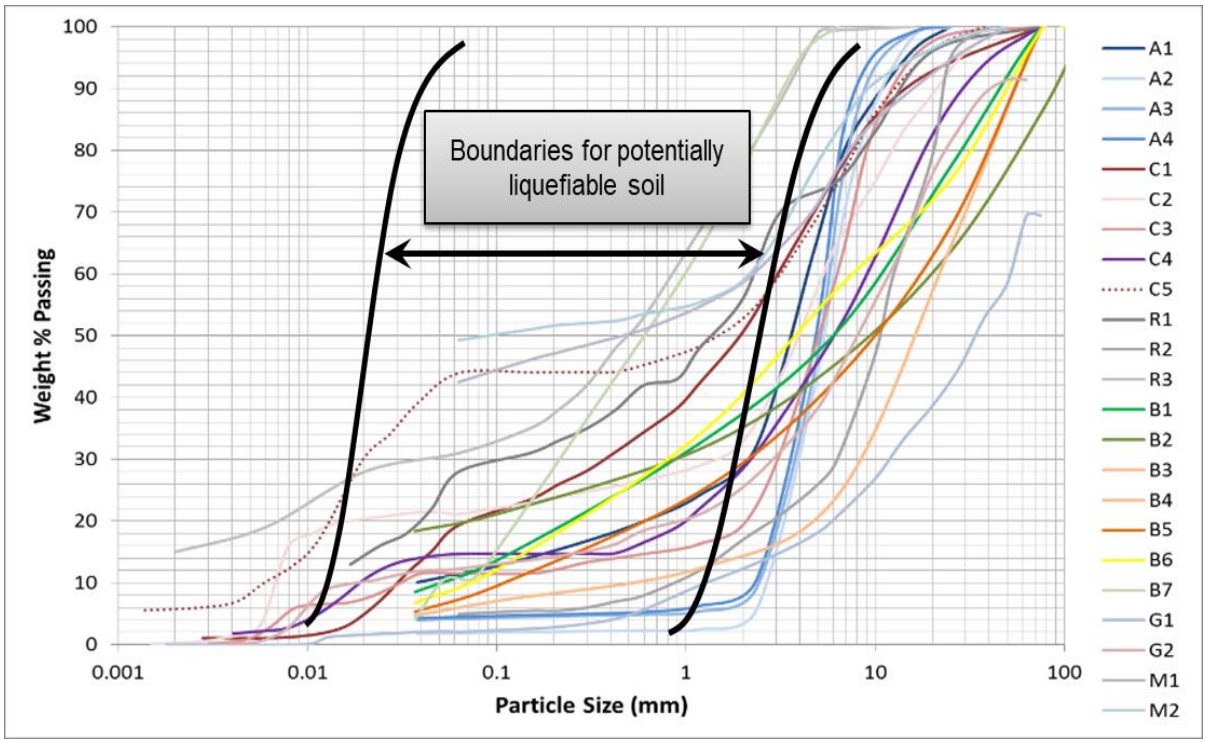

Source: Adapted from TSUCHIDA, 1970; GBWG, 2017

The cargo observations (Figure 35) have shown that the bauxite cargo within the vessel holds did not move significantly during the voyages undertaken, while cargo volume variation due to compaction ranged from 0% to 15%, reaching a 3% average. Laser scanning (Figure 36) and photogrammetry (Figure 37) techniques provided volume figures, which were related to weight figures from draught surveys to allow determinations of cargoes bulk densities, which ranged from 1.4 to 2.0 t/m^3. The records of pumped bilge water have shown that some bauxites exhibited substantial drainage, with up to 0.5% moisture reduction.

Figure 35 - Bauxite cargoes right after loaded at port of origin and right before discharging at port of destiny

Source: GBWG, 2017

Figure 36 - Images of laser scanning of bauxite cargoes within vessel holds

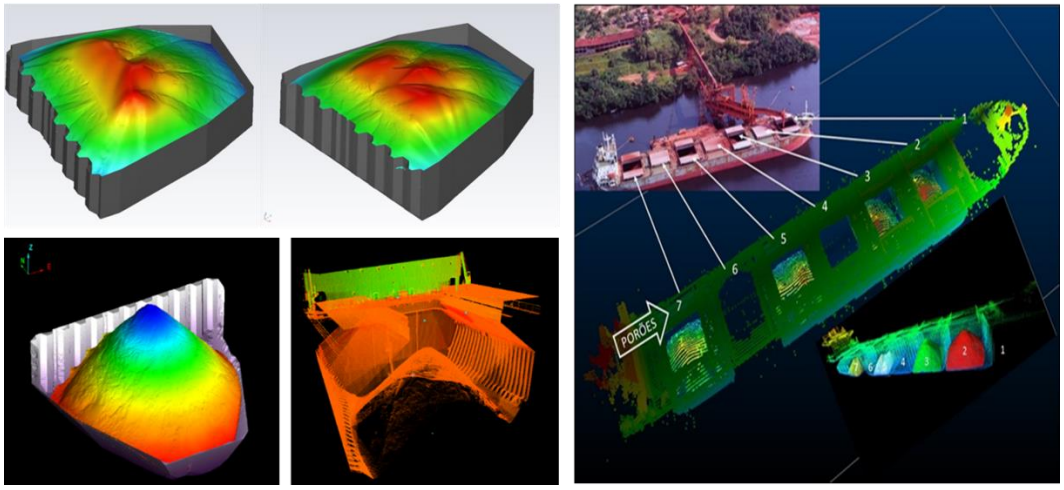

Source: GBWG, 2017

Figure 37 - Photogrammetry of bauxite cargoes within vessel holds

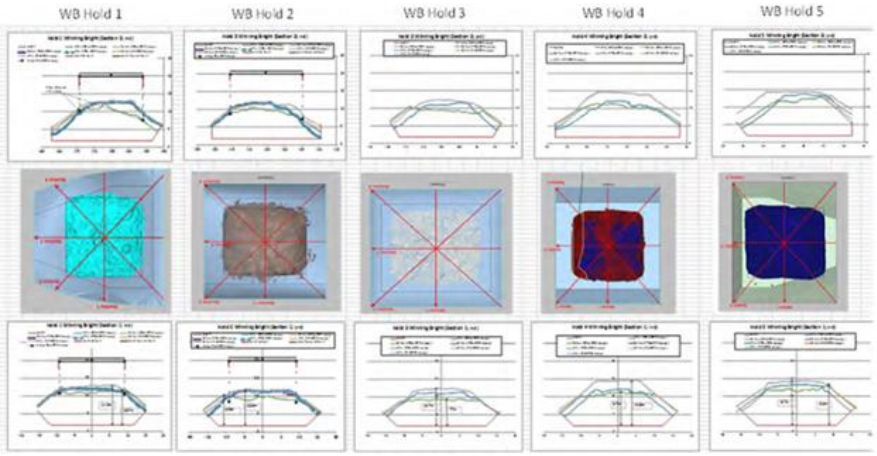

Source: GBWG, 2017

The ship motion modeling simulations showed that the maximum acceleration experienced on the simulated routes were similar and governed by encounters with tropical revolving storms (Figure 38). The accelerations and motions of smaller vessels (Handymax) were greater than those of larger vessels (Panamax and Capesize) and all vessels showed a natural roll period of about 10 seconds (or 0.1 Hz), while accelerations were less than 1G, typically 0.1G.

Figure 38 - Tropical revolving storms map

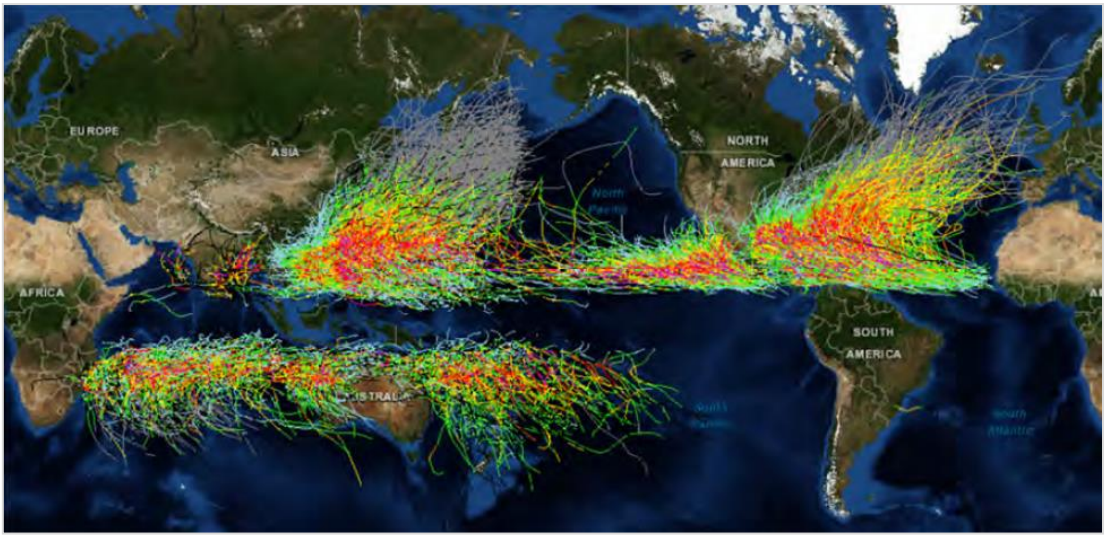

Source: GBWG, 2017

In CTTs, all bauxites tested showed resistance to cyclic stresses above those induced in shipping for all the voyage routes considering Handymax vessels, which are the

smaller vessels and also the ones that induce the largest cyclic stresses in the bauxite cargo. The CTTs results revealed that none of the bauxite samples liquefied in the tests carried with saturated samples under the undrained conditions at forces and induced cyclic stresses higher than those found in shipping.

Although no liquefaction was observed in the CTTs, it was noted that some finer bauxite samples exhibited excessive straining (Figure 39).

Figure 39 - Sample exhibiting no straining after CTT (left) and sample exhibiting significant straining after CTT (right)

Source: GBWG, 2017

The hexapod tests demonstrated moisture migration to the bottom of the sample pile for coarser bauxites tested with moisture content well above the typically shipped moistures (Figure 40). No liquefaction or sliding was observed for coarser bauxites, not even in tests carried with samples completely saturated. At the end of the tests, significant amounts of water were drained from the sample. In a real voyage, the cargo's drained water would be pumped out of the vessel hold through bilges system.

Figure 40 - Coarser bauxite sample after hexapod test

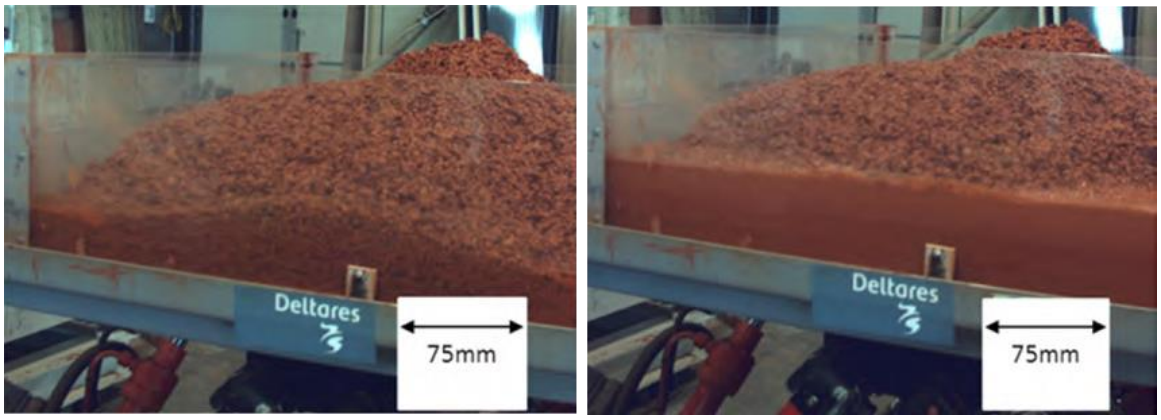

Source: GBWG, 2017.

Finer bauxites tested on hexapod sometimes exhibited slumping behavior in which the top of the cargo would flatten. As this happened, moisture was expelled from the sample to the corners within the sample container, forming a slurry of fine particles and water on the surface (Figure 41). At the end of the tests, many finer bauxite sample piles became flat due to slumping and erosion of the remaining sample pile by slurry. The final condition was often a flattened sample with a layer of slurry observed above a solid and drier cargo. The surface slurry could move from side to side of the container, while the solid cargo in the layer below did not move. If liquefaction had occurred, movement of the thick and solid bottom layer would have taken place which was not the case, as confirmed by the measurements of water pressure sensors.

Figure 41 - Finer bauxite sample after hexapod test

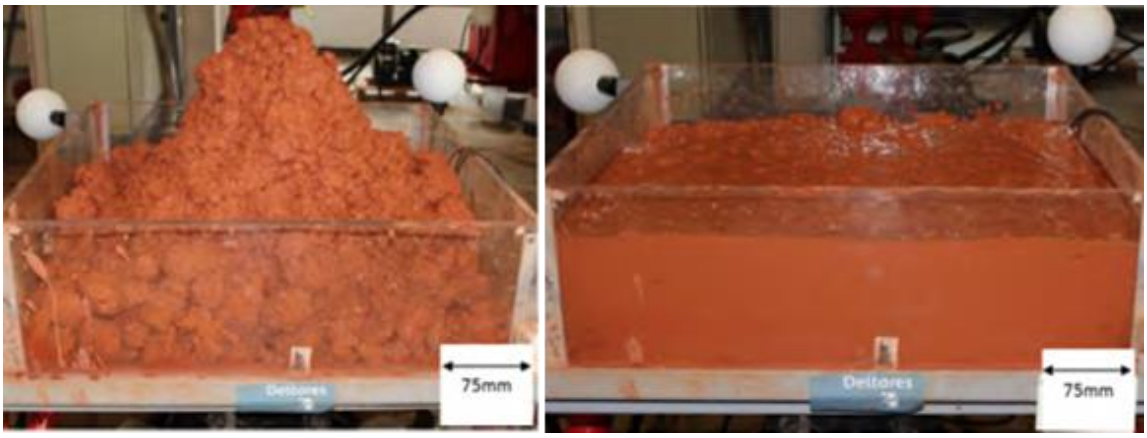

Source: GBWG, 2017.

As in the hexapod tests, the dynamic centrifuge tests conducted with samples containing moisture substantially higher than typically shipped showed drainage of water to the bottom for coarser bauxites, while finer bauxites exhibited the formation of a surface slurry of water and fine particles above a solid and drier layer. Water pressure sensors did not read any peak pressure that could indicate liquefaction and the only form of instability observed was the movement of the surface slurry for the finer bauxites tested.

After tests were carried, the samples inside the container were excavated and four layers were analyzed separately to assess the amounts of moisture along the cargo profile. After excavating part of the sample, it was noted that coarser bauxites held water between the structure of the particles, as shown in Figure 42. On the other hand, finer bauxites concentrated larger amounts of moisture and finer particles in the slurry surface (Figure 43), the result of dynamic separation of the initial cargo pile due to the cyclic motions.

Figure 42 - Side view and top view of coarse bauxite exhibiting water held between particles after the test

Source: GBWG, 2017

Figure 43 - Top views of fine bauxite exhibiting slurry surface and drier solid layer underneath after the test

Source: GBWG, 2017

Moisture determination of the different layers of fine and coarse bauxites tested confirmed the visual observation of higher amounts of water at the top for finer bauxites and higher amounts of water at the bottom for coarser bauxites (Figure 44).

Figure 44 - Moisture along the cargo sample profile for coarse and fine bauxites

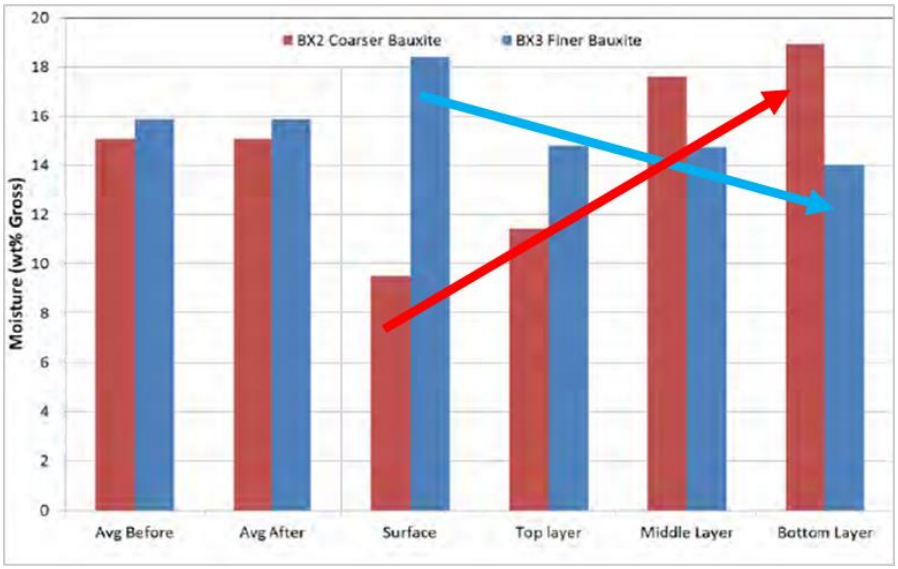

Source: GBWG, 2017

For the finer bauxites, the observation of slurry formation above a solid and drier layer

of cargo in the physical modeling tests conducted meet observations of conditions of cargoes after real voyages, according to reports from personnel involved in shipping and discharge operations. As below (Figure 45), vessel holds loaded with fine and wet bauxite cargoes may exhibit the formation of slurry above a drier layer of the cargo in ocean voyages.

Figure 45 - Vessel holds loaded with finer bauxites exhibiting slurry on the surface

Source: GBWG, 2017

Considering straining results from CTTs and the formation of free moving surface slurry in physical modeling tests as forms of instabilities, the GBWG established particle size boundaries to distinguish among fine bauxites that could become unstable when excessively wet and coarser bauxites that drained and did not exhibit such issues. Different combinations of particle size references were considered as a platform to separate “finer” bauxites from “coarser” bauxites. The 2.5 mm and 1 mm meshes were chosen as a basis due to the high correlation among them (Figure 46) and similar gradients in particle size distribution curves across the tested bauxites. It shall be highlighted that the tests were carried out taking into account all particle sizes within the tested samples, while 1 mm and 2.5 mm are only reference to allow the grouping bauxites according to different behaviors in order to reach a particle size criterion to distinguish finer bauxites that may exhibit some form of instability from coarser bauxites that do not.

Figure 46 - Correlation among percentage of particles passing 2.5 mm and 1 mm for the bauxites tested

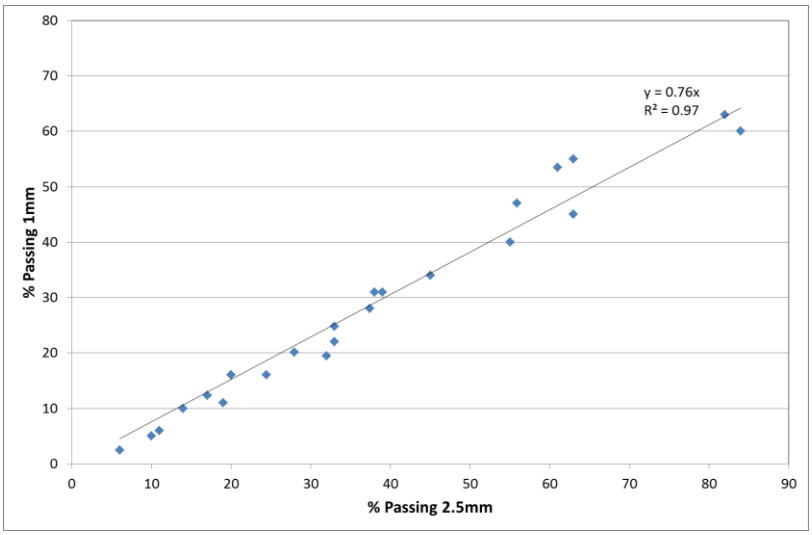

Source: GBWG, 2017

The results from CTT and physical modeling tests were compiled on a chart with 2.5 mm and 1 mm axis. The instability results (red triangles in Figure 47) are concentrated in a region of the chart that allows the determination of boundaries of percentage of particles passing 2.5 mm and 1 mm to classify finer cargoes as Group A and coarser cargoes as Group C. The first instability results were observed at approximately 37.5% passing 1 mm and 47.5% passing 2.5 mm. To assure substantial safety, the criterion proposed to classify cargoes as Group A was: more than 40% passing 2.5 mm and more than 30% passing 1 mm. The tested bauxites covered by the Group A criterion are those inside the green square on the chart.

Figure 47 - Overview of behaviors of tested bauxites shown in a "particles passing 2.5 mm and 1 mm" basis

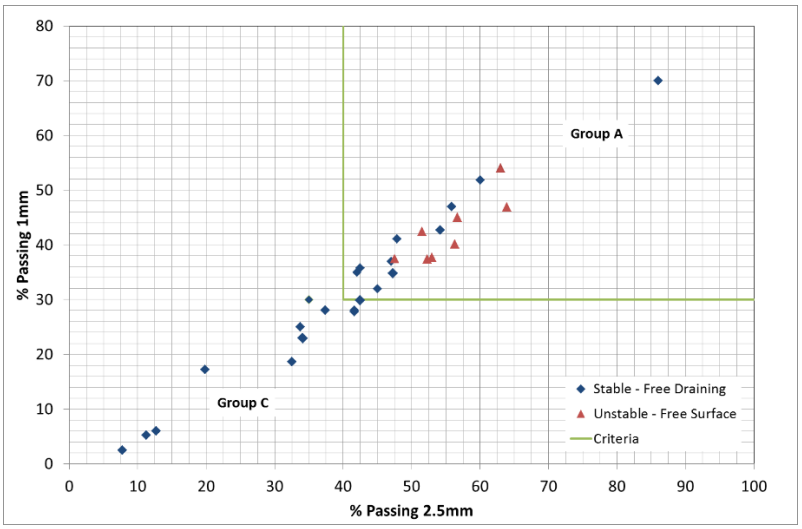

Source: GBWG, 2017

Based on the -2.5 mm and -1 mm size fractions, bauxite can be characterized as either coarse and Group C, or fine and Group A cargoes. Finer bauxites that are classified as Group A require TML determination to ensure that they are shipped at moisture contents below their TML. The standard Proctor/Fagerberg test method outlined in the IMSBC Code was modified by the GBWG to make it applicable to the range of bauxites shipped (GBWG, 2017). Modifications included a larger sample container to allow testing of larger particles, sample reconstitution where particles were still too large for the test, and the application of compaction energies in the test that are compatible with those observed in real cargoes after voyages for a given moisture range.

The calculated losses of GM of the ship due to a flattened bauxite cargo with a free moving slurry layer of 1 m height and 1.5 t/m^3 density showed no list of the vessel when 1, 2 or 3 vessel holds exhibit FSE. When more than 3 vessel holds are affected by free surface, negative initial stability is verified and the vessel develops a list, increasing the risk of instability towards capsizing and sinking of the vessel.

Table 1 - Loss of GM and vessel behavior due to FSE alone

No. of Holds with FSE	Loss of GM (m)	GM (m)	Vessel Behavior
None	0	6.86	Stable and stiff
1	2	4.78	Stable and soft
2	4	2.7	Stable and softer
3	6	0.63	Stable - "wobbling"
4	8	-1.45	List develops
5	10	-3.53	List progresses

Source: GBWG, 2017

The Handymax model with 2 and 3 ball bearings moving to simulate the FSE in 2 and 3 holds showed out of phase motions between the different holds, causing an irregular (“wobbling”) motion of the vessel (Figure 48). This atypical motion may be a confirmation sign noticed by the crew that the cargo is unstable due to excessive moisture. When 4 holds exhibit FSE, a significant list may take place (Figure 49).

Figure 48 - Handymax model behavior due to FSE with 2 and 3 holds exhibiting free slurry surface

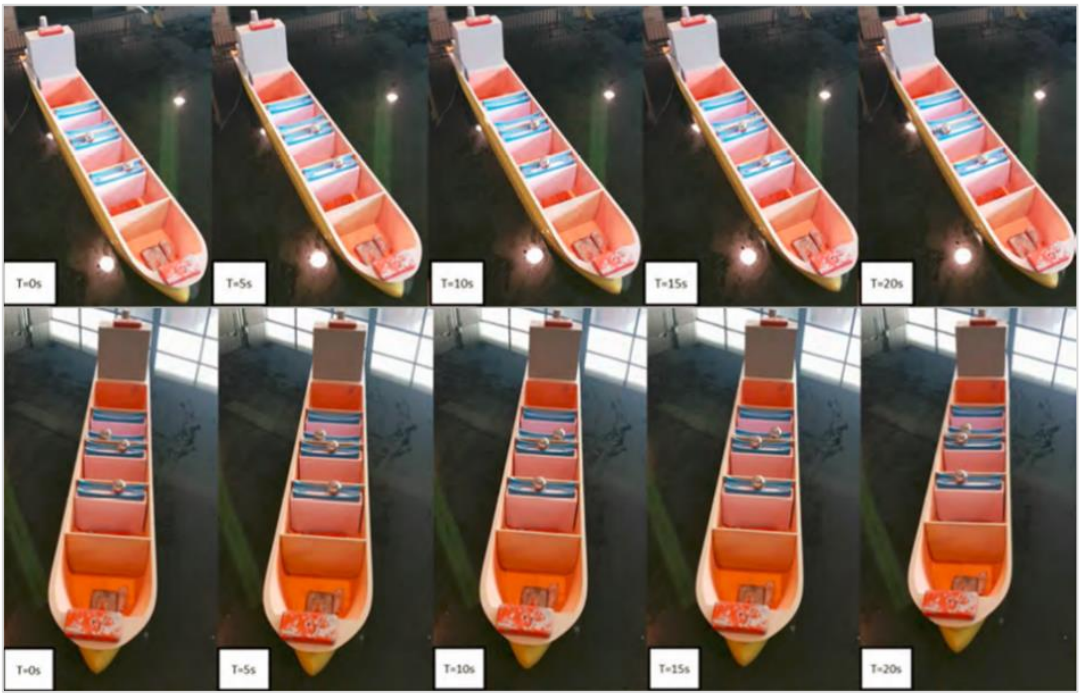

Source: GBWG, 2017

Figure 49 - Significant list developed: real vessels (top) and model vessel (bottom)

Source: GBWG, 2017

2.7.3 OVERVIEW OF CHANGES IN CLASSIFICATION OF BAUXITE CARGOES FOR MARITIME TRANSPORTATION

The research conducted by the GBWG was peer-reviewed by Imperial College London and presented in detail to the IMO in September of 2017 in a workshop held in IMO's headquarters, prior to the annual session of the Sub-Committee on Carriage of Cargoes and Containers (CCC). During CCC, an overview of the GBWG findings and recommendations were delivered to IMO delegates, who assessed the matter to amend policy on bauxite maritime transportation. The GBWGs recommendations related to bauxite classification based on particle size criterion and the TML test for finer bauxites were approved by the IMO. Following CCC, the IMO issued a Circular containing the schedules with characteristics and recommendations on carriage of BAUXITE FINES (Group A) (Figure 50) and BAUXITE (Group C) (

Figure 51) and also the test procedure to determine TML of Group A bauxites – the modified Proctor/Fagerberg test procedure for bauxite (IMO, 2017).

Figure 50 - Excerpt from Group A bauxite schedule in IMO's circular on bauxite carriage

ANNEX 2

DRAFT INDIVIDUAL SCHEDULE FOR BAUXITE OF GROUP A

BAUXITE FINES

The provisions of this schedule shall apply to Bauxite cargoes containing both:

.1 more than 30% of fine particles less than 1 mm (D_{30} < 1 mm); and

.2 more than 40% of particles less than 2.5 mm (D_{40} < 2.5 mm).

Notwithstanding the above provision, Bauxite cargo meeting the above criterion may be carried as a Group C cargo in accordance with the provisions of the individual schedule for BAUXITE where the shipper provides the master with a certificate, in accordance with the result of the test approved by the competent authority of port of loading*, stating that the moisture of the cargo freely drains from the cargo so that the degree of saturation is not liable to reach 70%.

Description

A reddish-brown to brownish-yellow clay-like and earthy mineral. Insoluble in water.

Characteristics

Angle of repose	Bulk density (kg/m^3)	Stowage factor (m^3/t)
Not applicable	1,100 to 2,000	0.50 to 0.91
Size	**Class**	**Group**
More than 30% of fine particles less than 1 mm and more than 40% of particles less than 2.5 mm	Not applicable	A

Source: IMO, 2017

Figure 51 - Excerpt from Group C bauxite schedule in IMO's circular on bauxite carriage

CCC.1/Circ.2/Rev.1
Annex 3, page 1

ANNEX 3

DRAFT INDIVIDUAL SCHEDULE FOR BAUXITE OF GROUP C

Note: The new texts are shown in grey shading and the proposed deletions are shown in ~~struck out with grey shading~~, based on the existing individual schedule for bauxite in the IMSBC Code.

BAUXITE

The provisions of this schedule shall apply to Bauxite cargoes

.1 containing either:

.1 30% or less of fine particles less than 1 mm ($D_{30} \geq 1$ mm); or

.2 40% or less of fine particles less than 2.5 mm ($D_{40} \geq 2.5$ mm); or

.3 both;

or

.2 where the shipper provides the master with a certificate, in accordance with the result of the test approved by the competent authority of port of loading*, stating that the moisture of the cargo freely drains from the cargo so that the degree of saturation is not liable to reach 70%.

Description

A reddish-brown to brownish~~,~~-yellow clay-like and earthy mineral. ~~Moisture content: 0% to 10%.~~ Insoluble in water.

Characteristics

Angle of repose	Bulk density (kg/m³)	Stowage factor (m³/t)
Not applicable	1,100 ~~1190~~ to 2,000 ~~1389~~	0.5 ~~0.72~~ to 0.91 ~~0.84~~
Size	**Class**	**Group**
~~70% to 90% lumps: 2.5 mm to 500 mm~~ ~~10% to 30% powder~~ Typically up to 500 mm	Not applicable	C

Source: IMO, 2017

As depicted from the latest circular schedules previously reproduced, Group C bauxites are those coarser cargoes containing less than 40% of particles passing 2.5 mm or less than 30% of particles passing 1 mm. These coarser cargoes exhibit enough permeability to drain and prevent moisture-related instabilities. On the other hand, Group A bauxite cargoes are those finer cargoes containing more than 40% of particles passing 2.5 mm and more than 30% of particles passing 1 mm.

To illustrate the application of the bauxite particle size criterion for cargo classification in which Group A cargoes are those containing more than 40% passing 2.5 mm and more than 30% passing 1 mm, examples are provided in Table 7.

Table 7 - Examples of classification of bauxite cargoes according to the established particle size criterion. B.C. stands for "bauxite cargo"

	B.C. 1	B.C. 2	B. C. 3	B. C. 4	B. C. 5	B. C. 6
- 2.5 mm	37	40	39	42	42	52
- 1.0 mm	28	30	32	28	32	39
Group	C	C	C	C	A	A

Source: Personal file

In the IMSB Code, a different particle size criterion to distinguish finer Group A cargoes and coarser Group C cargoes is established for iron ore, manganese ore, and coal. For these cargoes, the finer Group A cargoes are those containing 10% or more particles in weight passing 10 mm and 50% or more particles in weight passing 1 mm (IMO, 2018).

Following IMO's paths of regulation amendments, the Circular containing provisions on bauxite carriage is in effect since 2017, when it was issued, and its content will be published in the IMSBC Code 2020 version.

2.7.4 CONSIDERATIONS REGARDING THE BAUXITE INDUSTRY RESEARCH

I. The bauxite industry response to the 2015 tragic event involving bauxite transportation led to advancements in the understanding of the ore behavior during maritime transportation. For a practical approach, the bauxite cargo classification through particle size criteria and the TML test procedure for bauxite fines allow simple assessment of potential bauxite cargo instability risk during sea voyages. The IMO's regulatory changes based on the GBWG findings have improved the safety of worldwide bauxite shipping operations.

II. As per the latest IMO's regulatory provisions, coarser bauxite cargoes (those containing less than 40% in weight passing 2.5 mm or less than 30% in weight passing 1 mm) shall be shipped as Group C cargoes as they are not prone to moisture-related instabilities. On the other hand, finer bauxite cargoes (those

containing more than 40% in weight passing 2.5 mm and more than 30% in weight passing 1 mm) shall be shipped as Group A cargo, as they may become unstable during shipping if the moisture content exceeds its critical level, the TML. As a Group A bauxite producer and/or shipper, one shall be committed to managing moisture of the cargo in all stages of production chain from mining to shipping, providing accurate TML and moisture content figures to assure safe and compliant shipments.

III. The GBWG research showed that the bauxites tested did not liquefy under worst-case shipping conditions. However fine and excessively wet bauxites may exhibit a different instability mechanism under adverse sea conditions, in which the cargo undergoes dynamic separation where water and fine particles form a free slurry surface at the top of a solid and drier cargo. This better understanding of the mechanisms behind cargo instabilities may lead to advancements in monitoring cargoes and predicting potential instabilities, which would result in increased safety for the shipping community.

IV. The calculations of ship stability following the dynamic separation of the bauxite cargo and the model scale demonstrations indicate that Handymax vessels will develop a list when more than 3 cargo holds exhibit a free surface slurry layer of 1 m height and 1.5 t/m^3 density. Such cargo conditions will only occur if moisture content of bauxite fines cargo is above the determined TML. If this is the case, actions to be taken by captain and crew may be decisive to preserve the ship, the cargo and the lives of those on board, more importantly. Routine inspections of cargo may indicate formation of free surface slurry. If time and circumstances allow, corrections of course and speed along with correcting the list by ballasting may help in securing the stability of the vessel. If actions to preserve stability of the ship are not effective / cannot be taken in due time and severe list takes place, the crew shall be prepared to abandon the ship. This must be done with an awareness of potential limitations in launching lifeboats with the ship’s list and due care to dangers that may arise from ship rolling and sinking, including risks of being hit or suctioned in the water.

V. Due to the tests' results, the GBWG made recommendations on the definition of Group A cargoes as "liable to liquefy". Technically, this may not be the most accurate definition for those fine and substantially wet cargoes that may become unstable, since liquefaction may not be the only mode of instability for certain cargoes. A possible way forward would be classifying Group A cargoes as those that may present hazard due to moisture. This would provide a broader definition for Group A classification and make it analogous to the Group B definition: cargoes which possess chemical hazards. As the case for Group B cargoes, the schedules of Group A cargoes provide details on the risk associated with the hazard and provisions to assure safe shipping of the cargo.

3. ALCOA CORPORATION AND JURUTI MINE

Founded 130 years ago, Alcoa is a global industry leader in bauxite, alumina, and aluminum products. In 2018, the corporation accounted for 14,000 employees worldwide. With ownership of seven active bauxite mines globally (Figure 52) Alcoa is among the world's largest bauxite producers (ALCOA, 2019).

Figure 52 - Alcoa's mines: 4 wholly-owned by Alcoa and 3 joint ventures

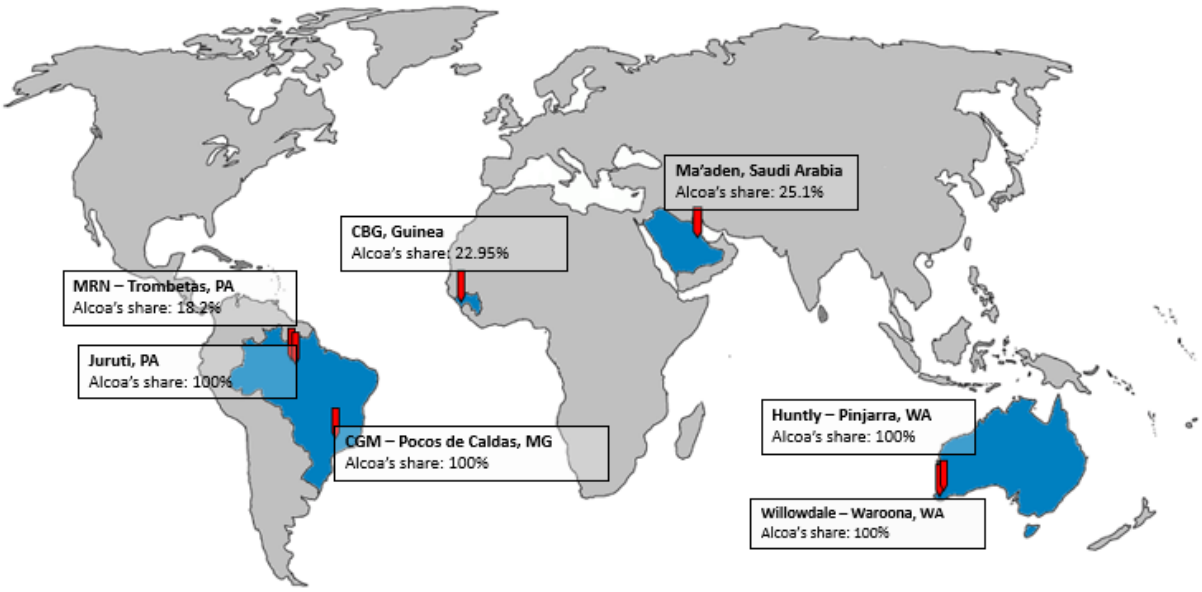

Source: personal file

The wholly-owned and operated mines in Western Australia (WA), Huntly and Willowdale, and Juruti in Brazil mined a combined annual record of 39.3 million dry metric tons of bauxite in 2018. The total shipped volume, including to Alcoa's own refinery system, was 46.9 million dry metric tons. Out of this total, 5.7 million dry metric tons of bauxite were shipped to third-party customers (ALCOA, 2019).

In line with Alcoa's strategy to grow the bauxite business, WA is increasing its sales to third-party customers towards 2.5 dry metric tons of bauxite per year and Juruti mine completed an expansion in 2018, increasing its annual capacity to 7.5 million metric tons. The primary customer base for third-party bauxite is located in Asia, particularly in China (ALCOA, 2019).

Alcoa's Juruti mine is located in Juruti city (Figure 53), Pará state, in the north region

of Brazil, where Alcoa's operations comprise bauxite mines, beneficiation plant, railroad and port (Figure 54). Typically, the Run of Mine (ROM) is beneficiated (washed) to reduce the amount of kaolinite, which is highly concentrated in size fractions below 0.037 mm. Most of the bauxite produced at the mine is washed, while bauxites that naturally contain lower amounts of kaolinite may be shipped without washing.

Figure 53 - Juruti mine location

Source: Google Maps

Figure 54 - Overview of key areas from Alcoa's Juruti complex, which comprises bauxite mines (top left), beneficiation plant (top right), 55km railroad (bottom left) and port (bottom right)

Source: Personal file

Since 2009, bauxite from Juruti mine has been mined and shipped by Alcoa. During this time, Alcoa has produced and shipped over 50 million tons of bauxite in over 900 shipments. Juruti production is secured in the long term by estimations of bauxite reserves summing up to 700 million metric tons of bauxite. In 2018, Juruti mine's production was 6.7 million tons of wet bauxite with average moisture of 13.5%.

4. MATERIALS AND METHODS

4.1 EFFECT OF SELECTED VARIABLES ON TML RESULTS OBTAINED BY PROCTOR/FAGERBERG TEST METHOD

Approximately 600 kg of washed bauxite and 600 kg of unwashed bauxite samples were collected by automated mechanical samplers cutting a flow of bauxite in the process of vessel loading at the port facility near the bauxite mine.

The washed and unwashed samples were scalped at 25.4 mm or 5 mm prior to compaction following the standard Proctor/Fagerberg test as a base and then applying a change in compaction energy using an alternative hammer. The standard Proctor/Fagerberg compaction effort consists of using the “C hammer”, which contains a 350 g mass dropped from a 20 cm height. The alternative compaction was carried with the “D hammer”, which contains a 150 g mass dropped from a 15 cm height (Figure 55 and Table 8.

Figure 55 - Compaction hammers D and C with guide tube (left) and without the guide tube (right)

Source: personal file

Table 8 - Features of hammers C and D

Hammer	Weight (g)	Drop height (cm)	Diameter (cm)	No. of compaction layers	No. of drops per layer	Energy (kJ/m^3)
C	350.0	20.0	5.0	5	25	85.8
D	150.0	15.0	5.0	5	25	27.6

Source: personal file

All tests were conducted in the Proctor mold of approximately 1,000 cm^3 volume with a removable extension piece and 100 mm of diameter, as in the standard Proctor/Fagerberg test method. To verify the effect of samples and test apparatus variations in the determined TML, the test program followed the factorial design of 3 variables and 2 levels described Table 9 and Table 10. The design of experiments and the analysis of results were done in software Excel and Minitab. The tests were carried in duplicate (always by the same team of 2 people) to provide the benefit of checking their repeatability and a total of 16 tests were carried in random order.

Table 9 - Variables tested and respective levels

Variables	Levels	
	-	+
(a) Bauxite type	washed	unwashed
(b) Top size	5 mm	25.4 mm
(c) Compaction hammer	C	D

Table 10 - Design of experiments followed

Variables	Test	Bauxite type	Top size	Hammer
(1)	1	-	-	-
a	2	+	-	-
b	3	-	+	-
ab	4	+	+	-
c	5	-	-	+
ac	6	+	-	+
bc	7	-	+	+
abc	8	+	+	+

All washed and unwashed bauxite samples of approximately 600kg each were firstly scalped at 25.4 mm. Half the amount of each bauxite sample type was separately scalped at 5 mm. For each one of the 16 Proctor/Fagerberg tests, an average of approximately 30 kg of bauxite was taken from long piles containing washed bauxite scalped at 5 mm, washed bauxite scalped at 25.4 mm, unwashed bauxite scalped at 5 mm and unwashed bauxite scalped at 25.4 mm (Figure 56 and Figure 57). Once a sample averaging 30 kg for each test was obtained, it was divided into 12 subsamples by a rotary divider. One of the subsamples was dried in the oven for moisture content determination in accordance with ISO 9033:1989 - Aluminium ores - Determination of the moisture content of bulk material. The dried subsample was ground, and a Jones riffles divider was used to get a portion of the subsample for determination of density of solids through water pycnometer in accordance with BS 1377-2: 1990 - Methods of test

for soils for civil engineering purposes - part 2: Classification tests.

Figure 56 - Sample preparation for Proctor/Fagerberg test starting at 600kg of each source of bauxite taken from port sampling tower

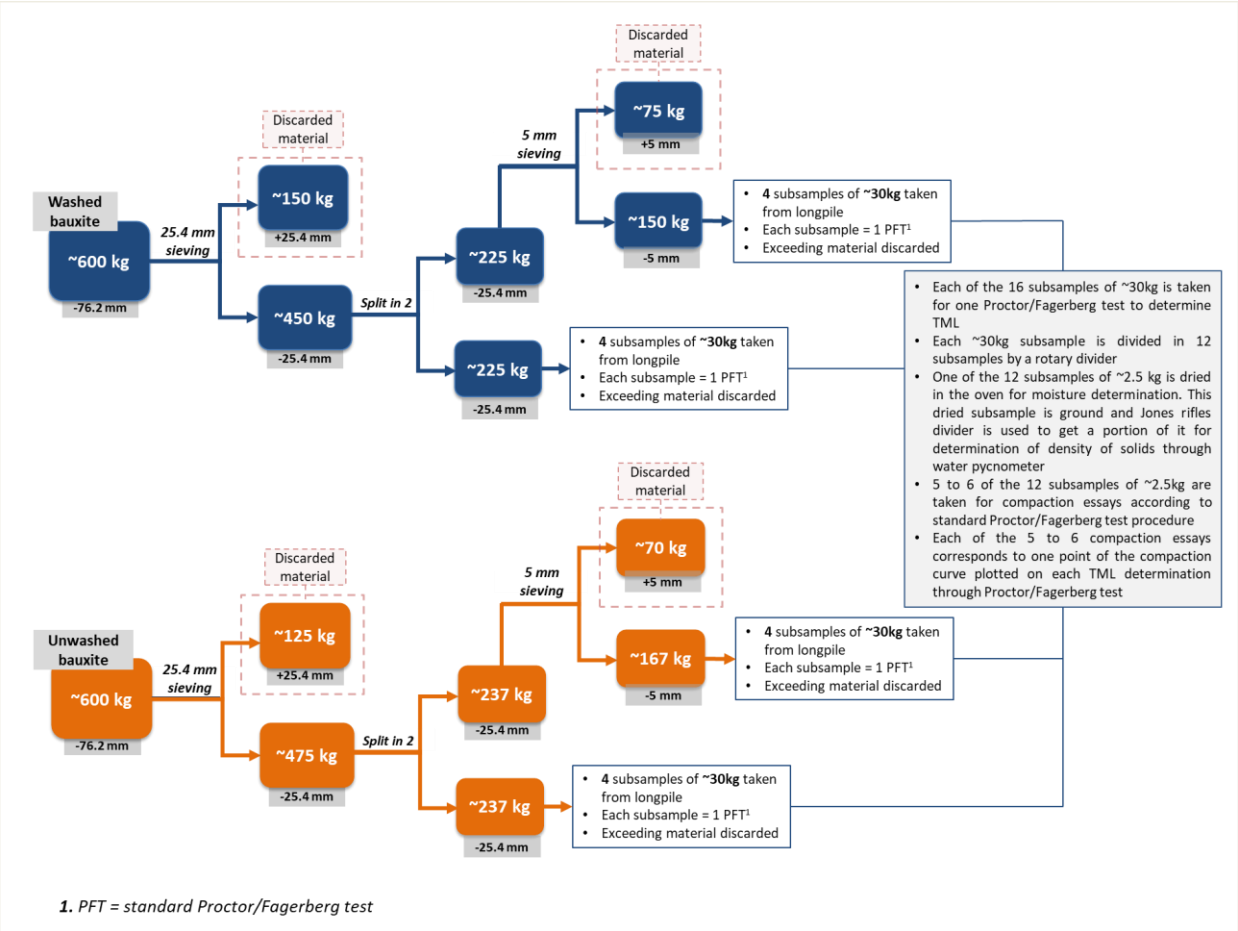

Figure 57 - Unwashed Bauxite as collected (left), scalped at 25.4 mm (middle) and scalped at 5 mm (right)

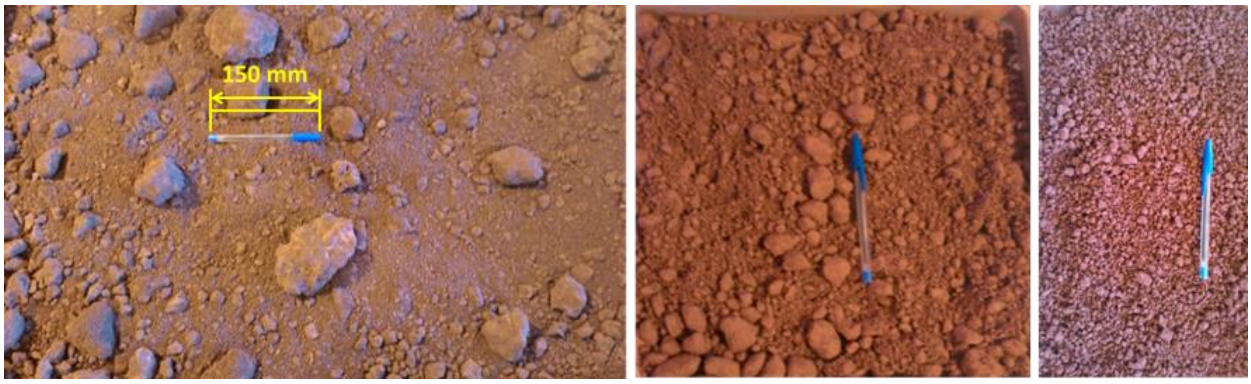

Source: personal file

To build the compaction curve, 5 to 6 subsamples at varying moisture contents were compacted. The adequate amount of water for each compaction essay was sprayed into the subsample, which was gently mixed for 5 minutes. Then, the mixed subsample was spread and divided into 5 portions using a spatula (Figure 58). The first portion was put in the cylindrical mold, leveled and tamped with the proper hammer (C or D) through 25 drops systematically distributed around the surface of the leveled subsample (Figure 59). The other 4 portions of the subsample went through the same process until tamping of the 5 layers was completed. After tamping the last layer, the extension piece of the mold cylinder was removed and the tamped subsample was leveled off along the brim of the mold, which contained a tamped subsample of approximately 1,000 cm^3 volume (Figure 60). The mold containing the tamped subsample was weighted, then the subsample was put in a tray and taken to the oven to dry in order to determine the moisture content of the material.

Figure 58 - Subsample divided in 5 parts to be tamped in 5 layers inside the mold.

Source: Personal file

Figure 59 – Tamping pattern of the 25 blows per layer

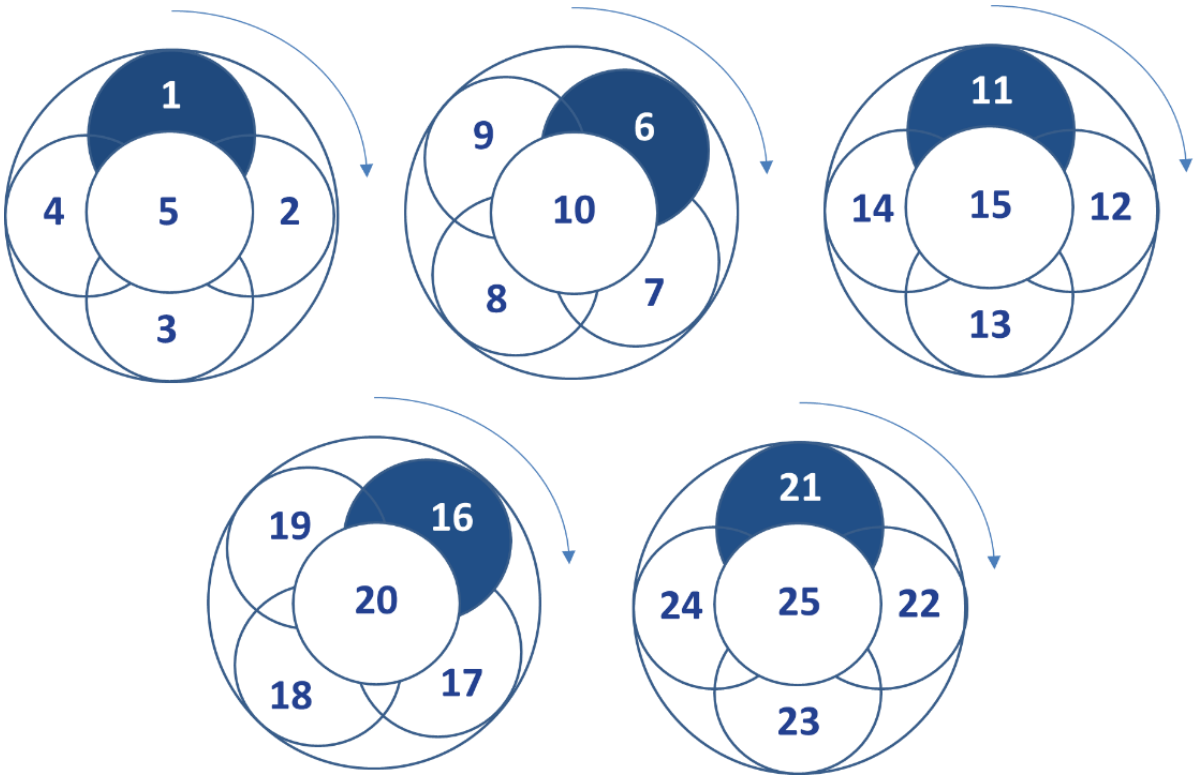

Source: Personal file

Figure 60 - Levelling off along the brim of the mold (left). Out of the mold subsamples (washed bauxite, 5 mm top size, tamped with C hammer) at approximately 13% of moisture (middle) and at approximately 16% of moisture (right)

Source: Personal file

After tamping, weighing and drying all 5 to 6 subsamples of each Proctor/Fagerberg test, the compaction curve could be plotted by using the previously determined solids density (d) to obtain the volumes required for calculating the parameters net water content in volume (e_v), void ratio (e) and degree of saturation (S) as per Equations 1,2

and 3. After the compaction curve was plotted on graph with net water content in volume (e_v) on the x-axis and void ratio (e) on the y-axis, the e_v corresponding to the intersection between compaction curve and 70% of saturation line was read and used to calculate the TML (gross water content in weight) as per Equation 11.

Equation 8

$$e_v = \frac{\text{Volume of water (cm}^3\text{)}}{\text{Volume of solids (cm}^3\text{)}}$$

Equation 9

$$e = \frac{\text{Volume of voids (cm}^3\text{)}}{\text{Volume of solids (cm}^3\text{)}}$$

Equation 10

$$S = \frac{e_v}{e}$$

Equation 11

$$TML = \frac{100e_v}{100d + e_v}$$

4.2 CASE STUDY ON PARTICLE SIZE CRITERION FOR BAUXITE CARGO CLASSIFICATION

The bauxite stockpiles at the port area (Figure 61) are reclaimed by bucket wheel reclaimer and the ore goes through conveyor belts to feed ship loaders operating at a rate of approximately 5,000 tons per hour. Most ships loaded in Juruti port are Panamax (Figure 62), while Handymax is also used.

Figure 61 - Port facility, highlighting pier and ship loader

Source: personal file

Figure 62 - Panamax vessel being loaded in Juruti

Source: Personal file

On the way between stockpiles and ship loaders, the conveyor belt goes through a sampling tower (Figure 63) containing automated mechanical samplers, which collect sample increments for every 1,000 tons of bauxite that pass through the sampling facility. Due to draught limitations in rivers navigated in the north region of Brazil, the ships typically carry up to 55,000 tons of bauxite. The collected samples undergo analysis of PSD, moisture content and chemistry. The PSD is measured through wet screening of dried samples at meshes 76.2 mm; 25.4 mm; 6.3 mm; 1.19 mm; 0.105 mm and 0.037 mm.

The particle size distribution of 486 shipments – from January of 2015 to April of 2019 – are analyzed. To verify the percentage of weight passing 1 mm, the trend for values of

weight percentage passing 1 mm was determined through trend calculations (using Excel software) based on values of weight percentages passing 6.3 mm and 1.19 mm. To verify the percentage of weight passing 2.5 mm, the year averages particle size distributions were plotted in Excel, the percentages of weight passing 2.5 mm were read and plotted against the values of percentage of weight passing 1 mm values in a scatter chart. The regression equation was applied to calculate the values of percentage passing 2.5 mm for each shipment.

Figure 63 - Port sampling facility

Source: personal file

5. RESULTS AND DISCUSSIONS

5.1 EFFECT OF SELECTED VARIABLES ON TML RESULTS OBTAINED BY PROCTOR/FAGERBERG TEST METHOD

The average density of solids of the washed bauxite samples was 2.62 g/cm^3 – with minimum at 2.60 g/cm^3 and maximum at 2.65 g/cm^3 –, while the average density of solids of the unwashed bauxite samples was 2.67 g/cm^3 – with minimum at 2.63 g/cm^3 and maximum at 2.7 g/cm^3. The main minerals contained in the sourced bauxites are gibbsite, kaolinite, hematite, goethite, and anatase (Table 11).

Table 11 - Typical mineralogical composition of bauxite from Juruti mine

Mineral	% of mass
Gibbsite ($Al(OH)_3$)	55 - 80
Kaolinite ($Al_2Si_2O_5(OH)_4$)	5 - 35
Hematite (Fe_2O_3)	10 - 20
Goethite ($FeO(OH)$)	2 - 5
Anatase (TiO_2)	1 - 3

Source: Personal file

The specific gravity of kaolinite and iron minerals are higher than those of gibbsite (Table 12) (MINERALOGY, 2019). The higher density of solids of unwashed bauxites is explained by the fact that the unwashed bauxites typically contain lower concentrations of gibbsite and higher amounts of kaolinite and iron oxides.

Table 12 - Specific gravity of minerals contained in Juruti bauxite

Mineral	Specific Gravity
Gibbsite ($Al(OH)_3$)	2.38 - 2.42
Kaolinite ($Al_2Si_2O_5(OH)_4$)	2.63
Hematite (Fe_2O_3)	5.26
Goethite ($FeO(OH)$)	4.27 - 4.29
Anatase (TiO_2)	3.79 - 3.97

Source: Mindat.org

The compaction curves built for each test are presented together in Figure 64. The samples that contain a higher void ratio for a given compaction effort have a higher amount of water at 70% saturation, thus returning higher TMLs. The larger amount of voids can simply be translated as more space to be filled with water. In some of the compaction curves (1, 2, 5, 6, 7, 8, 9, 10) it was possible to verify the OMC, which is a point of inflection at minimum void ratio (e) in the compaction curve. When the OMC was clearly identified, it was always above 80% saturation degree, providing a safety margin of at least 10% on the determination of the TML calculated at 70% of saturation.

Figure 64 - Compactions curves plotted for each test to check the e_v at interception between 70% saturation line and compaction curve

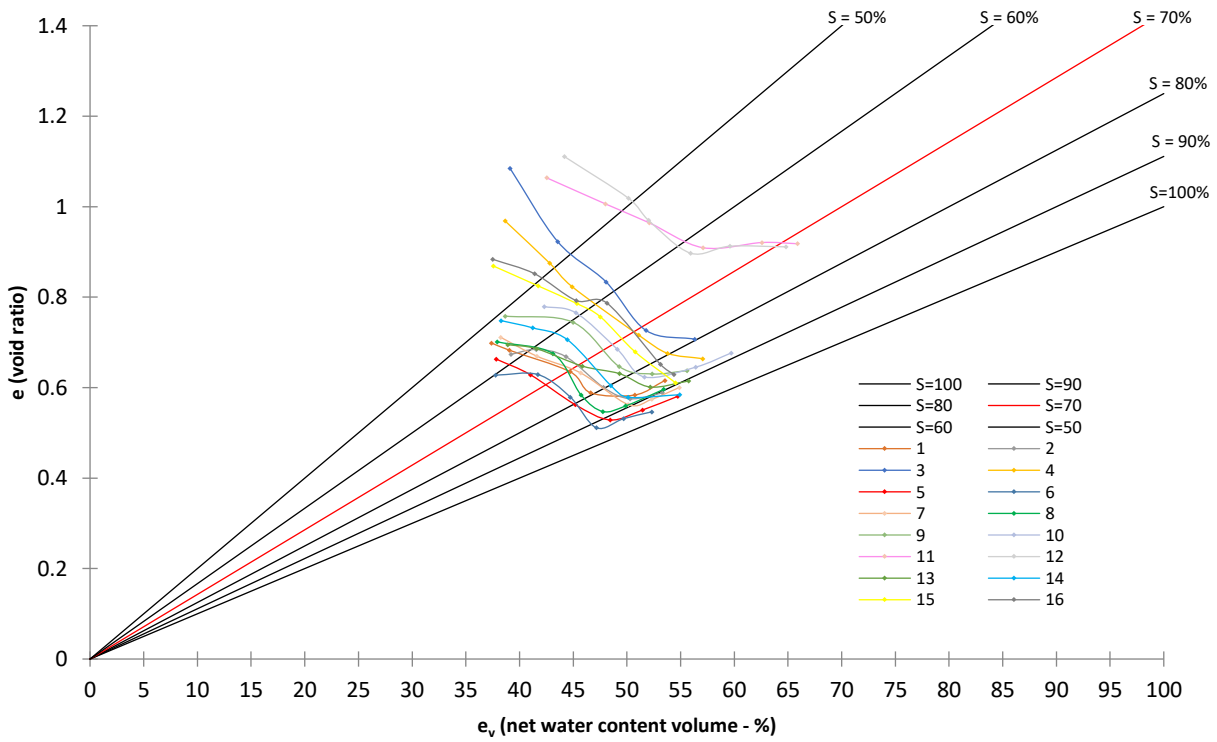

No clear correlation between saturation degree of the OMCs and energy of compaction or sample top size was observed. Tests 5 and 6 (Figure 65) were the only cases in which the OMC was above 90% saturation degree, so the TML calculated at 70% saturation degree provided a safety margin of more than 20%. These variations of compaction curves of tested bauxites were taken into account in the development of the Modified Proctor/Fagerberg test for Bauxite, as the test procedure allows TML calculation at 70% or 80% saturation, depending on the saturation in which the OMC occurs. When

the OMC cannot be clearly defined, a more conservative approach is adopted and TML is determined for 70% saturation degree (GBWG, 2017). In this study, all TMLs were calculated for net water content (e_v) read at 70% saturation degree, as in the standard Proctor/Fagerberg test.

Figure 65 - Compaction curves of tests 5 and 6, in which OMC above 90% saturation is observed

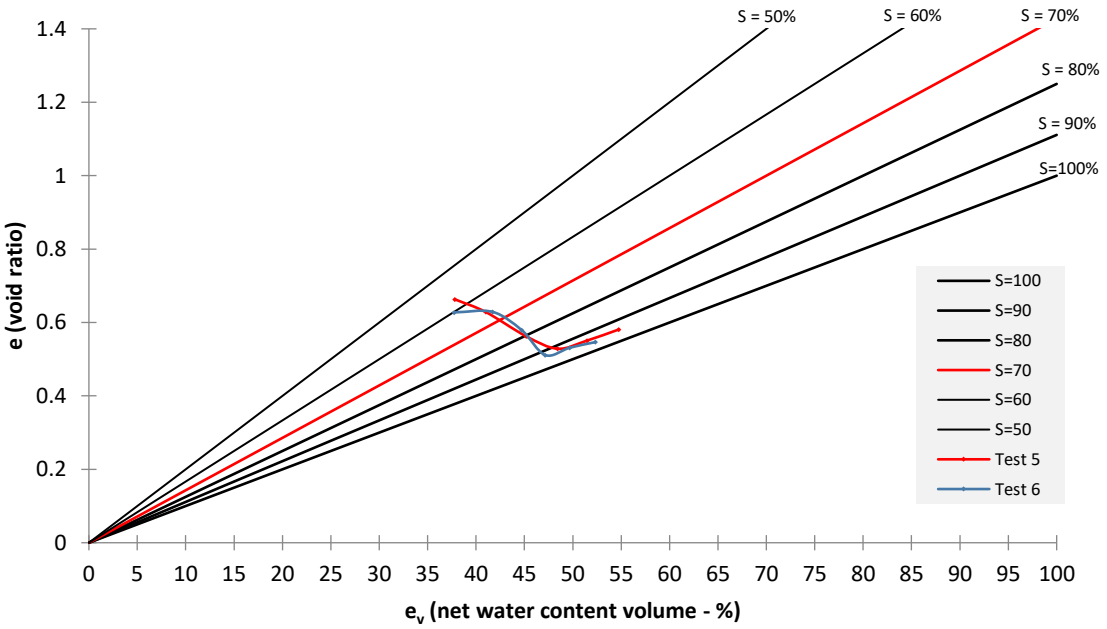

An overview of the test conditions and TMLs found in each of the 16 tests carried is presented in Table 13 and Figure 66. The TML is expressed in percentage of gross water content in mass and the average TML difference of tests carried in duplicate was 0.22% in absolute terms, showing good repeatability of the tests.

Table 13 - Test conditions and TML results

Test	Bauxite type	Top size	Hammer	TML (%)	Δ (%)	Average (%)
1	Washed	5 mm	C	14.38	0.26	14.50
2	Washed	5 mm	C	14.63		
3	Unwashed	5 mm	C	15.99	0.06	15.93
4	Unwashed	5 mm	C	15.86		
5	Washed	25.4 mm	C	13.93	0.25	14.06
6	Washed	25.4 mm	C	14.19		
7	Unwashed	25.4 mm	C	14.49	0.13	14.46
8	Unwashed	25.4 mm	C	14.42		
9	Washed	5 mm	D	15.38	0.27	15.50
10	Washed	5 mm	D	15.62		
11	Unwashed	5 mm	D	19.32	0.30	19.21
12	Unwashed	5 mm	D	19.11		
13	Washed	25.4 mm	D	14.85	0.24	14.98
14	Washed	25.4 mm	D	15.12		
15	Unwashed	25.4 mm	D	15.84	0.20	15.99
16	Unwashed	25.4 mm	D	16.14		

Figure 66 - Test conditions and TML results: blue bars identify washed bauxites and red bars identify unwashed bauxites

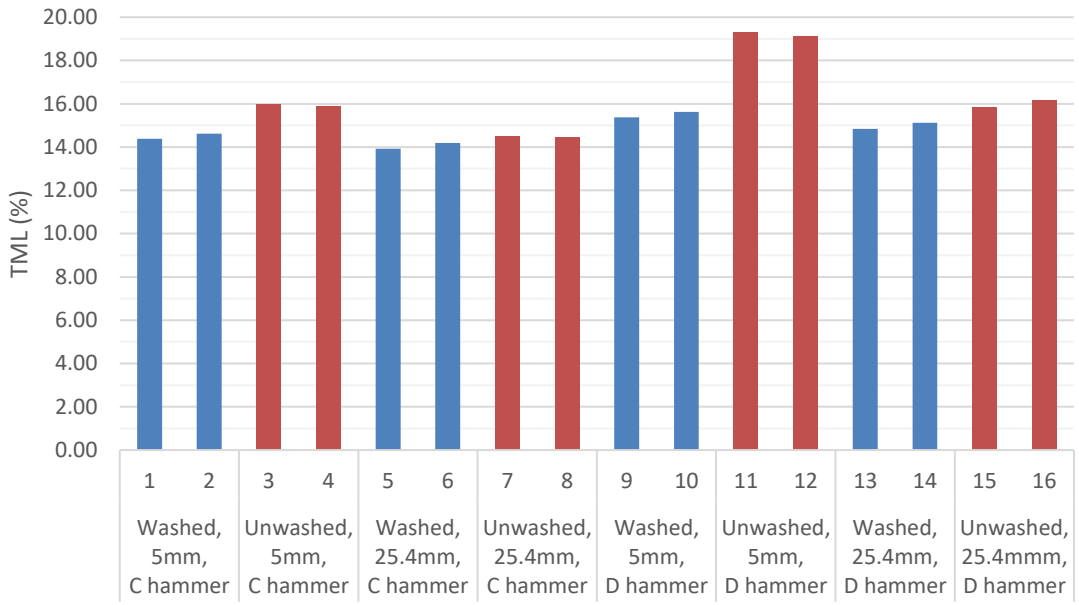

The D hammer led to higher TML figures, once it provides lower compaction than hammer C, allowing samples to maintain more voids and hold more water at any given saturation when compared to more compacted samples. When investigating the most adequate hammer to be adopted, an assessment of the bulk density of the cargo piles in vessel holds shall be taken into account, so the values of bulk density of the cargo as shipped can be used as a reference for the densities to be achieved in the laboratory test after compaction of the samples. Based on comprehensive research by world bauxite industry (GBWG, 2017), the Proctor/Fagerberg test modified for bauxite adopts the hammer D only, as it has been noted that the level of energy provided by this test method is enough to make samples reach bulk densities of actually shipped cargoes. The same is observed for other cargoes and the three accredited modifications of the standard Proctor/Fagerberg tests – notably the Modified Proctor/Fagerberg test for Iron Ore Fines, for Coal and for Bauxite – adopt the D hammer compaction effort (IMO, 2017, 2018).

The bauxites scalped at 25.4 mm returned lower TML figures when compared to those scalped at 5 mm. A more compacted condition was observed for those samples with wider particle size range in a way that the combination of larger particles at size fraction -25.4 mm +5 mm with finer particles at size fraction -5 mm led to a more packed particles' structure in the mold after tamping. Due to the potential removal of larger particles, the leveling off process carried after compacting bauxites scalped at 25.4 mm

took longer than the process carried after compacting bauxites scalped at 5 mm. Although not observed in this study, this may be a source of error, specially if an even coarser material is tested. The bauxite type affected the TML in a way that lower figures were found for washed bauxite from which most of the clay (kaolinite) was removed in the beneficiation process. The clay is a very fine and plastic material whose structure is made of microscopic layers of plates. This makes for higher surface area and volume of voids, enhancing the capacity of water absorption of clay. Therefore, the larger amounts of clay played a role in increasing the determined TML of those unwashed bauxite samples. In comparison with washed bauxites, the unwashed bauxites exhibited a higher difference in TML results for tests at different top sizes. This is explained by the concentration of clay that occurred when testing only the size fraction passing 5 mm, as seen in tests 3, 4, 11 and 12.

The bauxites classified as Group A cargoes (bauxite fines) are those containing more than 40% passing 2.5 mm and more than 30% passing 1 mm (IMO, 2018). Some bauxites, such as those covered in this study, may fit this Group A classification criterion and still contain some amount of coarse particles. To carry the compaction essays, scalping samples was a necessary step, since the as shipped material top size is 76.2 mm, containing amounts of large particles that could not be taken into the 100 mm diameter Proctor mold. The standard Proctor/Fagerbeg test procedure establishes that it shall be applied to test materials up to a top size of 5 mm while testing coarser materials shall be backed up by extensive investigation for adoption and improvement of the test method.

Scalping samples at 25.4 mm prior to testing reduces the concentration of fines and assures that tested samples will have particle size characteristics more similar to those of the as-shipped materials. Scalping samples at 25 mm became a sample preparation step on the Modified Proctor/Fagerberg test for Coal and also on the Modified Proctor/Fagerberg test for Bauxite. To compensate the particles larger than 25 mm removed on scalping, the Modified Proctor/Fagerberg test for Bauxite established a sample reconstitution in which the weight of particles larger than 25 mm removed shall be replaced by equivalent weight of particles in size fraction -25 mm +6.3mm, to improve the similarity between shipped material and tested samples, while still testing samples with a 25 mm top size. In addition to scalping at 25 mm and reconstitution at -25 mm

+6.3 mm, the Modified Proctor/Fagerberg test for Bauxite also replaced the standard Proctor mold by the larger standard mold applied on the California Bearing Ratio (CBR) test (ASTM, 1999). The later mold has 152 mm in diameter and 127 mm in height, presenting 2304.5 cm^3 of volume. The larger diameter and volume of the CBR mold made it a better fit to test particles with top size significantly larger than the 5 mm top size reference of the standard Proctor/Fagerberg test.

The effect of selected variables tested after factorial design assessed on Minitab is shown in Figure 67 and summarized in Figure 68. All three variables affected the TML of the bauxites tested. The single variable with the highest impact on the TML was the compaction hammer, which showed effect of 1.69%. The effect of bauxite type was 1.63% and effect of top size was -1,41%. The tests carried on the base condition (washed bauxite scalped at 5 mm and tamped with C hammer) returned average TML of 14.50%, while the average of all 16 tests was 15.58%. The lowest TML figures (13.93% and 14.19%) were found for washed bauxites scalped at 25.4 mm and compacted with C hammer, while highest TML figures (19.32% and 19.11%) were obtained in tests with unwashed bauxites scalped at 5 mm and compacted with D hammer.

Figure 67 - Minitab analysis on effect of selected variables on TML result

Session

Factorial Fit: TML versus Bauxite type; Top size; Hammer

Estimated Effects and Coefficients for TML (coded units)

Term	Effect	Coef	SE Coef	T	P
Constant		15,5794	0,04034	386,24	0,000
Bauxite type	1,6337	0,8169	0,04034	20,25	0,000
Top size	-1,4138	-0,7069	0,04034	-17,52	0,000
Hammer	1,6863	0,8431	0,04034	20,90	0,000
Bauxite type*Top size	-0,9337	-0,4669	0,04034	-11,57	0,000
Bauxite type*Hammer	0,7263	0,3631	0,04034	9,00	0,000
Top size*Hammer	-0,4562	-0,2281	0,04034	-5,66	0,000
Bauxite type*Top size*Hammer	-0,4213	-0,2106	0,04034	-5,22	0,001

S = 0,161342 R-Sq = 99,44% R-Sq(adj) = 98,96%

Analysis of Variance for TML (coded units)

Worksheet 1 ***

↓	C1-T	C2-T	C3-T	C4	C5	C6	C7	C8	C9	C10
	Bauxite type	Top size	Hammer	TML	StdOrder	RunOrder	Blocks	CenterPt		
1	Washed	5mm	C	14,38	1	1	1	1		
2	Washed	5mm	C	14,63	2	2	1	1		
3	Unwashed	5mm	C	15,99	3	3	1	1		
4	Unwashed	5mm	C	15,86	4	4	1	1		
5	Washed	25.4mm	C	13,93	5	5	1	1		
6	Washed	25.4mm	C	14,19	6	6	1	1		
7	Unwashed	25.4mm	C	14,49	7	7	1	1		
8	Unwashed	25.4mm	C	14,42	8	8	1	1		
9	Washed	5mm	D	15,38	9	9	1	1		
10	Washed	5mm	D	15,62	10	10	1	1		
11	Unwashed	5mm	D	19,32	11	11	1	1		
12	Unwashed	5mm	D	19,11	12	12	1	1		
13	Washed	25.4mm	D	14,85	13	13	1	1		
14	Washed	25.4mm	D	15,12	14	14	1	1		
15	Unwashed	25.4mm	D	15,84	15	15	1	1		
16	Unwashed	25.4mm	D	16,14	16	16	1	1		

Figure 68 - Results of the effects verified for the factorial design of three variables and 2 levels on TML results

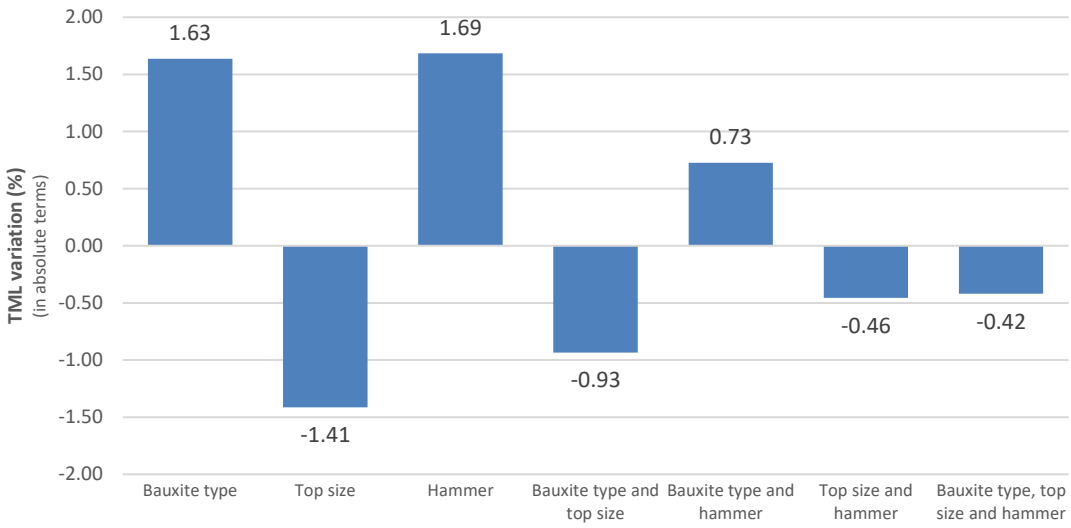

5.2 CASE STUDY ON PARTICLE SIZE CRITERION FOR BAUXITE CARGO CLASSIFICATION

The Juruti bauxite contains gibbsite as the mineral of interest and kaolinite as major contaminant, while hematite, goethite, and anatase are also found on the mineralogical composition. The shipped cargoes exhibit a wide range of particle sizes, containing clay, silt, sand, and gravel. The screen apertures used (76.2 mm; 25.4 mm; 6.3 mm; 1.19 mm; 0.105 mm and 0.037 mm) reflect relevant particle sizes for the operations process control and are related to separation and classifications operations in screens and hydro cyclones. During the time frame covered in this study, nearly 25 million tons of bauxite were shipped through those 486 shipments.

The particle sizes data of all 486 shipments show that sieve with the largest aperture (76.2 mm) has 88.2% to 100% passing, while sieve with the smallest aperture (0.037 mm) has 5.4% to 25.8% passing (Table 14). A variation range of more than 10% absolute between minimums and maximums can be observed for any given particle size. In relative terms, the widest variation between minimum and maximum values of “% passing” is observed for the 0.037 mm sieve. This is due to the fact that the washing process aims to remove the fraction <0.037 mm, where higher amounts of kaolinite is concentrated, but not all shipments consist of washed bauxite. Those shipments containing washed bauxites (or blends with higher amounts of washed bauxite) have

lower amounts of % passing 0.037 mm, while those containing unwashed bauxite (or blends with higher amounts of unwashed bauxite) have higher amounts of % passing 0.037 mm.

Table 14 - Statistics of "% passing" in different sieves for 486 shipments

	76.2 mm	25.2 mm	6.3 mm	1.19 mm	0.105 mm	0.037 mm
Mean (%)	99.2	76.4	52.2	36.4	17.5	12.5
σ (%)	1.9	5.9	5.2	3.7	2.6	2.5
Maximum (%)	100.0	90.3	65.4	45.5	29.5	25.8
Minimum (%)	88.2	60.9	39.0	25.6	9.1	5.4

The year average PSDs of 486 shipments from 2015 to 2019 (until the end of April) is exhibited below (Figure 69). It is noted that in 2016, the shipments contained more fines on average. This is due to a higher proportion of shipments containing unwashed bauxite in that year. On the other hand, years 2017, 2018 and 2019 have very similar PSD curves, in which it is observed lower amounts of fines in comparison to 2015 and 2016. This is explained by lower proportion of shipments containing unwashed bauxite, higher washing efficiency and mining of bauxites naturally containing less amounts of fines. In all years, the shipment's average PSDs exhibit more than 30% passing 1 mm. In years 2015 and 2016, more than 40% passing 2.5 mm is clearly seen, while in years 2017, 2018 and 2019, it is observed that the PSDs are very close to 40% passing 2.5 mm.

Figure 69 - PSD curves for year averages of shipments from 2015 to 2019

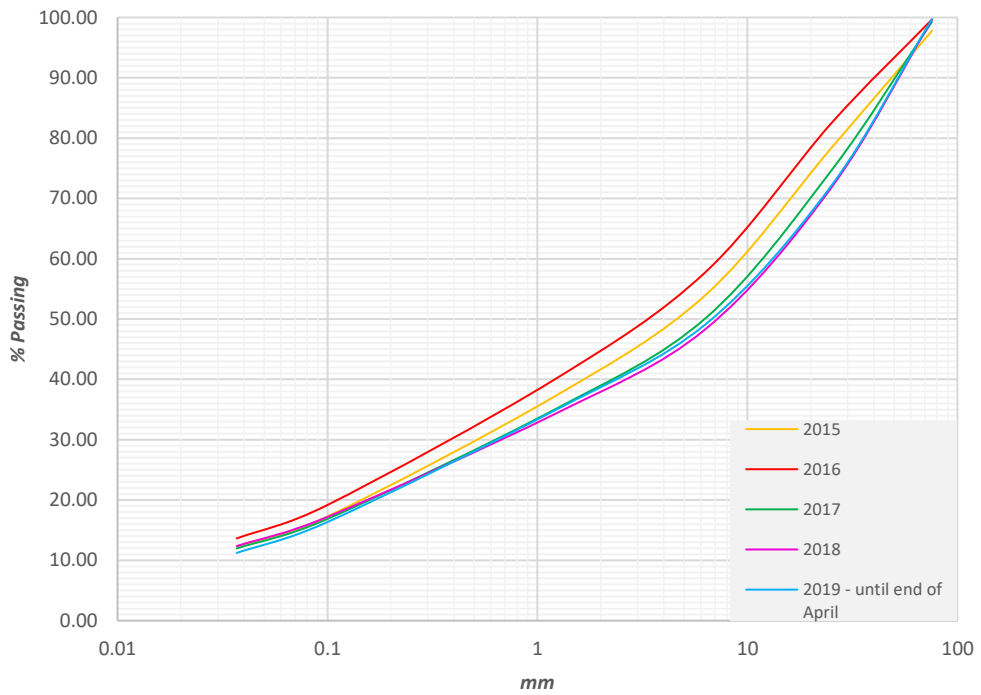

The percentage passing 6.3 mm and 1.19 mm in all the 486 shipments analyzed were used to determine the percentage passing 1 mm through trend calculation in Excel software. The average difference between percentage passing 1.19 mm and calculated percentage passing 1 mm was 0.59% in absolute terms. The minimum and the maximum difference in absolute terms were, respectively, 0.40% and 0.88%.

To calculate the percentage passing 2.5 mm for each shipment, the percentage passing 1 mm and 2.5 mm were read in the average PSDs of shipments per year and plotted in a scatter chart (Figure 70). A strong correlation with $R^2 = 0.997$ was obtained and the regression equation was applied to calculate the percentage passing 2.5 mm inputting the percentage passing 1 mm.

Figure 70 - Correlation and regression equation of % passing 2.5 mm and % passing 1 mm of shipments PSDs year averages

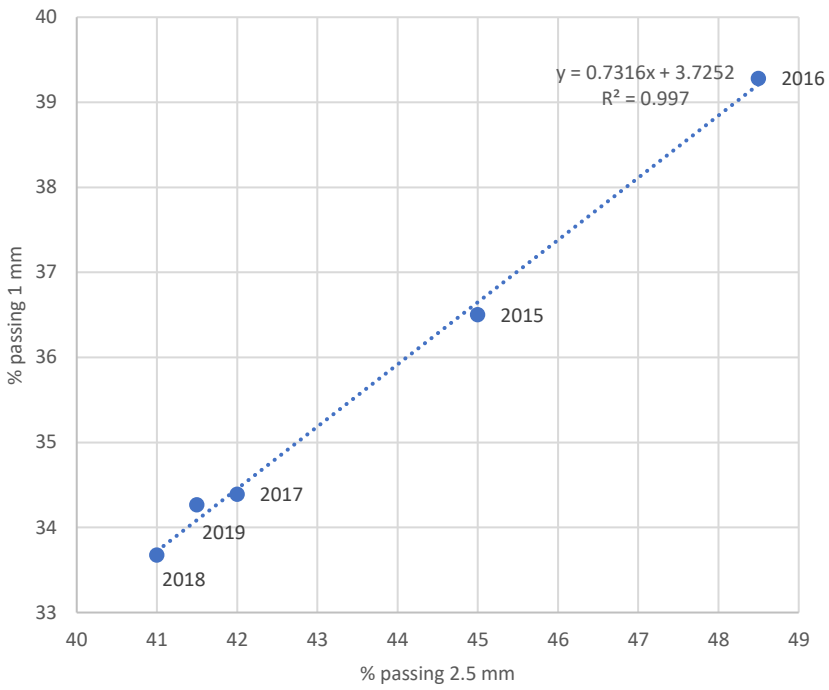

In 2015, IMO's circular entitled "Carriage of bauxites which may liquefy" established that bauxite cargoes containing more than 10% of moisture or more than 30% passing 2.5 mm should be shipped as Group A cargo – unless the cargo was assessed by the competent maritime authority and it was determined that it did not exhibit Group A properties (i.e. not prone to undergo instabilities due to moisture). This circular was a regulatory term in response to the bulk Jupiter incident and no joint research on bauxite behavior during shipping was provided at the time.

Due to moisture content and particle size distribution of the cargo, Alcoa started shipping bauxite as a Group A cargo in 2015. At the time, there was no TML test specific for bauxite and an adaptation of the general Proctor/Fagerberg test procedure was applied for TML determination. The adaptation consisted of scalping the samples at 5 mm and testing only the portion passing 5 mm, following the 5 mm top size reference of the test procedure. In addition to TML determination, Alcoa put in place a moisture management plan to assure moisture content of the shipped bauxite is always below the TML. In general, the plan consisted of i) adopting a reliable technique for expedite determination of moisture; and ii) provide a contingency stockpile of relatively drier bauxite in port area to adjust moisture level of shipped cargo, if necessary.

In September of 2017, the IMO issued a new circular on the regulation of bauxite carriage by the light of the findings of the bauxite industry research on bauxite behavior during shipping. The particle size criterion established demanded the bauxite shipper to analyze its shipments particle size database to properly assess its bauxite cargo Group. As per updated regulation, the cargo would be i) Group A if containing more than 40% passing 2.5 mm and more than 30% passing 1 mm; ii) Group C if containing less than 40% passing 2.5 mm or less than 30% passing 1 mm. For TML determination of the Group A bauxite cargoes, the IMO circular of 2017 prescribed the Modified Proctor/Fagerberg test procedure for bauxite. The average PSD of 289 bauxite shipments from January 2015 to August 2017 showed an average of ~45% passing 2.5 mm and ~36% passing 1 mm (Figure 71).

Figure 71 - Average and boundaries of curves of particle size distributions of 289 bauxite shipments from January 2015 to August 2017

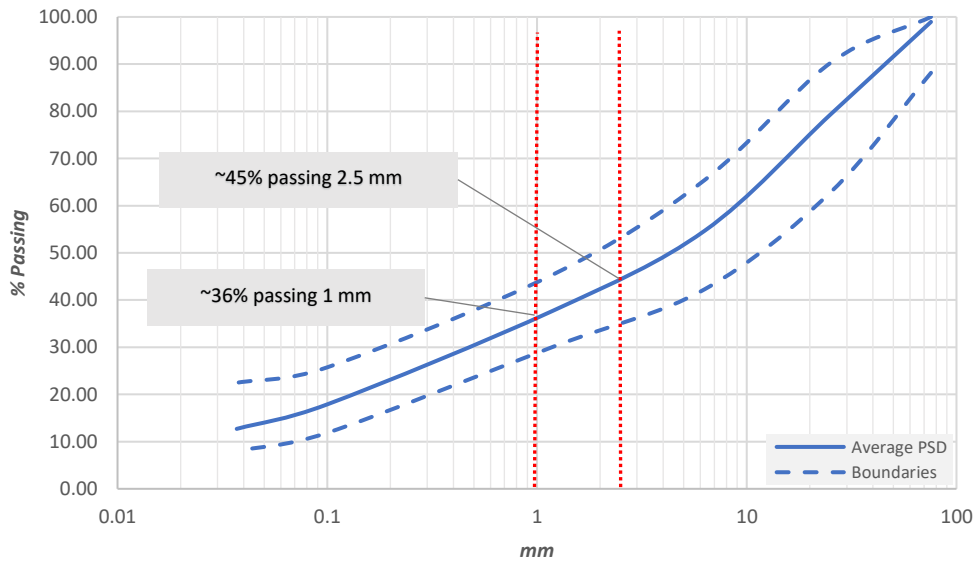

It was observed that 89% of the shipments from January 2015 to August 2017 carried cargoes with PSD falling into Group A classification according to the latest regulation. Since the shipments PSD information is obtained after processing samples taken while the ship is loaded, the PSD information is available only after the ship has already departed. In a practical approach, the 11% of the cargoes shipped exhibiting Group C PSDs would probably be shipped as Group A cargo to avoid any potential unsafe and uncompliant situation due to inaccuracies in predicting the PSDs to be shipped. As depicted from chart below (Figure 72), 100% of the shipments on this 2015-17 period

had more than 35% passing 2.5 mm and more than 25% passing 1 mm. This means that if a safety margin of 5% is considered, all shipments should be preventively shipped as Group A.

Figure 72 - Percentage of weight passing 2.5 mm and 1 mm of the 289 bauxite shipments from January 2015 to August 2017

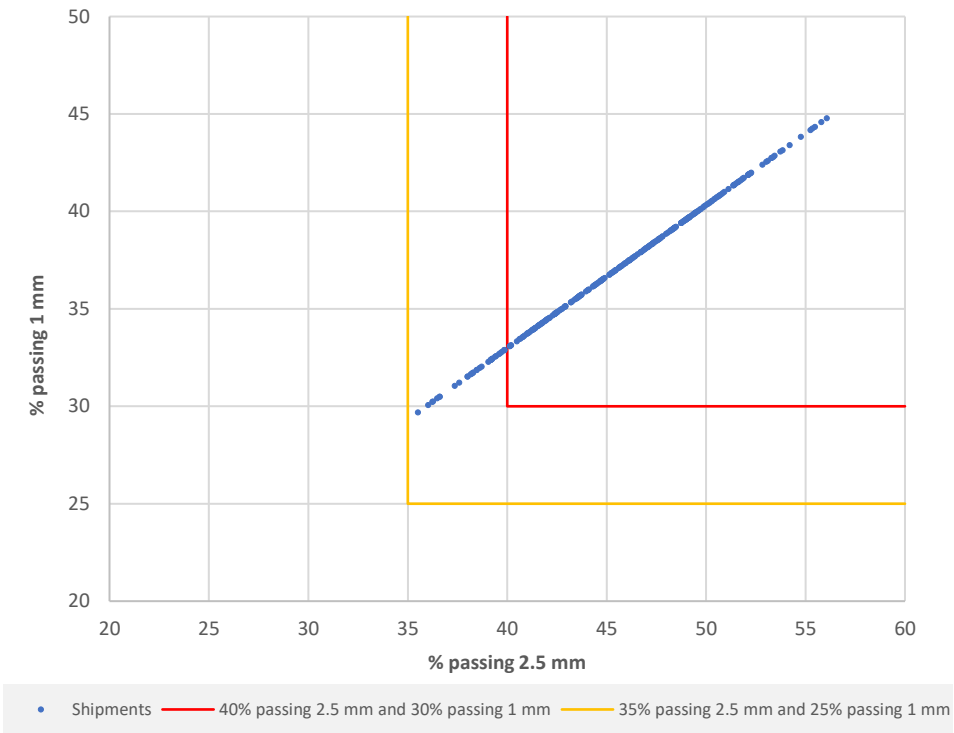

Following the particle size criterion for bauxite cargo classification as established by the IMO in 2017, these analyzes supported the classification of all cargoes as Group A by Alcoa. Soon after the IMO circular of 2017, the laboratory of Alcoa in Juruti became accredited by the Brazilian Maritime Authority to carry the Modified Proctor/Fagerberg test procedure for bauxite. This way, the Group A bauxite shipped would have the TML determined in accordance with the test method specific for bauxite.

From September of 2017 to April of 2019, Juruti accounted for 196 shipments of bauxite shipped as Group A cargo. The PSD database was assessed to verify the likelihood of variation in cargo classification for future shipments. The average PSD of those 196 bauxite shipments showed an average of ~40% passing 2.5 mm and ~33% passing 1 mm (Figure 73).

Figure 73 - Average and boundaries of curves of particle size distributions of 289 bauxite shipments from September 2017 to April 2019

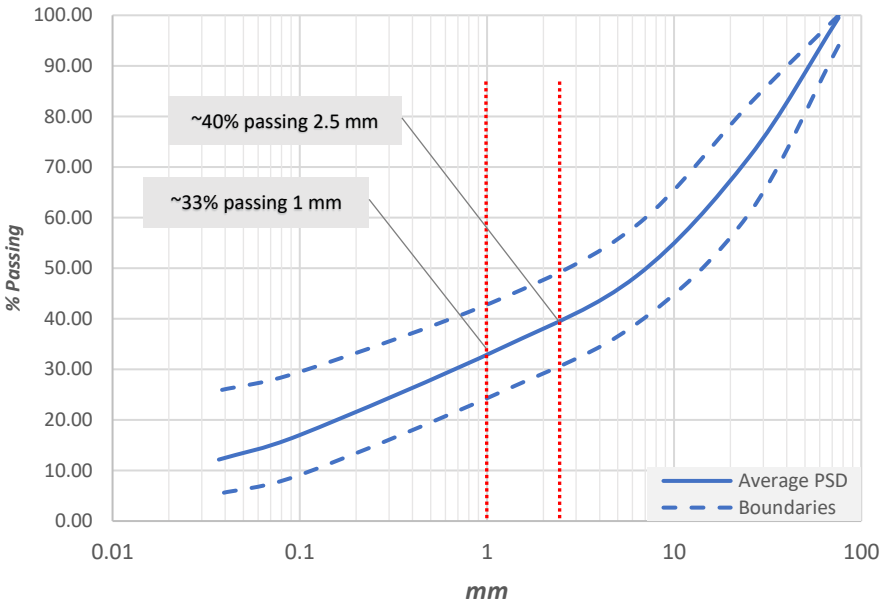

The bauxite cargoes shipped on the 2017-19 period are coarser than those shipped on the 2015-17 period, although PSDs of most of the shipments still relate to Group A bauxite cargo. It was noted that 59% of the shipments from September 2017 to April 2019 carried cargoes with PSD falling into Group A classification. Considering a 5% safety margin on the particle size criterion for bauxite cargo classification, 94% of the shipments on this 2017-19 period falls on the range of more than 35% passing 2.5 mm and more than 25% passing 1 mm (Figure 74). Again, a cautious and practical approach is shipping all bauxite cargoes as Group A to avoid any potential unsafe and uncompliant situation due to inaccuracies in predicting the PSDs to be shipped.

Figure 74 - Percentage of weight passing 2.5 mm and 1 mm of the 196 bauxite shipments from September 2017 to April 2019

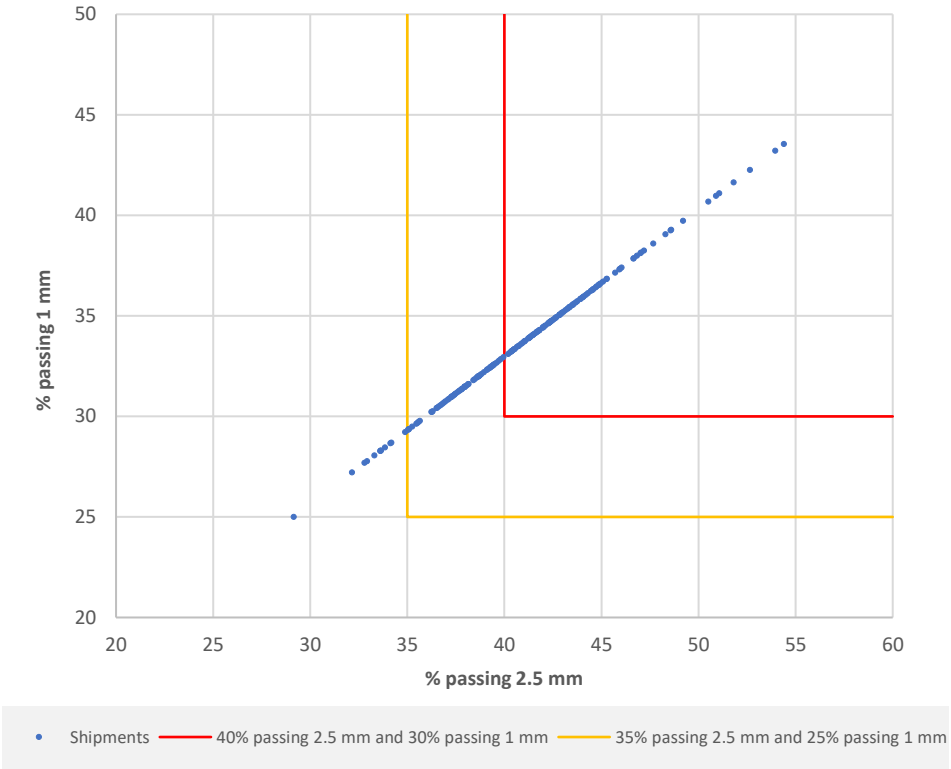

To allow shipping part of the bauxite produced as Group C cargo and another part as Group A cargo without any risk of improper classification, it would be necessary to separate the bauxite to be shipped in two ranges of particle sizes. Such separation would add to production cost and could be pursued if relevant cost benefits– such as lower insurance or freight – related to shipping Group C cargoes instead of Group A cargoes are found.

It shall be noted that shipping Group A cargoes is a standard operation in the global trade. These cargoes will be safely shipped, provided moisture content and TML of the cargo are properly determined. Alcoa gained experience in practical aspects related to shipping Group A cargoes in the past years, showing commitment to safe and compliant shipping of bauxite. The relevant IMO provisions on Group A bauxite shipping have been duly followed by Alcoa, whose moisture content and TML determination procedures are certified by the Brazilian Maritime Authority.

6. CONCLUSIONS

6.1 EFFECT OF SELECTED VARIABLES ON TML RESULTS OBTAINED BY PROCTOR/FAGERBERG TEST METHOD

I. The tests conducted through factorial design showed that changes in bauxite processing, sample top sizes, and compaction hammer applied affected TML results in Proctor/Fagerberg tests. The unwashed bauxites with larger amounts of clay resulted in higher TML figures and so did the application of the D hammer instead of the C hammer. Scalping samples at 25.4 mm instead of 5 mm returned lower TML figures. The test variation with highest impact (1.69% in absolute terms) on TML result was the hammer, followed by bauxite type and sample top size.

II. The variations on standard Proctor/Fagerberg tests covered in this study provide insights on how the TML for a given material varies when improvements on the test method are made to make it more suitable to test such material. Due to particle size distributions and bulk density of shipped bauxite cargoes, the original Proctor/Fagerberg test is not an adequate choice to determine the TML of Group A bauxite cargoes. The apparatus and procedures improvements made on this test method to make it more suitable to test bauxites are reflected on the Modified Proctor/Fagerberg test procedure for bauxite, which adopts: sample reconstitution to make particle size distribution of test samples more similar to that of shipped cargoes; the D hammer to match in-hold bulk density of shipped bauxite cargoes; the larger CBR mold to more properly test larger particles contained in bauxites; the possibility to calculate the TML at 70% or 80% saturation, depending on the verified optimum moisture content. The Modified Proctor/Fagerberg test procedure for bauxite is the recommended test to determine the TML of Group A bauxites since its first publication through an IMO Circular in September 2017.

6.2 CASE STUDY ON PARTICLE SIZE CRITERION

I. The capsizing event of a ship carrying wet and fine bauxite cargo in 2015 led to significant effort from the industry on research to better assess the behavior of bauxite during maritime transportation. The IMO's regulatory changes based on the bauxite industry findings have improved safety at sea and must be known and followed by those involved in bauxite shipping operations worldwide. The bauxite cargo classification through particle size criteria allows simple assessment of bauxite cargo instability risk.

II. The assessment of the PSDs database of Alcoa's bauxite shipments from Juruti showed that 89% out of 289 shipments from 2015-17 have PSDs of Group A cargo ad 59% out of 196 shipments from 2017-19 have PSDs of Group A cargo. Given a 5% safety margin, over 95% of the 485 shipments analyzed fall into Group A. From a practical and cautious approach, all cargoes are shipped as Group A.

III. Alcoa's case study of bauxite production and shipping operations in Brazil provides an example of cargo classification according to latest IMO's regulatory provisions. Such provisions brought implementation of new procedures to be followed and parameters to be closely watched in all stages of production chain from mining to shipping. As a Group A bauxite producer and/or shipper, one shall be committed to manage moisture of the cargo and to provide accurate TML and moisture content figures to assure safe and compliant shipments.

7. REFERENCES

ACARP. **Australian Coal Association Research Program. TML0036 - Coal Transportable Moisture Limit Project.** Technical Submission to the Australian Maritime Safety Authority (AMSA), 2014.

AHMAD, K.; KASSIM, K. A.; TAHA, M. R. Electroosmotic Flows and Electromigrations During Electrokinetic Processing of Tropical Residual Soil. **Malaysian Journal of Civil Engineering**, v. 18, n. 2, p. 74–88, 2006. Available at: <https://mjce.utm.my/index.php/MJCE/article/view/185>.

ALCOA. **2018 Annual Report**. Available at: <https://investors.alcoa.com/~/media/Files/A/Alcoa-IR/documents/annual-reports-and-proxy-information/annual-report-2018.pdf>.

AMSA. **Dynamic separation of cargoes**Australian Maritime Safety Authority, 2017. Available at: <https://www.amsa.gov.au/vessels-operators/cargoes-and-dangerous-goods/dynamic-separation-cargoes>. Access on: 25 jun. 2018.

ASTM. **ASTM designation C230-standard specification for flow table for use in tests of hydraulic cement.** West Conshohocken American Society for Testing and Materials, 1952.

ASTM. **ASTM designation C124-method of test for flow of portland-cement concrete by use of the flow table.** West ConshohockenAmerican Society for Testing and Materials, 1971.

ASTM. **ASTM D1883-99, Standard test method for CBR (California Bearing Ratio) of Laboratory Compacted Soils.** WestAmerican Society for Testing and Materials, 1999.

BARDOSSY G., A. G. J. J. Lateritic Bauxites. **Developments in Economic Geology**, v. 27, 1990.

BMTA. **"M.V Bulk Jupiter" — Report of the Marine Safety Investigation into the Loss of a Bulk Carrier in the South China Sea on January 2nd 2015**. Available at: <https://www.bahamasmaritime.com/wp-content/uploads/2015/08/Bulk-Jupiter-Final-Report-August-2015.pdf>.

BSI. **BS 1377-2: 1990 - Methods of test for soils for civil engineering purposes - part 2: Classification tests.** British Standards Institution, 1996.

BUREAU VERITAS; THE LONDON P&I CLUB; TMC MARINE. **Reducing the Risk of Liquefaction - Operational guidance for vessels that carry cargoes which may liquefy**, 2018. Available at: < https://www.londonpandi.com/media/2142/reducing-the-risk-of-liquefaction-operational-guidance-for-vessels-that-carry-cargoes-which-may-liquefy.pdf >

CHEN, W. et al. Investigation into the ship motion induced moisture migration during

seaborne coal transport. **Advanced Powder Technology**, v. 28, n. 11, p. 3004–3013, 2017. Available at: <https://doi.org/10.1016/j.apt.2017.09.011>.

CHEN, W. et al. Modelling the stability of iron ore bulk cargoes during marine transport. **Powder Technology**, v. 326, p. 255–264, 2018.

CLARKSON, R. S. Global bauxite trade: going the extra mile. 2017. Available at: <https://www.hellenicshippingnews.com/global-bauxite-trade-going-the-extra-mile/>.

CORREIA, G. et al. Research into the behavior of bauxite during shipping: an overview of the Global Bauxite Working Group (GBWG) findings. In: **36th International ICSOBA Conference, 2018**. Available at: <https://icsoba.org/sites/default/files/Papers2018/BAUXITE/BX06 - Research into the Behavior of Bauxite During Shipping an Overview of the Global Bauxite Working Group Findings.pdf>.

DAOUD, S. et al. Numerical analysis of cargo liquefaction mechanism under the swell motion. **Marine Structures**, v. 57, p. 52–71, 2018. Available at: <https://doi.org/10.1016/j.marstruc.2017.09.003>.

ESELLER-BAYAT, E. et al. Liquefaction response of partially saturated sands. I: Experimental results. **Journal of Geotechnical and Geoenvironmental Engineering**, v. 139, n. 6, p. 863–871, 2013.

EVANS, T. et al. Development and performance of a rolling table used on a centrifuge. **International Journal of Physical Modelling in Geotechnics**, p. 1–8, 2018.

FAGERBERG, B. Hazards of shipping granular ore concentrates. **Canadian Mining Journal**, v. 856, p. 53–57, 1965.

FAGERBERG, B.; STAVANG, A. Determination of critical moisture contents in ore concentrates carried in cargo vessels. In: **1st International Symposium on Transport and Handling of Minerals**, Vancouver, Canada, 1971.

FERREIRA, R. F. et al. Limite De Umidade Transportável De Minérios De Ferro : Transportable Moisture Limit of Iron Ores : Regulatory and. p. 16–23, 2017.

FERREIRA, R. F.; PEREIRA, T. M.; LIMA, R. M. F. A model for estimating the PFD80 transportable moisture limit of iron ore fines. **Powder Technology**, v. 345, p. 329–337, 2019. Available at: <https://doi.org/10.1016/j.powtec.2019.01.024>.

FREYSSINET, P.H., BUTT, C.R.M., MORRIS, R.C., PLANTONE, P. Ore forming processes related to lateritic weathering. **Economic Geology**, v. 1905, 2005.

GBWG. **Global Bauxite Working Group Report on Research into the Behaviour of Bauxite during Shipping**. 2017. Available at: <https://www.bahamasmaritime.com/wp-content/uploads/2017/10/CCC-4-INF.10.pdf>.

GOLD PALM GLOBAL BHD. **Bulk carrier fleet**. 2019. Available at:

<ahvm.com.my/services/general-information-on-sand-export/>. Access on: 15 mar. 2019.

GRANT, K.; UK P&I CLUB. **Bulletin 602 - 9/08 - Shipping nickel ore - Indonesia**. Available at: <https://www.ukpandi.com/fileadmin/uploads/uk-pi/LP Documents/LP_Bulletins/Bulletin 602.pdf>. Access on: 21 ago. 2018.

GREENWOOD, N. N.; EARNSHAW, A. **Chemistry of the Elements**. Butterworth Heinemann, 1997.

HASAN, M. et al. Basic and Morphological Properties of Bukit Goh Bauxite. **IOP Conference Series: Materials Science and Engineering**, v. 318, n. 1, 2018.

HASAN, M.; AZIZ, S. H.; WAN JUSOH, W. N. Basic Properties of Gebeng Bauxite in Accordance to IMSBC Code. **Indian Journal of Science and Technology**, v. 10, n. 7, p. 1–5, 2017.

HAZEN, A. Hydraulic Fill Dams. **Transactions of the American Society of Civil Engineers**, v. 83, n. 1, p. 1717–1745, 1920.

IAI. **International Aluminum Institute**. Available at: <http://www.worldaluminium.org/media/filer_public/2018/05/18/170518_sbmg_final.pdf >.

IMO. **Circular CCC1./ Circ.2: Carriage of bauxites that may liquefy**LondonInternational Maritime Organization, 2015. Available at: <http://www.imo.org/en/MediaCentre/Documents/CCC.1-Circ.2 - Carriage Of Bauxite That May Liquefy (Secretariat).pdf>.

IMO. **Circular CCC1./ Circ.2/Rev.1: Carriage of bauxites that may liquefy**LondonInternational Maritime Organization, 2017. Available at: <http://www.imo.org/en/MediaCentre/PressBriefings/Documents/CCC.1-Circ.2-Rev.1 - Carriage Of Bauxite Which May Liquefy.pdf>.

IMO. **International Maritime Solid Bulk Cargoes Code**. 2018. ed. London: International Maritime Organization, 2018.

INTERCARGO. **Bulk carrier casualty report**. 2019. Available at: <https://www.intercargo.org/wp-content/uploads/2019/04/INTERCARGO-MEDIA-RELEASE_24_04_2019.pdf>.

IOFTWG. **Report 3: Iron Ore Proctor Fagerberg Test. Iron Ore Fines Technical Working Group Submission for Evaluation and Verification: Iron Ore Fines Proctor-Fagerberg Test**. 2013. Available at: <http://ironorefines-twg.com/report-3-iron-ore-proctor-fagerberg-test/%0D%0A%0D%0A>.

ISHIHARA, K. Stability of natural deposits during earthquakes. In: **11th International Conference on Soil Mechanics and Foundation Engineering**, San Francisco, USA, 1985. Available at:

<https://www.issmge.org/uploads/publications/1/34/1985_01_0007.pdf>.

ISO. **ISO 9033:1989 - Aluminium ores - Determination of the moisture content of bulk material.** International Organization for Standardization, 1989.

JU, L. et al. Numerical investigation of rolling response of a 2D rectangular hold, partially filled with moist bulk cargo. **Ocean Engineering**, v. 142, n. July, p. 348–362, 2017.

JU, L. et al. **Numerical investigation of solid bulk cargo liquefaction. Ocean Engineering**, 2018.

JU, L.; VASSALOS, D.; BOULOUGOURIS, E. **Numerical assessment of cargo liquefaction potential. Ocean Engineering**, 2016.

KAI, A.; NICK, C.; BROOKSBELL. **Iron Ore Fines Loading Issues – India**. Available at: <ttp://www.ukpandi.com/loss-prevention/article/660-10-09-iron-ore-fines-loading-issues-india-925/>. Access on: 14 jun. 2019.

LEE, H. L. Nickel ore bulk liquefaction a handymax incident and response. **Ocean Engineering**, v. 139, n. September 2016, p. 65–73, 2017.

MINERALOGY, H. I. of. **Mindat.org**. Available at: <https://www.mindat.org/>. Access on: 15 jul. 2019.

MUNRO, M. C.; MOHAJERANI, A. Moisture content limit of iron ore fines for the prevention of liquefaction in bulk carriers. v. 40, n. October, p. 193–224, 2014.

MUNRO, M. C.; MOHAJERANI, A. Moisture content limits of Iron Ore Fines to prevent liquefaction during transport: Review and experimental study. **International Journal of Mineral Processing**, v. 148, p. 137–146, 2016a. Available at: <http://dx.doi.org/10.1016/j.minpro.2016.01.019>.

MUNRO, M. C.; MOHAJERANI, A. Corrigendum to “Moisture content limits of iron ore fines to prevent liquefaction during transport: Review and experimental study” [Int. J. Miner. Process. 148 (2016) 137–146]. **International Journal of Mineral Processing**, v. 157, p. 174, 2016b.

MUNRO, M. C.; MOHAJERANI, A. Liquefaction Incidents of Mineral Cargoes on Board Bulk Carriers. **Advances in Materials Science and Engineering**, v. 2016, p. 1–20, 2016c.

MUNRO, M. C.; MOHAJERANI, A. Variation of the geotechnical properties of Iron Ore Fines under cyclic loading. **Ocean Engineering**, v. 126, n. June 2015, p. 411–431, 2016d. Available at: <http://dx.doi.org/10.1016/j.oceaneng.2016.09.006>.

MUNRO, M. C.; MOHAJERANI, A. A review of the newly developed method used to prevent Liquefaction of iron ore fines on bulk carriers. **Australian Geomechanics Journal**, v. 51, n. 1, p. 43–52, 2016e.

MUNRO, M. C.; MOHAJERANI, A. Cyclic Behavior of Iron Ore Fines on Board Bulk Carriers: Scale Model Analysis. **Journal of Materials in Civil Engineering**, v. 29, n. 7, p. 04017046, 2017a.

MUNRO, M. C.; MOHAJERANI, A. Bulk cargo liquefaction incidents during marine transportation and possible causes. **Ocean Engineering**, v. 141, n. May, p. 125–142, 2017b. Available at: <http://dx.doi.org/10.1016/j.oceaneng.2017.06.010>.

MUNRO, M. C.; MOHAJERANI, A. Laboratory scale reproduction and analysis of the behaviour of iron ore fines under cyclic loading to investigate liquefaction during marine transportation. **Marine Structures**, v. 59, n. February, p. 482–509, 2018.

NEXT GENERATION. **Ships and Rig stability for non Naval Architect**. Available at: <http://kimwhye.blogspot.com/2013/06/ship-and-offshore-rig-stability-for-non.html>. Access on: 21 ago. 2018.

PROCTOR, R. Fundamental principles of soil compaction. **Engineering News Record**, v. 3, n. 9, p. 245–248, 1933a.

PROCTOR, R. Description of field and laboratory test methods. **Engineering News Record**, v. 3, n. 10, p. 286–289, 1933b.

RNLI. **Free surface effect**. Available at: <https://www.youtube.com/watch?v=zzJVYs1kgJ4%0A%0A>. Access on: 20 ago. 2019.

ROSE, T. P. Solid Bulk Shipping : Cargo Shift, Liquefaction and the Transportable Moisture Limit. p. 1–195, 2014. Available at: <http://www2.eng.ox.ac.uk/civil/publications/theses/rose>.

SANDVIK, K.; REIN, A. Safe transport at sea of bulk mineral cargoes. **Bulk Solids Handling**, v. 12, p. 79–83, 1992.

SLADEN, J. A.; D'HOLLANDER, R. D.; KRAHN, J. The liquefaction of sands, a collapse surface approach. **Canadian Geotechnical Journal**, v. 22, n. 4, p. 564–578, 1985.

SMITH, P. Hydrometallurgy The processing of high silica bauxites — Review of existing and potential processes. **Hydrometallurgy**, v. 98, n. 1–2, p. 162–176, 2009.

SURVEY, U. S. G. **Mineral Commodity Summaries**. 2019. Available at: <https://minerals.usgs.gov/minerals/pubs/mcs/2019/mcs2019.pdf>.

TAYLOR, R. N.; SKINNER, J. H. **Instability of Granular Cargo in Bulk Carrier Ships**. 1998.

TERZAGHI, K. Erdbaumechanik auf Bodenphysikalischen Grundlagen. **Franz Deuticke**, 1925.

TERZAGHI, K. **Theoretical Soil Mechanics**. [s.l.] John Wiley & Sons, Inc., 1943.

THE HONG KONG MARINE DEPARTMENT. **Report of investigation into the sinking**

of M.V. Huil Ong on 20 May 2005 The Hong Kong Special Administrative Region - Marine Department - Marine Accident investigation, 2005. Available at: <https://www.mardep.gov.hk/en/publication/pdf/mai050520_f.pdf>.

TSUCHIDA. Prediction and Countermeasure Against Liquefaction in Sand Deposits. In: **Seminar in the Port and Harbor Research Institute**, Yokosuka, Japan: Ministry of Transport, 1970.

VEFNÁMSKEID, P. **Plato Vefnámskeid, 2019**. Available at: <https://plato.is/stability_of_fishing_vessels/equilibrium/>. Access on: 20 ago. 2019.

WARTSILA. **Metacentric height**. Available at: <https://www.wartsila.com/encyclopedia/term/metacentric-height>. Access on: 20 ago. 2019a.

WARTSILA. **Free surface effect**. Available at: <https://www.wartsila.com/encyclopedia/term/free-surface-effect>. Access on: 20 ago. 2019b.

WIJDEVELD, A.; EVANS, T.; PENNEKAMP, J. Use of tensiometers to determine the Moisture Characterization Point in ores. p. 1104–1111, 2016.

WILLIAMS, K. et al. Exigências de Limite De Umidade Transportável (TML) para Transporte Marítimo de Minério de Ferro. **45º Seminário de Redução de Minério de Ferro**, p. 661–680, 2017. Available at: <https://abmproceedings.com.br/ptbr/article/exigencias-de-limite-de-umidade-transportavel-tml-para-transporte-maritimo-de-minerio-de-ferro>.

ZHANG, J.; WU, W.; HU, J. Study on the Sloshing of Nickel Ore Slurries With Three Different Moisture Contents. **Journal of Offshore Mechanics and Arctic Engineering**, v. 139, n. 3, p. 032001, 2017.

ZOGRAFAKIS, K. **The Problem of Cargo Liquefaction in the Maritime Industry**. 2014. Strathclyde University, 2014. Available at: <http://dspace.lib.ntua.gr/dspace2/bitstream/handle/123456789/38354/zografakisk_liquefaction.pdf?sequence=1>.

8. APPENDIX

The individual tables and charts of the 16 TML tests described in the section "EFFECT OF SELECTED VARIABLES ON TML RESULTS OBTAINED BY PROCTOR/FAGERBERG TEST METHOD" are displayed on this appendix.

Test 1

Proctor/Fagerberg test - Reading the TML

Density of solids (d)	2.65
Mass of mold (A)	4671.50
Volume of mold	998.19

Test number	Target moisture (%)	Mass of mould + sample (g) B	Mass of tray	Mass of wet sample + tray (g)	Mass of dry sample + tray (g)	Measured gross water content (%) W_1	Net water content (%) e_v	Void ratio (%v) e	Dry density (g/cm^3) Y	Degree of saturation (%) S	Wet bulk density (g/cm^3)	Mass of wet sample (g) C	Mass of dry sample (g) D	Mass of water (g) E	Net water content (%) W
1	13	6448.40	390.30	2175.30	1954.60	12.36	**37.39**	**0.70**	1.56	53.51	1.78	1776.9	1557.2	219.7	14.1
2	14	6475.20	486.70	2298.40	2065.70	12.84	**39.05**	**0.68**	1.57	57.21	1.81	1803.7	1572.0	231.7	14.7
3	15	6562.10	619.00	2516.50	2242.60	14.43	**44.71**	**0.64**	1.62	70.38	1.89	1890.6	1617.7	272.9	16.9
4	16	6629.70	580.00	2543.60	2249.80	14.96	**46.63**	**0.59**	1.67	79.23	1.96	1958.2	1665.2	293.0	17.6
5	17	6661.60	403.70	2397.80	2077.30	16.07	**50.75**	**0.58**	1.67	86.94	1.99	1990.1	1670.2	319.9	19.2
6	18	6639.40	566.60	2537.50	2206.30	16.80	**53.53**	**0.62**	1.64	86.94	1.97	1967.9	1637.2	330.7	20.2

ev read at 70% degree of saturation	44.50
TML (%)	14.38

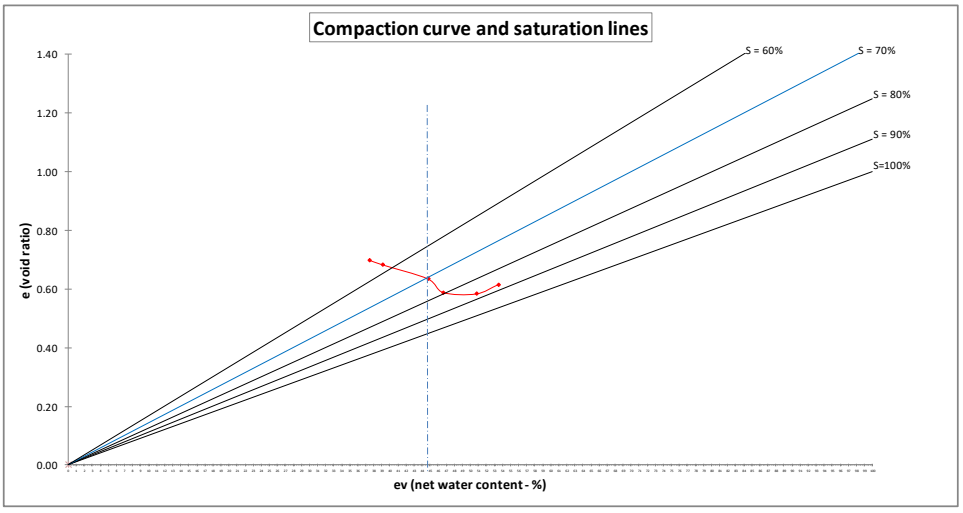

Test 2

Proctor/Fagerberg test - Reading the TML

Density of solids (d)	2.65
Mass of mold (A)	4671.50
Volume of mold	998.19

Test number	Target moisture	Mass of mould + sample	Mass of tray	Mass of wet sample + tray	Mass of dry sample + tray	Measured gross water content	Net water content	Void ratio	Dry density	Degree of saturation	Wet bulk density	Mass of wet sample	Mass of dry sample	Mass of water	Net water content
	(%)	(g)		(g)	(g)	(%)	(%)	(%v)	(g/cm^3)	(%)	(g/cm^3)	(g)	(g)	(g)	(%)
		B				W_1	e_v	e	Y	S		C	D	E	W
1	13	6485.90	459.70	2281.40	2046.70	12.88	**39.19**	**0.67**	1.58	58.19	1.82	1814.4	1580.6	233.8	14.8
2	14	6488.20	426.80	2250.00	2002.90	13.55	**41.55**	**0.68**	1.57	60.71	1.82	1816.7	1570.5	246.2	15.7
3	15	6522.10	352.90	2211.60	1945.30	14.33	**44.32**	**0.67**	1.59	66.30	1.85	1850.6	1585.5	265.1	16.7
4	16	6622.50	426.80	2382.10	2083.20	15.29	**47.82**	**0.60**	1.66	79.64	1.95	1951.0	1652.8	298.2	18.0
5	17	6669.20	342.30	2344.70	2025.30	15.95	**50.29**	**0.58**	1.68	87.40	2.00	1997.7	1679.0	318.7	19.0
6	18	6671.90	324.30	2328.00	1992.40	16.75	**53.31**	**0.59**	1.67	90.61	2.00	2000.4	1665.4	335.0	20.1

ev read at 70% degree of saturation	45.40

TML (%)	14.63

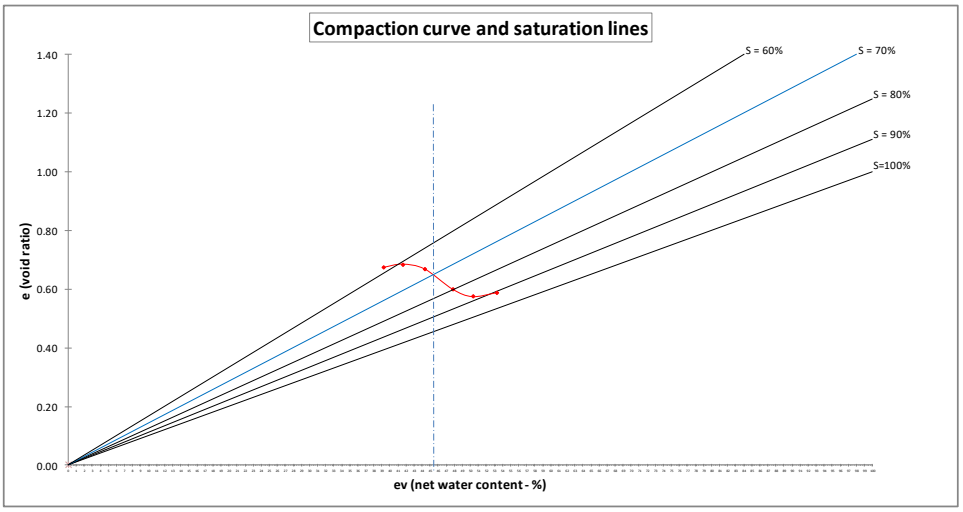

Test 3

Proctor/Fagerberg test - Reading the TML

Density of solids (d)	2.70
Mass of mold (A)	4671.50
Volume of mold	998.19

Test number	Target moisture	Mass of mould + sample	Mass of tray	Mass of wet sample + tray	Mass of dry sample + tray	Measured gross water content	Net water content	Void ratio	Dry density	Degree of saturation	Wet bulk density	Mass of wet sample	Mass of dry sample	Mass of water	Net water content
	(%)	(g)		(g)	(g)	(%)	(%)	(%v)	(g/cm^3)	(%)	(g/cm^3)	(g)	(g)	(g)	(%)
		B				W_1	e_v	e	Y	S		C	D	E	W
1	13	6151.80	879.50	2359.40	2172.10	12.66	**39.12**	**1.08**	1.30	36.08	1.48	1480.3	1292.9	187.4	14.5
2	14	6299.30	873.80	2500.80	2274.80	13.89	**43.55**	**0.92**	1.40	47.20	1.63	1627.8	1401.7	226.1	16.1
3	15	6403.00	854.80	2585.30	2323.80	15.11	**48.06**	**0.83**	1.47	57.66	1.73	1731.5	1469.8	261.7	17.8
4	16	6532.10	873.30	2732.50	2433.30	16.09	**51.78**	**0.73**	1.56	71.30	1.86	1860.6	1561.2	299.4	19.2
5	17	6579.60	888.30	2800.40	2470.40	17.26	**56.32**	**0.71**	1.58	79.65	1.91	1908.1	1578.8	329.3	20.9

ev read at 70% degree of saturation	51.40

TML (%)	15.99

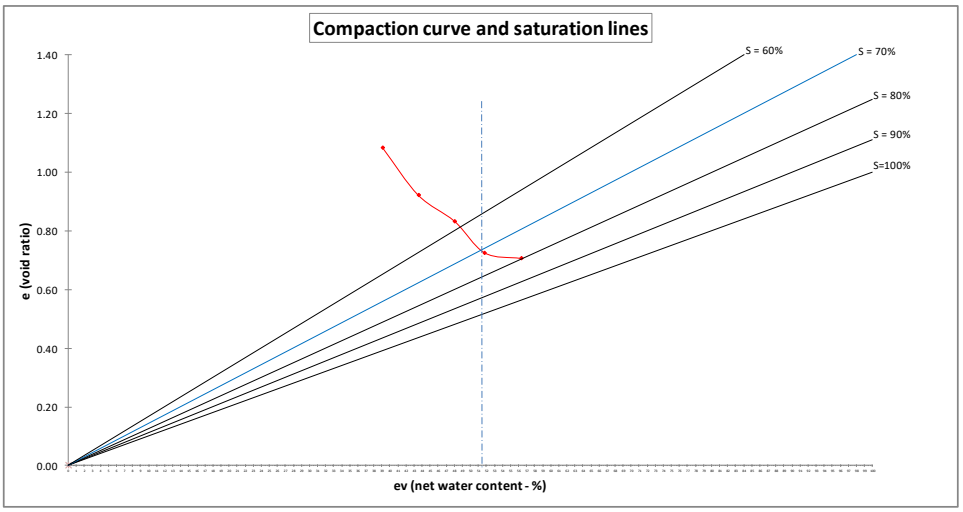

Test 4

Proctor/Fagerberg test - Reading the TML

Density of solids (d)	2.69
Mass of mold (A)	4671.50
Volume of mold	998.19

Test number	Target moisture	Mass of mould + sample	Mass of tray	Mass of wet sample + tray	Mass of dry sample + tray	Measured gross water content	Net water content	Void ratio	Dry density	Degree of saturation	Wet bulk density	Mass of wet sample	Mass of dry sample	Mass of water	Net water content
	(%)	(g)		(g)	(g)	(%)	(%)	(%v)	(g/cm^3)	(%)	(g/cm^3)	(g)	(g)	(g)	(%)
		B				W_1	e_v	e	Y	S		C	D	E	W
1	13	6231.60	880.50	2440.50	2244.50	12.56	**38.65**	**0.97**	1.37	39.91	1.56	1560.1	1364.1	196.0	14.4
2	14	6331.00	898.60	2558.30	2330.50	13.73	**42.80**	**0.88**	1.43	48.88	1.66	1659.5	1431.7	227.8	15.9
3	15	6390.30	863.20	2581.40	2335.60	14.31	**44.91**	**0.82**	1.48	54.56	1.72	1718.8	1472.9	245.9	16.7
4	16	6533.30	875.40	2736.70	2439.60	15.96	**51.09**	**0.72**	1.57	71.34	1.87	1861.8	1564.6	297.2	19.0
5	17	6593.90	882.40	2805.00	2484.70	16.66	**53.77**	**0.68**	1.61	79.55	1.93	1922.4	1602.1	320.3	20.0
6	18	6627.50	888.30	2863.10	2517.50	17.50	**57.06**	**0.66**	1.62	85.94	1.96	1956.0	1613.7	342.3	21.2

ev read at 70% degree of saturation	50.70

TML (%)	15.86

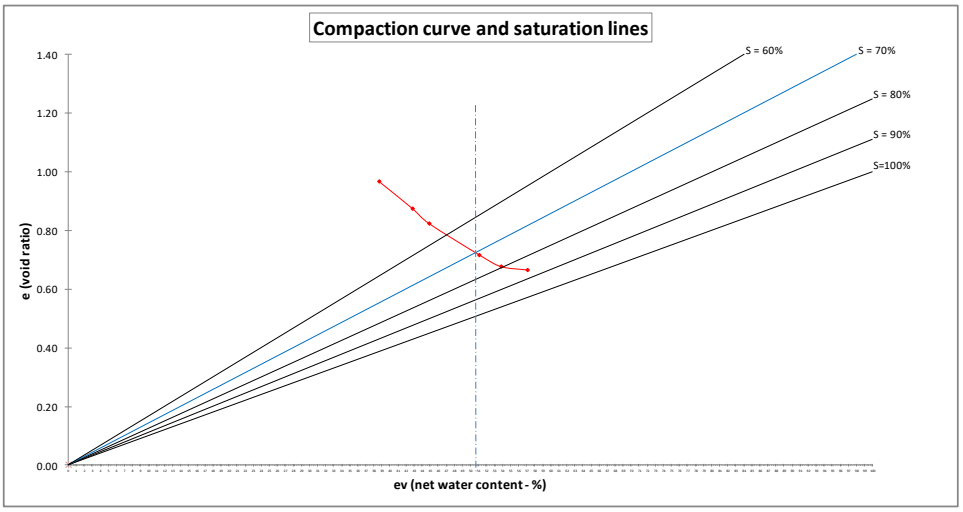

Test 5

Proctor/Fagerberg test - Reading the TML

Density of solids (d)	2.62
Mass of mold (A)	4671.50
Volume of mold	998.19

Test number	Target moisture	Mass of mould + sample	Mass of tray	Mass of wet sample + tray	Mass of dry sample + tray	Measured gross water content	Net water content	Void ratio	Dry density	Degree of saturation	Wet bulk density	Mass of wet sample	Mass of dry sample	Mass of water	Net water content
	(%)	(g)		(g)	(g)	(%)	(%)	(%v)	(g/cm^3)	(%)	(g/cm^3)	(g)	(g)	(g)	(%)
		B				W_1	e_v	e	Y	S		C	D	E	W
1	13	6470.90	869.30	2668.30	2441.40	12.61	**37.81**	**0.66**	1.58	57.02	1.80	1799.4	1572.4	227.0	14.4
2	14	6528.80	873.30	2729.30	2478.10	13.53	**41.01**	**0.63**	1.61	65.25	1.86	1857.3	1605.9	251.4	15.7
3	15	6634.30	873.80	2835.50	2546.90	14.71	**45.19**	**0.56**	1.68	80.38	1.97	1962.8	1674.0	288.8	17.2
4	16	6698.70	886.80	2911.40	2595.50	15.60	**48.44**	**0.53**	1.71	91.64	2.03	2027.2	1710.9	316.3	18.5
5	17	6689.40	887.50	2900.80	2570.30	16.42	**51.46**	**0.55**	1.69	93.46	2.02	2017.9	1686.6	331.3	19.6
6	18	6671.50	876.40	2871.50	2526.70	17.28	**54.74**	**0.58**	1.66	94.24	2.00	2000.0	1654.4	345.6	20.9

ev read at 70% degree of saturation	42.40

TML (%)	13.93

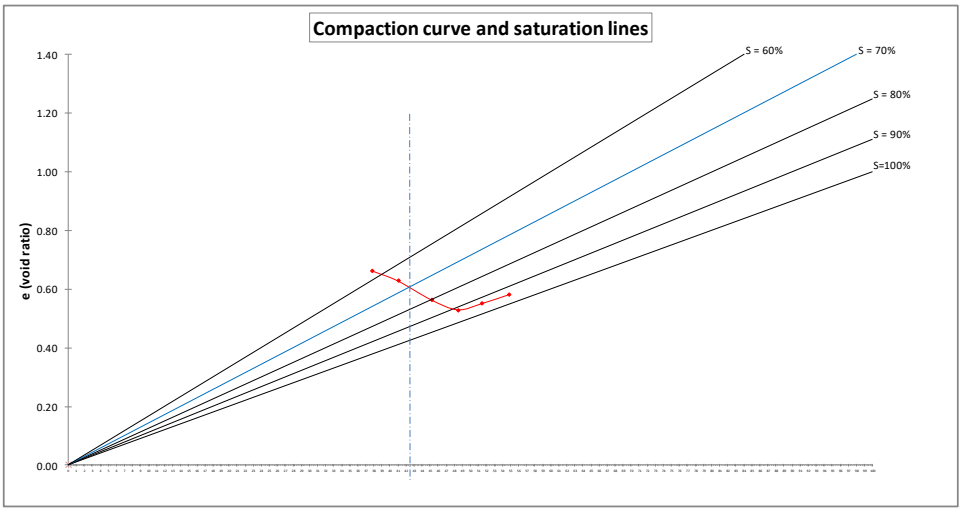

Test 6

Proctor/Fagerberg test - Reading the TML

Density of solids (d)	2.60
Mass of mold (A)	4671.50
Volume of mold	998.19

Test number	Target moisture	Mass of mould + sample	Mass of tray	Mass of wet sample + tray	Mass of dry sample + tray	Measured gross water content	Net water content	Void ratio	Dry density	Degree of saturation	Wet bulk density	Mass of wet sample	Mass of dry sample	Mass of water	Net water content
	(%)	(g)		(g)	(g)	(%)	(%)	(%v)	(g/cm^3)	(%)	(g/cm^3)	(g)	(g)	(g)	(%)
		B				W_1	e_v	e	Y	S		C	D	E	W
1	13	6497.70	352.90	2187.20	1954.60	12.68	**37.76**	**0.63**	1.60	60.17	1.83	1826.2	1594.6	231.6	14.5
2	14	6520.30	426.80	2281.60	2025.20	13.82	**41.71**	**0.63**	1.60	66.31	1.85	1848.8	1593.2	255.6	16.0
3	15	6597.80	389.30	2320.70	2037.20	14.68	**44.73**	**0.58**	1.65	77.24	1.93	1926.3	1643.5	282.8	17.2
4	16	6700.30	428.80	2461.30	2149.30	15.35	**47.15**	**0.51**	1.72	92.23	2.03	2028.8	1717.4	311.4	18.1
5	17	6690.20	520.30	2538.60	2214.80	16.04	**49.68**	**0.53**	1.70	93.51	2.02	2018.7	1694.8	323.9	19.1
6	18	6687.40	394.50	2409.20	2071.70	16.75	**52.32**	**0.55**	1.68	95.74	2.02	2015.9	1678.2	337.7	20.1

ev read at 70% degree of saturation	43.00

TML (%)	14.19

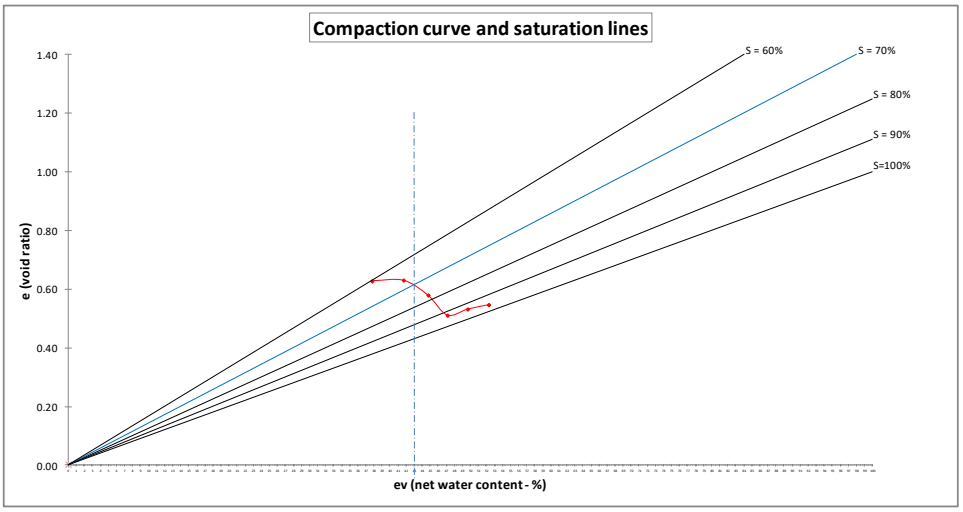

Test 7

Proctor/Fagerberg test - Reading the TML

Density of solids (d)	2.65
Mass of mold (A)	4671.50
Volume of mold	998.19

Test number	Target moisture	Mass of mould + sample	Mass of tray	Mass of wet sample + tray	Mass of dry sample + tray	Measured gross water content	Net water content	Void ratio	Dry density	Degree of saturation	Wet bulk density	Mass of wet sample	Mass of dry sample	Mass of water	Net water content
	(%)	(g)		(g)	(g)	(%)	(%)	(%v)	(g/cm^3)	(%)	(g/cm^3)	(g)	(g)	(g)	(%)
		B				W_1	e_v	e	Y	S		C	D	E	W
1	13	6440.20	873.80	2642.40	2419.40	12.61	**38.23**	**0.71**	1.55	53.75	1.77	1768.7	1545.7	223.0	14.4
2	14	6504.70	873.30	2706.40	2457.60	13.57	**41.62**	**0.67**	1.59	62.16	1.84	1833.2	1584.4	248.8	15.7
3	15	6571.70	872.10	2771.20	2491.80	14.71	**45.71**	**0.63**	1.62	72.31	1.90	1900.2	1620.6	279.6	17.3
4	16	6684.30	874.20	2883.50	2564.00	15.90	**50.11**	**0.56**	1.70	89.05	2.02	2012.8	1692.7	320.1	18.9
5	17	6683.50	854.80	2860.20	2529.60	16.49	**52.31**	**0.57**	1.68	91.10	2.02	2012.0	1680.3	331.7	19.7
6	18	6666.90	869.30	2857.00	2516.00	17.16	**54.88**	**0.60**	1.66	91.44	2.00	1995.4	1653.1	342.3	20.7

ev read at 70% degree of saturation	44.90

TML (%)	14.49

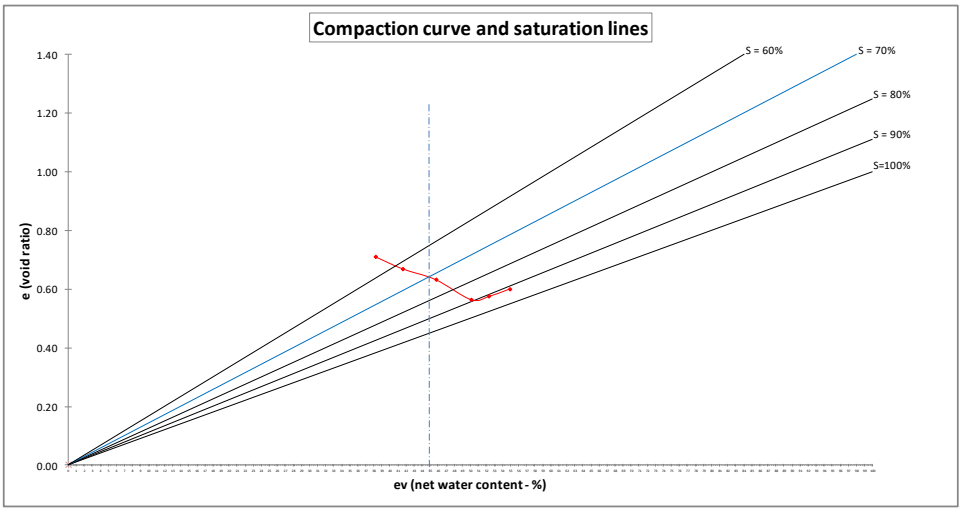

Test 8

Proctor/Fagerberg test - Reading the TML

Density of solids (d)	2.64
Mass of mold (A)	4671.50
Volume of mold	998.19

Test number	Target moisture	Mass of mould + sample	Mass of tray	Mass of wet sample + tray	Mass of dry sample + tray	Measured gross water content	Net water content	Void ratio	Dry density	Degree of saturation	Wet bulk density	Mass of wet sample	Mass of dry sample	Mass of water	Net water content
	(%)	(g)		(g)	(g)	(%)	(%)	(%v)	(g/cm^3)	(%)	(g/cm^3)	(g)	(g)	(g)	(%)
		B				W_1	e_v	e	Y	S		C	D	E	W
1	13	6442.90	390.50	2164.10	1941.40	12.56	**37.91**	**0.70**	1.55	54.06	1.77	1771.4	1549.0	222.4	14.4
2	14	6501.40	394.50	2226.00	1968.90	14.04	**43.11**	**0.68**	1.58	63.84	1.83	1829.9	1573.0	256.9	16.3
3	15	6623.80	426.80	2376.60	2088.70	14.77	**45.73**	**0.58**	1.67	78.36	1.96	1952.3	1664.0	288.3	17.3
4	16	6682.80	352.90	2361.50	2053.80	15.32	**47.76**	**0.55**	1.71	87.27	2.01	2011.3	1703.2	308.1	18.1
5	17	6680.60	393.00	2397.80	2079.20	15.89	**49.88**	**0.56**	1.69	89.16	2.01	2009.1	1689.8	319.3	18.9
6	18	6656.60	394.90	2376.60	2043.10	16.83	**53.42**	**0.60**	1.65	89.61	1.99	1985.1	1651.0	334.1	20.2

ev read at 70% degree of saturation	44.50

TML (%)	14.42

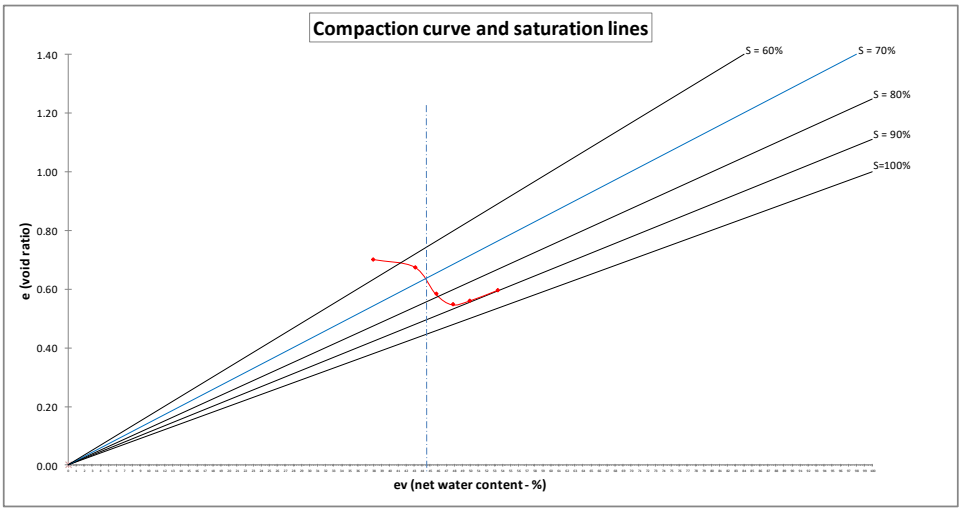

Test 9

Proctor/Fagerberg test - Reading the TML

Density of solids (d)	2.63
Mass of mold (A)	4671.50
Volume of mold	998.19

Test number	Target moisture	Mass of mould + sample	Mass of tray	Mass of wet sample + tray	Mass of dry sample + tray	Measured gross water content	Net water content	Void ratio	Dry density	Degree of saturation	Wet bulk density	Mass of wet sample	Mass of dry sample	Mass of water	Net water content
	(%)	(g)		(g)	(g)	(%)	(%)	(%v)	(g/cm^3)	(%)	(g/cm^3)	(g)	(g)	(g)	(%)
		B				W_1	e_v	e	Y	S		C	D	E	W
1	13	6384.30	252.90	2066.00	1833.60	12.82	**38.67**	**0.76**	1.50	51.01	1.72	1712.8	1493.3	219.5	14.7
2	14	6433.80	353.60	2115.90	1858.50	14.61	**44.98**	**0.74**	1.51	60.42	1.77	1762.3	1504.9	257.4	17.1
3	15	6564.40	459.70	2340.10	2043.40	15.78	**49.27**	**0.65**	1.60	76.19	1.90	1892.9	1594.2	298.7	18.7
4	16	6602.30	470.60	2388.40	2070.10	16.60	**52.34**	**0.63**	1.61	83.04	1.93	1930.8	1610.3	320.5	19.9
5	17	6613.50	426.80	2363.50	2025.60	17.45	**55.58**	**0.64**	1.61	87.19	1.95	1942.0	1603.2	338.8	21.1

ev read at 70% degree of saturation	47.80

TML (%)	15.38

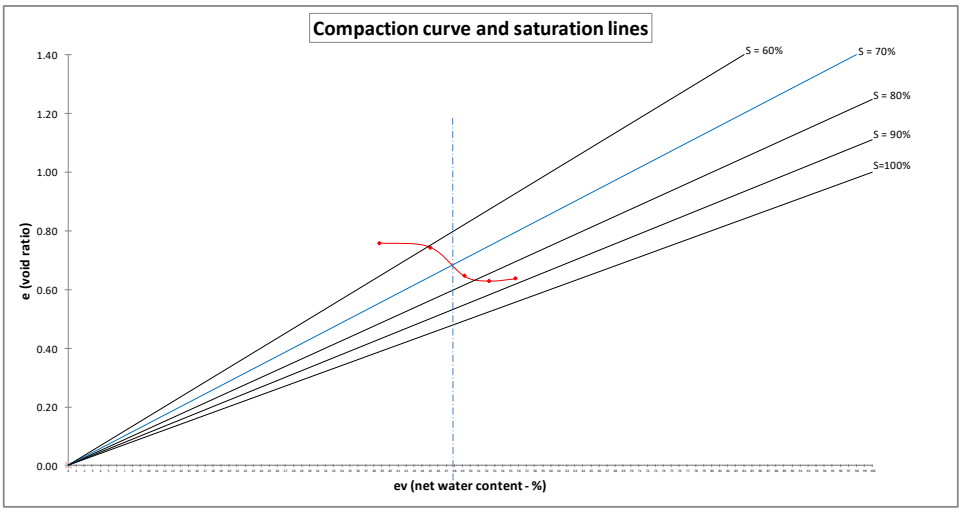

Test 10

Proctor/Fagerberg test - Reading the TML

Density of solids (d)	2.63
Mass of mold (A)	4671.50
Volume of mold	998.19

Test number	Target moisture	Mass of mould + sample	Mass of tray	Mass of wet sample + tray	Mass of dry sample + tray	Measured gross water content	Net water content	Void ratio	Dry density	Degree of saturation	Wet bulk density	Mass of wet sample	Mass of dry sample	Mass of water	Net water content
	(%)	(g)		(g)	(g)	(%)	(%)	(%v)	(g/cm^3)	(%)	(g/cm^3)	(g)	(g)	(g)	(%)
		B				W_1	e_v	e	Y	S		C	D	E	W
1	13	6384.20	466.20	2179.30	1942.00	13.85	**42.29**	**0.78**	1.48	54.27	1.72	1712.7	1475.5	237.2	16.1
2	14	6414.50	426.80	2168.60	1912.90	14.68	**45.25**	**0.77**	1.49	59.13	1.75	1743.0	1487.1	255.9	17.2
3	15	6520.70	391.30	2240.20	1949.30	15.73	**49.11**	**0.68**	1.56	71.72	1.85	1849.2	1558.3	290.9	18.7
4	16	6606.10	392.20	2324.70	2007.50	16.41	**51.65**	**0.62**	1.62	82.84	1.94	1934.6	1617.1	317.5	19.6
5	17	6609.30	394.90	2326.40	1985.30	17.66	**56.41**	**0.65**	1.60	87.41	1.94	1937.8	1595.6	342.2	21.4
6	18	6592.80	458.80	2372.70	2018.50	18.51	**59.73**	**0.68**	1.57	88.26	1.92	1921.3	1565.7	355.6	22.7

ev read at 70% degree of saturation	48.70

TML (%)	15.62

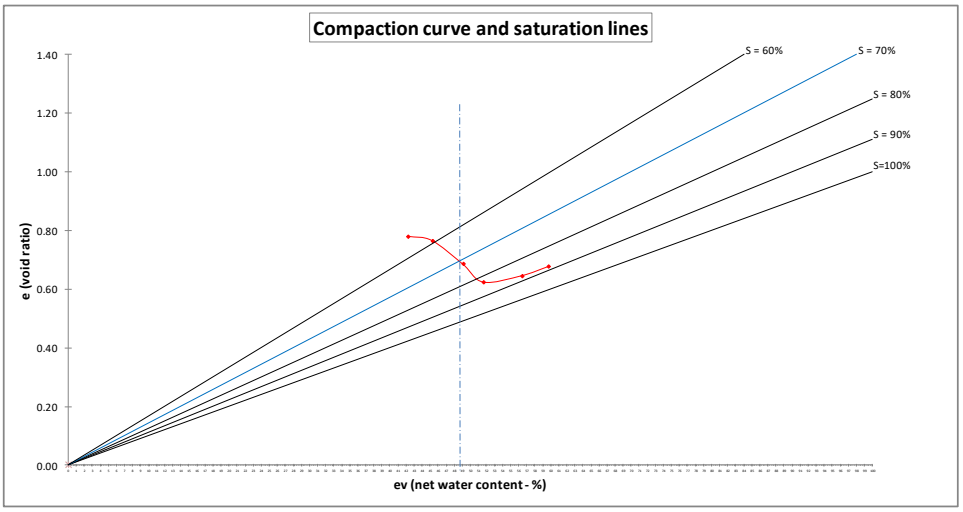

Test 11

Proctor/Fagerberg test - Reading the TML

Density of solids (d)	2.69
Mass of mold (A)	4671.50
Volume of mold	998.19

Test number	Target moisture	Mass of mould + sample	Mass of tray	Mass of wet sample + tray	Mass of dry sample + tray	Measured gross water content	Net water content	Void ratio	Dry density	Degree of saturation	Wet bulk density	Mass of wet sample	Mass of dry sample	Mass of water	Net water content
	(%)	(g)		(g)	(g)	(%)	(%)	(%v)	(g/cm^3)	(%)	(g/cm^3)	(g)	(g)	(g)	(%)
		B				W_1	e_v	e	Y	S		C	D	E	W
1	14	6178.20	381.20	1884.40	1679.20	13.65	**42.53**	**1.06**	1.30	39.97	1.51	1506.7	1301.0	205.7	15.8
2	15	6248.60	466.20	1960.40	1734.20	15.14	**47.99**	**1.01**	1.34	47.69	1.58	1577.1	1338.4	238.7	17.8
3	16	6303.30	426.80	2060.80	1795.70	16.22	**52.09**	**0.96**	1.37	54.03	1.63	1631.8	1367.1	264.7	19.4
4	17	6376.20	390.50	2120.40	1817.60	17.50	**57.08**	**0.91**	1.41	62.77	1.71	1704.7	1406.3	298.4	21.2
5	18	6394.60	394.40	2122.50	1796.40	18.87	**62.57**	**0.92**	1.40	67.95	1.73	1723.1	1397.9	325.2	23.3
6	19	6414.20	391.30	2146.00	1800.80	19.67	**65.88**	**0.92**	1.40	71.75	1.75	1742.7	1399.9	342.8	24.5

ev read at 70% degree of saturation	64.40
TML (%)	19.32

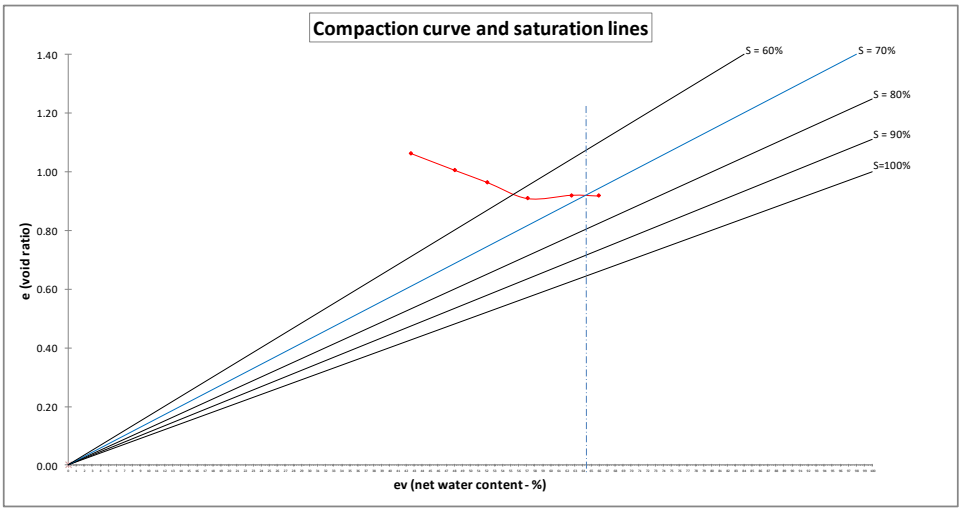

Test 12

Proctor/Fagerberg test - Reading the TML

Density of solids (d)	2.70
Mass of mold (A)	4671.50
Volume of mold	998.19

Test number	Target moisture	Mass of mould + sample	Mass of tray	Mass of wet sample + tray	Mass of dry sample + tray	Measured gross water content	Net water content	Void ratio	Dry density	Degree of saturation	Wet bulk density	Mass of wet sample	Mass of dry sample	Mass of water	Net water content
	(%)	(g)		(g)	(g)	(%)	(%)	(%v)	(g/cm^3)	(%)	(g/cm^3)	(g)	(g)	(g)	(%)
		B				W_1	e_v	e	Y	S		C	D	E	W
1	14	6157.10	390.30	1884.70	1674.60	14.06	**44.17**	**1.11**	1.28	39.76	1.49	1485.6	1276.7	208.9	16.4
2	15	6254.50	389.30	1980.40	1731.20	15.66	**50.14**	**1.02**	1.34	49.22	1.59	1583.0	1335.1	247.9	18.6
3	16	6303.30	426.80	2065.40	1800.70	16.15	**52.02**	**0.97**	1.37	53.64	1.63	1631.8	1368.2	263.6	19.3
4	17	6386.20	394.50	2116.80	1821.30	17.16	**55.92**	**0.90**	1.42	62.32	1.72	1714.7	1420.5	294.2	20.7
5	18	6391.60	392.50	2117.50	1805.60	18.08	**59.59**	**0.91**	1.41	65.30	1.72	1720.1	1409.1	311.0	22.1
6	19	6420.10	390.50	2120.20	1785.40	19.36	**64.80**	**0.91**	1.41	71.12	1.75	1748.6	1410.1	338.5	24.0

ev read at 70% degree of saturation	63.80

TML (%)	19.11

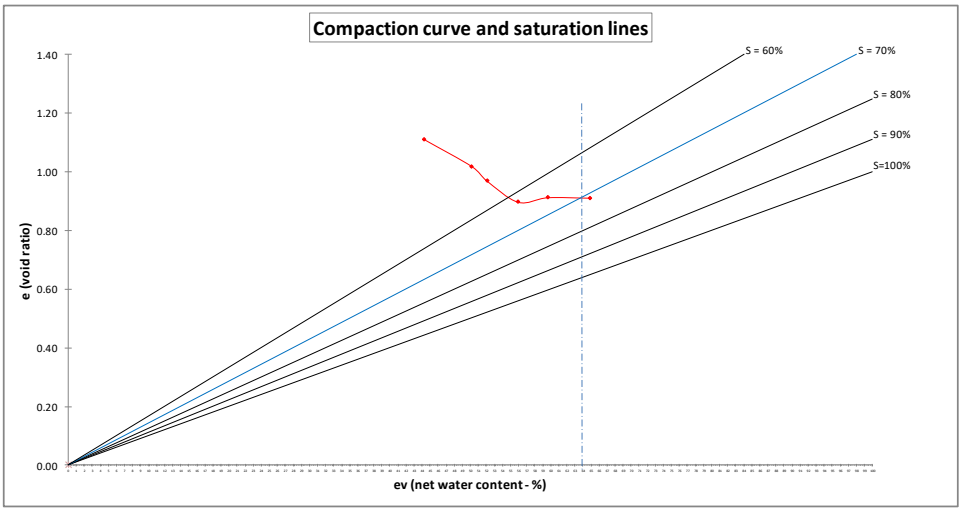

Test 13

Proctor/Fagerberg test - Reading the TML

Density of solids (d)	2.61
Mass of mold (A)	4671.50
Volume of mold	998.19

Test number	Target moisture	Mass of mould + sample	Mass of tray	Mass of wet sample + tray	Mass of dry sample + tray	Measured gross water content	Net water content	Void ratio	Dry density	Degree of saturation	Wet bulk density	Mass of wet sample	Mass of dry sample	Mass of water	Net water content
	(%)	(g)		(g)	(g)	(%)	(%)	(%v)	(g/cm^3)	(%)	(g/cm^3)	(g)	(g)	(g)	(%)
		B				W_1	e_v	e	Y	S		C	D	E	W
1	13	6437.70	395.00	2161.00	1932.00	12.97	**38.89**	**0.69**	1.54	55.96	1.77	1766.2	1537.2	229.0	14.9
2	14	6462.80	395.40	2186.50	1940.40	13.74	**41.57**	**0.69**	1.55	60.60	1.79	1791.3	1545.2	246.1	15.9
3	15	6530.40	403.60	2261.80	1984.20	14.94	**45.84**	**0.65**	1.58	70.78	1.86	1858.9	1581.2	277.7	17.6
4	16	6570.90	388.50	2286.80	1985.10	15.89	**49.32**	**0.63**	1.60	78.18	1.90	1899.4	1597.5	301.9	18.9
5	17	6623.70	406.50	2356.50	2031.60	16.66	**52.18**	**0.60**	1.63	86.77	1.96	1952.2	1626.9	325.3	20.0
6	18	6629.70	385.30	2340.60	1996.40	17.60	**55.76**	**0.61**	1.62	90.71	1.96	1958.2	1613.5	344.7	21.4

ev read at 70% degree of saturation	45.50

TML (%)	14.85

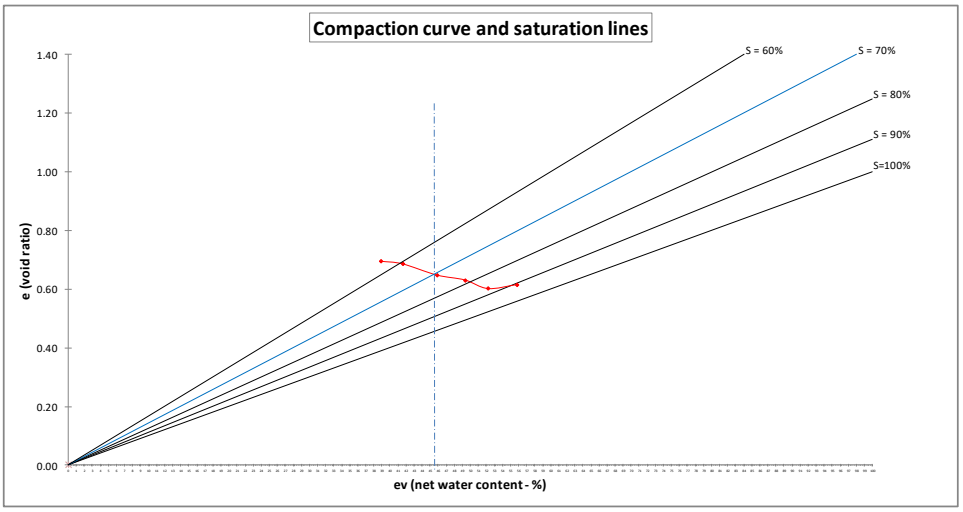

Test 14

Proctor/Fagerberg test - Reading the TML

Density of solids (d)	2.60
Mass of mold (A)	4671.50
Volume of mold	998.19

Test number	Target moisture	Mass of mould + sample	Mass of tray	Mass of wet sample + tray	Mass of dry sample + tray	Measured gross water content	Net water content	Void ratio	Dry density	Degree of saturation	Wet bulk density	Mass of wet sample	Mass of dry sample	Mass of water	Net water content
	(%)	(g)		(g)	(g)	(%)	(%)	(%v)	(g/cm^3)	(%)	(g/cm^3)	(g)	(g)	(g)	(%)
		B				W_1	e_v	e	Y	S		C	D	E	W
1	13	6374.70	394.90	2099.00	1880.30	12.83	**38.28**	**0.75**	1.49	51.17	1.71	1703.2	1484.6	218.6	14.7
2	14	6407.60	458.80	2194.40	1956.80	13.69	**41.24**	**0.73**	1.50	56.34	1.74	1736.1	1498.4	237.7	15.9
3	15	6452.80	391.30	2146.10	1889.90	14.60	**44.45**	**0.71**	1.52	62.96	1.78	1781.3	1521.2	260.1	17.1
4	16	6590.80	426.80	2343.70	2042.30	15.72	**48.51**	**0.60**	1.62	80.25	1.92	1919.3	1617.5	301.8	18.7
5	17	6632.20	466.20	2422.60	2106.50	16.16	**50.10**	**0.58**	1.65	86.58	1.96	1960.7	1643.9	316.8	19.3
6	18	6655.60	390.30	2363.50	2019.40	17.44	**54.92**	**0.58**	1.64	93.98	1.99	1984.1	1638.1	346.0	21.1

ev read at 70% degree of saturation	46.30

TML (%)	15.12

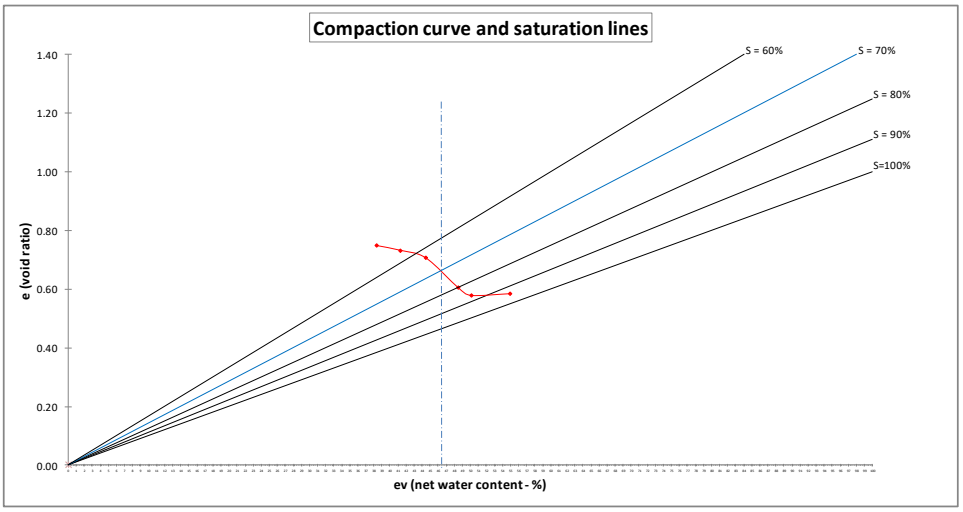

Test 15

Proctor/Fagerberg test - Reading the TML

Density of solids (d)	2.63
Mass of mold (A)	4671.50
Volume of mold	998.19

Test number	Target moisture	Mass of mould + sample	Mass of tray	Mass of wet sample + tray	Mass of dry sample + tray	Measured gross water content	Net water content	Void ratio	Dry density	Degree of saturation	Wet bulk density	Mass of wet sample	Mass of dry sample	Mass of water	Net water content
	(%)	(g)		(g)	(g)	(%)	(%)	(%v)	(g/cm^3)	(%)	(g/cm^3)	(g)	(g)	(g)	(%)
		B				W_1	e_v	e	Y	S		C	D	E	W
1	13	6276.90	403.70	2008.70	1808.10	12.50	**37.57**	**0.87**	1.41	43.24	1.61	1605.4	1404.8	200.6	14.3
2	14	6338.30	393.80	2060.20	1832.00	13.69	**41.73**	**0.82**	1.44	50.59	1.67	1666.8	1438.5	228.3	15.9
3	15	6395.00	393.50	2116.80	1863.40	14.70	**45.34**	**0.79**	1.47	57.70	1.73	1723.5	1470.1	253.4	17.2
4	16	6436.20	394.70	2160.60	1890.30	15.31	**47.53**	**0.76**	1.50	62.83	1.77	1764.7	1494.6	270.1	18.1
5	17	6536.70	470.60	2333.00	2031.70	16.18	**50.76**	**0.68**	1.57	74.74	1.87	1865.2	1563.4	301.8	19.3
6	18	6639.40	873.80	2833.20	2496.70	17.17	**54.53**	**0.61**	1.63	89.30	1.97	1967.9	1629.9	338.0	20.7

ev read at 70% degree of saturation	49.50

TML (%)	15.84

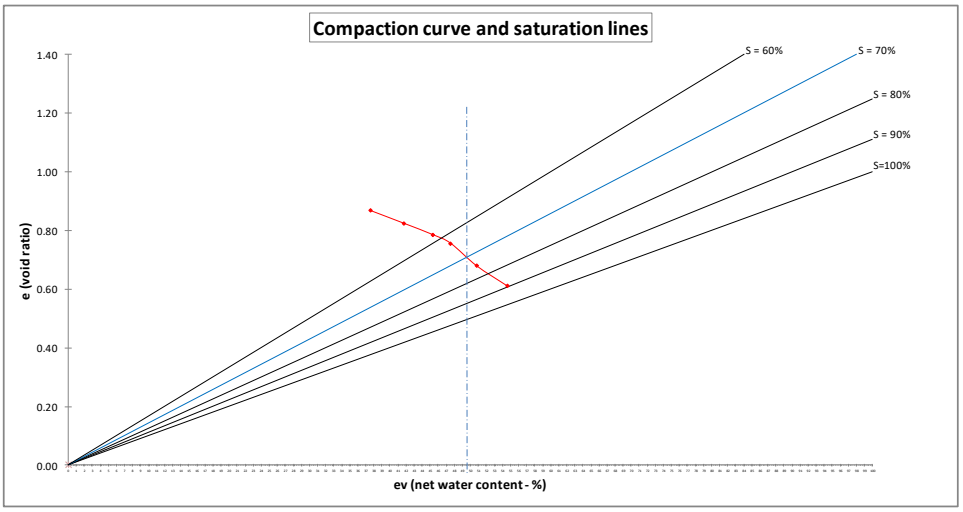

Test 16

Proctor/Fagerberg test - Reading the TML

Density of solids (d)	2.63
Mass of mold (A)	4671.50
Volume of mold	998.19

Test number	Target moisture	Mass of mould + sample	Mass of tray	Mass of wet sample + tray	Mass of dry sample + tray	Measured gross water content	Net water content	Void ratio	Dry density	Degree of saturation	Wet bulk density	Mass of wet sample	Mass of dry sample	Mass of water	Net water content
	(%)	(g)		(g)	(g)	(%)	(%)	(%v)	(g/cm^3)	(%)	(g/cm^3)	(g)	(g)	(g)	(%)
		B				W_1	e_v	e	Y	S		C	D	E	W
1	13	6263.90	332.00	1924.80	1726.00	12.48	**37.51**	**0.88**	1.40	42.44	1.60	1592.4	1393.6	198.8	14.3
2	14	6312.50	324.30	1965.90	1742.60	13.60	**41.41**	**0.85**	1.42	48.62	1.64	1641.0	1417.8	223.2	15.7
3	15	6388.40	333.50	2049.70	1797.60	14.69	**45.29**	**0.79**	1.47	57.15	1.72	1716.9	1464.7	252.2	17.2
4	16	6409.60	322.40	2059.20	1790.50	15.47	**48.14**	**0.79**	1.47	61.18	1.74	1738.1	1469.2	268.9	18.3
5	17	6582.10	325.60	2231.30	1911.10	16.80	**53.11**	**0.65**	1.59	81.52	1.91	1910.6	1589.6	321.0	20.2
6	18	6615.90	323.10	2261.10	1929.10	17.13	**54.37**	**0.63**	1.61	86.40	1.95	1944.4	1611.3	333.1	20.7

ev read at 70% degree of saturation	50.60

TML (%)	16.14